Public-data File 85-31

A PRELIMINARY REPORT ON THE INVESTIGATION OF GEOTHERMAL ENERGY RESOURCE POTENTIAL OF THE EASTERN COPPER RIVER BASIN, ALASKA

By

E.M. Wescottt and D.L. Turner

Alaska Division of
Geological and Geophysical Surveys

1985

THIS REPORT HAS NOT BEEN REVIEWED FOR
TECHNICAL CONTENT (EXCEPT AS NOTED IN
TEXT) OR FOR CONFORMITY TO THE
EDITORIAL STANDARDS OF DGGS.

794 University Avenue, Basement
Fairbanks, Alaska 99701

A Preliminary Report on the Investigation of the Geothermal Energy Resource Potential of the Eastern Copper River Basin, Alaska

(Draft Version of Final Report)

Eugene M. Wescott and Donald L. Turner
Editors and Co-Principal Investigators

Submitted to the Alaska Division of Geological and Geophysical Surveys
RSA 82-5X-670

December 1982

Executive Summary

This report consists of a review of the available geological, geochemical and geophysical data on parts of the Eastern Copper River Basin with emphasis on the mud volcanoes, and the results of geophysical and geochemical studies carried out by the Geophysical Institute and Alaska DGGS personnel in Summer 1982. The purpose of this work is to evaluate the possible existence of geothermal energy resources in the Copper River Basin. There is ample reason to suspect that the area may contain geothermal prospects although there are no obvious surface manifestations such as hot springs, geysers, etc. The area is situated on the flanks of a volcano - Mt. Drum, which was active as late as 200,000 years ago and which is thought to have retained significant amounts of residual heat at high levels within the volcano.

There are two groups of mud volcanoes in this area: the Tolsona group west of Glenallen and the Klawasi group east of Glenallen. The Tolsona group is characterized by high methane and helium gas content. The presence of methane in an overpressured zone near 5,000 ft. depth in the nearby Pan American Moose Creek #1 well strongly suggests that the Tolsona group result from mud and gas reaching the surface from this overpressured zone. The Klawasi group, however, produce predominantly CO_2 gas with a minor helium content. The CO_2 may result from decomposition of limestones, or calcium carbonate cemented sedimentary rocks (Motyka, personal communication, 1982). The geothermometry of the waters coming from the Klawasi mud volcanoes has so far produced contradictory results: some indicate a cold water source while others indicate a source of greater than 150°C (Motyka, private communica-

tion, 1982). For this reason the Klawasi mud volcano area was a focal point of the 1982 survey.

There are no wildcat wells in the area. The AMOCO Ahtna A-1 well about 13 miles from the mud volcanoes is the closest hole. It shows an overpressured zone near 2,300 ft. depth and greenstone basement rocks near 5,000 ft. depth. Gravity and aeromagnetic data suggest that the basement in the Klawasi group area may be even deeper.

Ground water in the area as shown by water wells in populated areas is saline and thus of low resistivity. This fact ruled out the use of artificial source electrical surveys because it would take unrealistic amounts of current to penetrate to the depths of interest, and geothermal sources would produce only small contrasts. Instead, we conducted self-potential surveys to look for anomalous areas. The other principle reconnaissance survey technique was sampling the soil and soil gas for anomalous helium content - a method demonstrated to be a useful indicator of geothermal areas.

Gravity and magnetic surveys cannot directly indicate geothermal resources, but they are very useful for interpreting geologic structures associated with or responsible for helium or self-potential anomalies. The Alaska DGGS contracted with ERTEC Airborne Systems Inc. to fly an aeromagnetic survey of the area during the field season. The airborne survey was augmented by our ground magnetic measurements. We also ran a much more detailed gravity survey over the area than was previously available.

The results of the various surveys are presented in separate sections of this report. The final section sums up the analysis in terms of possible geothermal prospects. No combination of geophysical and geochemical measurements can unequivocally prove the presence of geothermal resources at depth where there are no obvious surface manifestations. Test drilling is the

only sure method to prove a resource. Our measurements have discovered at least three areas of interest. An area of several square miles centered over a well-defined gravity high has anomalous helium flux, a steep positive self-potential gradient, and apparently a negative magnetic anomaly. Taken singly each measurement might be explained otherwise, but together they all point to a geothermal resource at depth. A second large area of anomalous helium flux is associated with a gravity low, a magnetic low and a negative self-potential gradient. The suggested source of this second anomalous area is a mud diapir driven by a heat source. A third area is also of interest although no detailed gravity nor any self-potential data were taken there. It is located near the junction of the Tazlina and Copper Rivers, on the road system. It contains the highest anomalous helium value found in our survey. Logistically it would be the easiest area for further detailed exploration and test drilling.

The final chapter of this report considers these data and makes recommendations for future work to evaluate the geothermal potential of the area.

TABLE OF CONTENTS

CHAPTER 1 - SUMMARY AND EVALUATION OF GEOLOGIC, GEOCHEMICAL AND GEOPHYSICAL DATA RELEVANT TO GEOTHERMAL ENERGY EXPLORATION IN THE EASTERN COPPER RIVER BASIN, ALASKA, by Donald L. Turner, Eugene M. Wescott and Christopher J. Nye 1

INTRODUCTION 1

FIGURE 1-1. 2

REGIONAL SETTING 3

THE WRANGELL VOLCANOES 4

BASIN STRUCTURE AND STRATIGRAPHY 9

STRUCTURE 9

STRATIGRAPHY 10

MUD VOLCANOES 12

MORPHOLOGY 12

GAS AND WATER ANALYSIS 13

TABLE 1-1. 14

ORIGIN OF THE MUD VOLCANOES 15

FIGURE 1-2. 17

TABLE 1-2. 18

TABLE 1-3 19

IMPLICATIONS OF THE MUD VOLCANOES FOR GEOTHERMAL EXPLORATION 20

FIGURE 1-3. 21

PREVIOUS GEOPHYSICAL AND GEOCHEMICAL SURVEYS 22

FIGURE 1-4. 23

TABLE 1-4. 25

FIELD WORK PLAN 28

GRAVITY 28

MAGNETICS 29

SELF POTENTIAL SURVEY 29

HELIUM SOIL GAS SURVEY 29

COPPER RIVER BASIN BIBLIOGRAPHY 31

CHAPTER 2 - A HELIUM SOIL SURVEY IN THE EASTERN COPPER RIVER BASIN, ALASKA, by Donald L. Turner and Eugene M. Wescott 48

CHARACTERISTICS AND SOURCES OF HELIUM 48

FIGURE 2-1. 50

FIGURE 2-2. 51

FIGURE 2-3. 52

EXPLORATION TECHNIQUES 53

SAMPLING METHODS 54

FIGURE 2-4. 55

RESULTS 57

FIGURE 2-5. 59

TABLE 2-1. 62

APPENDIX A 68

APPENDIX B 70

CHAPTER 3 - MERCURY SOIL SAMPLING IN THE EASTER COPPER RIVER BASIN, ALASKA, By Eugene M. Wescott 74

INTRODUCTION 74

RESULTS 74

TABLE 3-1. 76

FIGURE 3-1. 77

CHAPTER 4 - A GRAVITY SURVEY OF PART OF THE EASTERN COPPER RIVER BASIN, ALASKA, by Eugene M. Wescott, Becky Petzinger, Gary Bender, William Witte and Donald L. Turner 78
INTRODUCTION 78
PHYSICAL PROPERTY MEASUREMENTS 79
GRAVITY SURVEY 79
FIGURE 4-1. 82
FIGURE 4-2. 83
TABLE 4-1. 85
TABLE 4-2 86
CHAPTER 5 - A SELF-POTENTIAL SURVEY IN THE EASTERN COPPER RIVER BASIN, ALASKA, by Eugene M. Wescott and Gary Bender 90
INTRODUCTION 90
THE KLAWASI MUD VOLCANO GROUP SELF-POTENTIAL SURVEYS 92
FIGURE 5-1. 94
FIGURE 5-2. 95
FIGURE 5-3. 96
FIGURE 5-4. 97
FIGURE 5-5. 99
FIGURE 5-6. 100
FIGURE 5-7. 101
DISCUSSION OF SELF-POTENTIAL SURVEYS 102
FIGURE 5-8. 103
REFERENCES 104
CHAPTER 6 - AEROMAGNETIC SURVEYS OF PART OF THE EASTERN COPPER RIVER BASIN by Eugene M. Wescott 105
INTRODUCTION 105

DISCUSSION OF MAGNETIC RESULTS 105

CHAPTER 7 - SUMMARY AND RECOMMENDATIONS by Eugene M. Wescott and Donald L. Turner 109

FIGURE 7-1. 111

ACKNOWLEDGEMENTS 113

CHAPTER 1

SUMMARY AND EVALUATION OF GEOLOGIC, GEOCHEMICAL AND GEOPHYSICAL DATA RELEVANT TO GEOTHERMAL ENERGY EXPLORATION IN THE EASTERN COPPER RIVER BASIN, ALASKA

by

Donald L. Turner[1], Eugene M. Wescott[1] and Christopher J. Nye[2]

[1]Geophysical Institute
University of Alaska, Fairbanks
Fairbanks, Alaska 99701

[2]Earth Science Board
University of California
Santa Cruz, California 95064

INTRODUCTION

The Copper River Basin is an intermontane structural basin ranging from 150 to 1200 m (500 - 4,000 ft.) above sea level and rimmed by 1,370 to 5,000 m (4,500 - 16,500 ft.) peaks of the Alaska Range and the Talkeetna, Chugach and Wrangell Mountains. Rock units bordering the basin range in age from middle (?) Paleozoic to Tertiary and consist dominantly of schist, greenstone, graywacke, slate, shale and sandstone, locally associated with minor amounts of altered limestone, tuffs and basalt flows, and are intruded by a wide variety of igneous rocks. The Tertiary to Quaternary andesite lavas of the Wrangell Mountains form the eastern border of the basin. A generalized geologic map of the basin is shown in Figure 1.

Two groups of mud volcanoes occur in the basin. The Tolsona group consists of several gas seeps and four cones ranging in height from 25 to 60 ft. and occurring immediately north of the Glenn Highway, about 12 - 15 miles west of Glenallen. Three of these cones are active, and discharge methane and nitrogen, and water containing dissolved chlorides of sodium and calcium. The Drum group of three mud volcanoes occurs about 7 - 15 miles east of the Copper River, on the lower part of the western flank of Mt. Drum. These three cones range in height from 150 ft. (Lower Klawasi) to 310 ft. (Shrub). The three cones discharge CO_2 and warm NaCl and bicarbonate waters. The small size of all of these cones and their lack of included angular rock fragments suggest that they formed by gradual accretion of mud, rather than by explosive activity (Nichols and Yehle, 1961).

One or more of the Drum group of mud volcanoes may have been formed by hydrothermal activity, as possibly suggested by the geothermometry of their discharged waters. However, other non-thermal models can also be suggested for their formation, as will be discussed later. In general, the anticipated

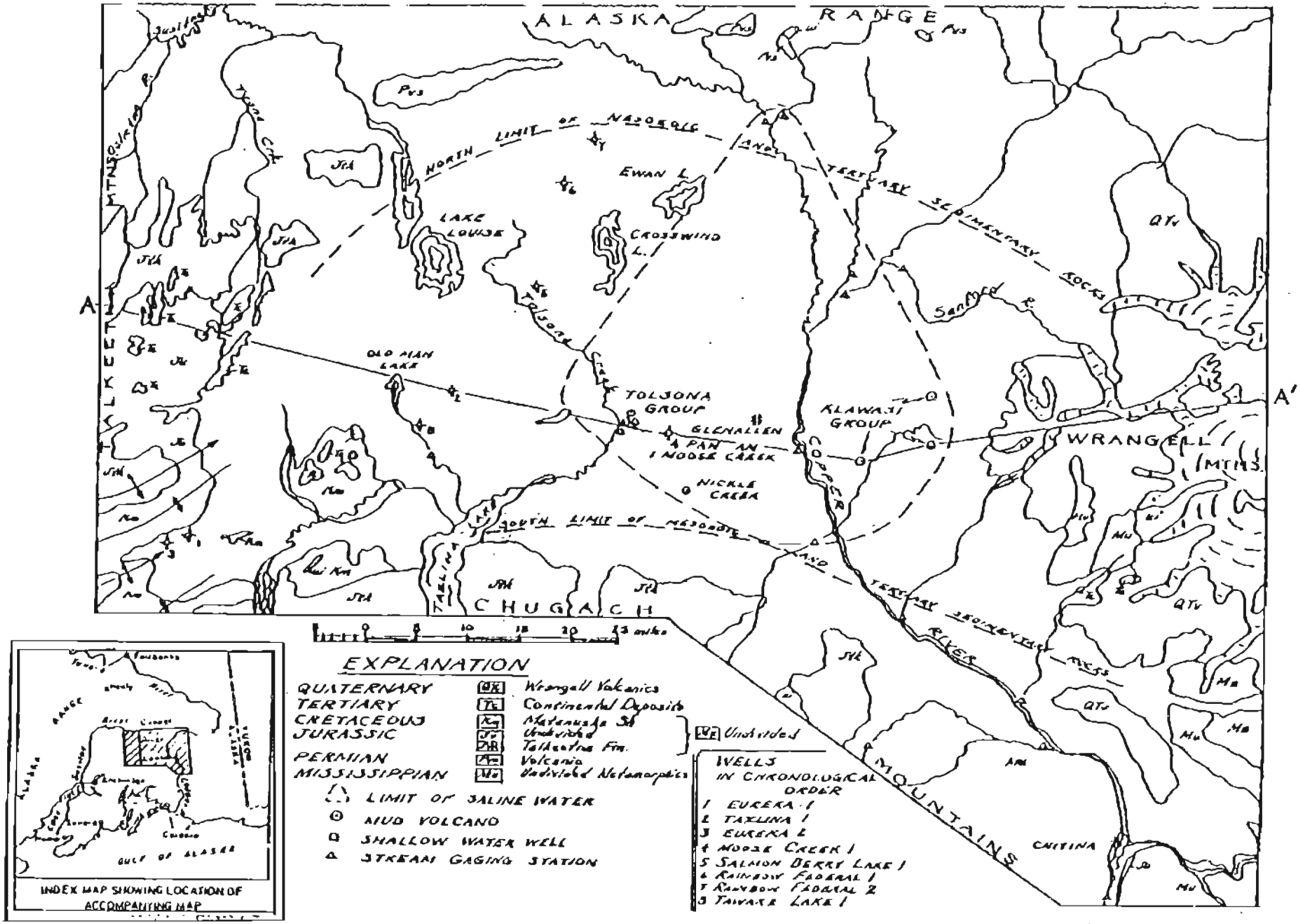

Figure 1-1. Generalized geologic map of the Copper River Basin (Foresman, 1970).

high heat flow in the region of the Wrangell volcanoes, the suspected presence of abundant subsurface acquifers in the basin, the inferred presence of subsurface impermeable lava flows and claystone beds which could serve as cap rocks, and perhaps the presence of the mud volcanoes themselves, all suggest that the easternmost part of the Copper River Basin is a promising area for geothermal energy exploration.

REGIONAL SETTING

The geographic setting of the Copper River Basin is shown in Figure 1. The Cenozoic topographic and structural basin covers 5,400 sq. mi. rimmed by 4,500 to 16,500 ft. mountain peaks. It is poorly drained; the impounded water resulting in numerous lakes, ponds and swamps connected by meandering streams and rivers. Exterior drainage is accomplished only by the Copper River which has incised a deep canyon through the Chugach Range to the south, and by the Oshetna River which combines with the Susitna River to cut through the Talkeetna Mountains to the west. The basin is barred from drainage to the north by low hills that form the south margin of the Alaska Range, and on the east by the great volcanic cones of the Wrangell Mountains.

Glacial, lacustrine and alluvial deposits which probably exceed 1,000 ft. where thickest cover the basin, effectively concealing older rocks (Mendenhall, 1905). There are, however, a few areally restricted outcrops of continental deposits of Eocene age. In the east part of the basin the Quaternary deposits are several hundred feet thick. The basin lies in the zone of discontinuous permafrost. Permafrost is probably present everywhere in the basin except beneath large lakes and major streams. It lies 1 - 2 ft. below the surface in some muskegs, 2 - 5 ft. in lacustrine and fine-grained glacial deposits and six to more than ten ft. in. granular alluvial and

glacial deposits. It generally ranges from 100 to 200 ft. thick, has a high ice content and is marginal in temperature, about -0.5 to -1.5°C. The permafrost is in a delicate state of equilibrium, and construction projects can result in considerable surface subsidence (Schultz and Smith, 1965).

Underlying most of the western part of the basin are Cretaceous shale and sandstone of the Matanuska Formation and semi-consolidated continental Tertiary sandstone and conglomerate with a few lignitic beds (Miller, et al., 1959). To the east, however, an aeromagnetic survey suggests that Tertiary lavas and Pleistocene unconsolidated deposits underlie a thin veneer of Quaternary cover, and extend at least as far west as the Copper River (Andreasen, 1964).

The northern margin of the basin is formed by isolated hills of Permian volcanic rocks that merge northward into mountains made up of basalt and andesite of Permian and Triassic age. The Wrangell Mountains bordering the east part of the basin are Tertiary-to-Quaternary volcanoes which have erupted vast amounts of andesitic lava over surrounding older rocks. The flows have slowly forced the channel of the Copper River westward until it now flows around the great volcanic massif in a huge arc. The hills bordering the southeast corner of the basin are formed of metamorphic rocks of Mississippian age. Metamorphosed sedimentary rocks of Mesozoic age are exposed in the hills at the extreme southeast margin of the basin.

THE WRANGELL VOLCANOES

Wrangell Mountains on the east side of the Copper River Basin are composed of an elongate massif of Neogene and Quaternary calcalkaline volcanoes. Of these volcanoes, Mt. Wrangell alone is still active, as shown by increased heat flux at the summit over the last 15 years and historic steam

and possible ash eruptions (Motyka et al., 1980). Since Mt. Wrangell is active it may mark the location of a significant heat source in the upper crust. Also, since Mt. Wrangell is roughly equidistant from the two major Alaskan population centers and is situated near existing transportation corridors it is uniquely suited as a potential major geothermal resource.

The Wrangell Mountains lie between a demonstrably transform boundary to the east and a classic arc-trench system to the west. The Wrangells are offset 240 km south from the main trend of the Aleutian-Alaska Peninsula volcanic arc. Seaward of the Wrangells lie the St. Elias and Chugach Mountains, which are large thrust-faulted ranges locally over 5600 m. high. The Wrangell Volcanics were erupted through an allochthonous terrain of Paleozoic and Mesozoic carbonates, fine clastics and pillow basalts which extends southward at least as far as Vancouver Island. This terrain has been named Wrangellia by Jones and others (1977). Wrangellia is thought to have been in its present position by the mid-Cretaceous (Jones and others, 1977), although the exact timing of suturing is not well constrained. Wrangellia's allochthonous nature probably has little bearing on the origin of rocks as young as the Wrangell Lava.

Previous work on the Wrangell volcanoes has been, with a few notable exceptions, of a reconnaissance nature. All areas underlain by the Wrangell Lava (a formational name given to young volcanic rocks of the Wrangell Mountains by Mendenhall in 1905) have been mapped at a scale of 1:250,000, in addition, Mt. Drum and several quadrangles to the north and northwest of Mt. Wrangell have been mapped more recently at 1:63,360. The few major element analyses reported with this mapping have emphasized that the Wrangell Lava is broadly typical of convergent margins. Field investigations coupled with K-Ar ages (Richter and Smith, 1976; Deininger and Turner, unpub. data) also show

that volcanism has occurred from Miocene through Pleistocene times. There are virtually uneroded volcanic edifices, Mt. Wrangell itself being the largest.

Two groups have done work relating to the total heat budget of specific volcanoes. Richter and others (1979) have mapped Mt. Drum at 1:63,360. They have documented a two cycle series of andesitic cone building followed by satellitic dacite dome emplacement. Using information from petrographic, geochemical and geochronologic studies, they suggested that a shallow magma chamber has been crystallizing since the volcano became extinct about a quarter of a million years ago. They estimate that about 8.4×10^{20} joules of thermal energy remain in the system (Smith and Shaw, 1979), thus making Drum one of Alaska's largest thermal reservoirs. It should be noted that this estimate is based on interpretations of volcanic plumbing and magma chamber size that are not clearly mandated by the available data.

Benson and coworkers at the University of Alaska have been carrying out glaciological research at Mt. Wrangell for nearly two decades (see Benson and Motyka, 1979, for a review). They are attempting to use the total ice budget of the mountain to estimate geothermal heat production. By knowing the net ice loss due to melting and ablation and the latent heat of the ice-water phase change, as well as the geothermal gradient of the few snow free areas, total heat flux can be measured. This is a labor and time intensive method which is frequently hindered by poor working conditions, but it should ultimately provide an accurate measure of heat flux. Estimates of an average of several hundred megawatts of heat production from the summit region alone over a period of a thousand years are indicated. Their detailed surveying and air photogrametry have also enabled them to accurately measure ice loss due to the surges in heat supplied to one of the postcaldera cones during the past 15 years.

Nye has spent ten weeks in two summers doing field work on Mt. Wrangell. The primary goal of the field work was to locate all exposures of flows derived from Wrangell and to infer stratigraphic relationships between these flows. A representative sample of over 150 flows and a few pyroclastic rocks have been collected from the morphologic Mt. Wrangell. K-Ar ages, preliminary major element concentrations and concentrations of Rb, Sr, Zr, Y, Nb, and Ni have been measured on selected samples. These data, in conjunction with previously published data and field observations, permit the following conclusions.

A major, previously unrecognized, pre-Wrangell volcano (informally named the Chetaslina vent) is partially buried under the southwestern flank of Wrangell volcano. A sample from the 2,300 m. level of the Chetaslina vent yielded K-Ar age of 0.98 ± 0.03 m.y., and samples from a thick sequence of superposed flows northwest of the Chetaslina glacier which may have been derived from this vent are as young as 0.42 ± 0.03 m.y. The eroded remnants of the Chetaslina vent are overlain by flows derived from Wrangell volcano. At the 2000 ft. level one of these flows yielded a K-Ar age of 0.08 ± 0.02 m.y. The Chetaslina vent and Wrangell volcano are, considering the nearly million year time span of activity, likely to represent two separate volcanic events. Because of their spatial proximity they will be referred to together as Mt. Wrangell. The presence of the Chetaslina vent indicates that a substantial part of Mt. Wrangell's volume is older than Wrangell volcano. Thus, Wrangell volcano, the youngest of the Pleistocene cones of the western Wrangells, is volumetrically smaller than it appears, and, depending on the volume of the Chetaslina vent buried under Wrangell volcano, may be substantially smaller than Mts. Drum, Sanford or Jarvis.

Dates from the Chetaslina vent are older than expected, and indicate that the major volcanoes of the western Wrangells are in large part coeval. Mt. Drum was active between 0.24 and 0.9 m.y. (Miller and others, ms. in prep.) Basal Mt. Sanford lavas yield K-Ar ages around 0.8 m.y. (Miller and others, ms. in prep.). Mt. Jarvis' activity embraced a time span including 0.75 ± 0.03 m.y. (this study) and 1.63 ± 0.42 m.y. (Richter and others, 1977).

Although age data from the south flank of Mt. Wrangell do not exist, the preliminary data suggest that the western Wrangells have not been built by construction of spatially and temporally separate volcanic centers. Instead, volcanism seems to have been dominant during the first half of the last million years, with several volcanoes active at once, and may have been dying out since that time.

If the preerosion shape of the Wrangell volcanoes is taken to be a simple cone with apex at the present (or inferred in the case of Mt. Drum) summit and edge at the apparent edge of the mountain then the volumes of the edifices may be readily calculated. All of the Pleistocene cones are of roughly the same dimension and have mean volumes three times greater than the largest of the Cascade volcanoes. The construction of these large, closely spaced volcanoes over the relatively short time span indicated by the radiometric ages suggests that the rate of edifice production in the Wrangells is about five times greater than that reported from other circum-Pacific volcanoes (30 km^3/m.y./km of arc length. This suggests that a quantity of heat vastly greater than normal was transported into the upper crust during this period.

The region around Mt. Wrangell is a likely target for geothermal exploration because it is the only active volcanic center with a location central to Alaskan population concentrations and transportation corridors. Mt. Wrangell is the last of an exceptionally voluminous group of Pleistocene

volcanoes and represents the waning of a major magmatic pulse. During the first half of the last million years, edifice production rates and presumably heat transport rates were an order of magnitude greater than elsewhere in circum-Pacific magmatic arcs. Some of this heat is expected to have been retained by shallow magma chambers which may have fed the prehistoric eruptions at the summit of Mt. Wrangell.

BASIN STRUCTURE AND STRATIGRAPHY

STRUCTURE

The Copper River Basin is both a structural and a topographic basin. Quaternary glacial and alluvial deposits and local continental deposits of Eocene age are present over most of the basin and conceal the older rocks. Pre-Eocene rocks form eastward-trending arcs that are concave south (Payne, 1955). These arcs have existed since Mesozoic and earliest Tertiary time. They are delineated by the strike of geologic contacts, faults and topographic features. Two arcuate belts of lower Jurassic and older rocks containing numerous plutonic bodies are called the Seldovia and Talkeetna geanticlines. These geanticlines trend eastward through the northern part of the Chugach Mountains and the northern half of the Copper River Basin, respectively. Between these geanticlines lies a belt of middle Jurassic to late Cretaceous marine sediments called the Matanuska geosyncline (Figure 1). These rocks trend into the Copper River Basin from the Matanuska Valley on the west and from the Chitina Valley on the southeast, but they are exposed at only a few places within the basin itself (Andreasen et al., 1964).

STRATIGRAPHY

Thus far, the only detailed stratigraphic studies of the basin are proprietary studies by various oil companies. However, two cross sections based on eight wells drilled to depths of approximately 2,800 to 8,800 ft. have been published by the Alaska Geological Society (Church et al., 1969). These sections cover the central, southern, and southeastern parts of the basin. The easternmost well, Pan American Moose Creek Unit No. 1, was drilled to a total depth of 7,869 ft. This well is located approximately 20 miles ENE of the Lower Klawasi mud volcano and about five miles east of the Tolsona group of mud volcanoes. It penetrated the following section:

0 - 920 ft.	Quaternary and Tertiary? (Note: Nichols and Yehle (1961) state that the southeast part of the basin, perhaps including the Tolsona group, is underlain by semi-consolidated Tertiary sandstone and conglomerate with a few lignite beds).
Unconformity	**********
920 - 4,125 ft.	U. Cretaceous - Matanuska Formation marine shales with occasional fine-grained sandstones.
4,125 - 4,820 ft.	Basal Upper Cretaceous - Basal Matanuska Formation fine-grained marine sandstones with minor interbedded shales.
Unconformity	**********
4,820 - 6,755 ft.	Lower Cretaceous Kennicott and possibly Nelchina Formations - marine shales with two fine-grained quartzose sandstone units in the lower middle portion of the drilled interval. The uppermost of these sandstones produced a water flow with methane, along with tar shows.
Unconformity	**********
6,755 - 7,869 T.D.	Upper Jurrasic Naknek and Chitina Formations - marine tuffaceous sandstones and shales.

The Middle Jurrasic Tuxedni Formation, consisting of marine shales and interbedded sandstones is believed to underlie the Naknek and Chitina Formations, based on subsurface extrapolations from deeper wells to the west.

Two additional wells have been drilled for the Ahtna Corp., by Amoco near Gulkana, about 12 and 15 miles, respectively, northwest of the Lower Klawasi mud volcano. Stratigraphic information from these wells is now in the public domain. The following information is available for these wells:

AMOCO Ahtna No. 1 - Sec. 18., T6N, R1W

Total Depth 7,941 ft.

Temp. at T.D. 138°F

Encountered "bedrock" at T.D.

1,080 ft.	Top of Matanuska Formation based on paleontology. Dominantly shale with some sandstone near base of section. No Nelchina Formation present.
6,710 ft.	Top of Jurassic based on paleontology. This is either Naknek or Talkeetna Formation. Sandstone composed of metavolcanic grains.
7,700 ft.	Basement - Talkeetna Formation massive greenstone. Density 2.7 to 2.8.

A slight gas show consisting almost entirely of methane, and a "fairly strong" water flow were encountered at 7,100 ft. The flow died out quickly and there was no indication of a highly overpressured zone as occurs in the Moose Creek well discussed above. The final shut in pressure was 3,220 psi, which is approximately equivalent to the formation pressure at the T. D. of 7,941 ft. This pressure gives a calculated pressure gradient of about 0.45 lbs./ft., essentially equivalent to the normal hydrostatic gradient. A thin coal bed was noted at 4,530 ft.

AMOCO Ahtna No. A-1 - Sec. 22, T5N, R1W

Total Depth - 5577 ft.

Temp. at T.D. - 118°F

Encountered "bedrock" at T.D.

710 ft.	Miocene sediments - clays, gravels, siltatone, shales.
1,020 ft.	Top of Matanuska Formation - mostly siltstone with a few sand layers.
4,864 ft.	Talkeetna Formation - primarily siltstone with a limestone layer from 5,025 to 5,045 ft. and some thin tuff layers.
5,575 ft.	Basement - probable greenstone with some quartzite.
From 2,100 to 2,300 ft.	There were natural gas shows and indications of carbons in the drilling mud. Near 2,337 ft. the hole collapsed and there was a salt water flow. The mud weight was increased from 8.9 to 15.6 pounds per gallon (81% of lithostatic pressure). Further salt water flow was indicated at 2,520 ft. where the mud weight was increased to 16 ppg.

MUD VOLCANOES

MORPHOLOGY

The two grups of mud volcanoes in the basin have been described in detail by Nichols and Yehle (1961) and Grantz et al. (1962). The morphology, surface water temperatures, and estimated discharge rates of these mud volcanoes are shown in the following table from Nichols and Yehle (1961).

In the Klawasi group (Figure 1) the Shrub and Upper Klawasi cones have drumlinoid profiles and are mantled by glacial drift consisting of coarse, gravelly sand and striated erratics up to 5 ft. in diameter. In contrast, Lower Klawasi has a nearly symmetrical cone which has no traces of glacial drift or glacio-lacustrine deposits. Lower Klawasi has clearly had cone-

building activity much later in time than the other two mud volcanoes in the Drum group as evidenced by large numbers of killed spruce trees standing.

In the Tolsona group (Figure 1) the Nickel Creek mud volcano is similar to the Shrub and Upper Klawasi cones, while the Shepard and Tolsona cones are miniature replicas of the Lower Klawasi cone. The Tolsona cones all lie below nearby strandlines from the glacial lake and are capped by probable glacio-lacustrine deposits. The low, broad shield-type cones of Lower Klawasi, Shepard, Tolsona No. 1 and Tolsona No. 2 have apparently developed during or after melting of the glaciers in the basin. However, the springs which built all of the mud volcanoes could be much older than the present cones.

GAS AND WATER ANALYSES

Gas and water analyses from the mud volcanoes and springs have been reported by Nichols and Yehle (1961) and Grantz et al. (1962). All gas samples from the Drum (Klawasi) group are dominantly carbon dioxide gases with minor amounts of nitrogen. The Tolsona group gases, however, have 48% or more methane and a negligible amount of CO_2, the remainder being largely nitrogen. These striking differences suggested to these authors that the gases are derived from entirely different sources, with the Tolsona group, probably being derived from buried marsh or coal deposits. Gas in the Drum group, however may emanate in part from volcanic sources, although their extremely high CO_2 content is enigmatic.

The water of the Drum group is also believed by Nichols and Yehle (1961) to possibly include a volcanic component. All of the spring waters analyzed are highly saline, but there are significant differences, most notably the relatively high bicarbonate content of the Drum group, along with their significantly higher silica, magnesium, sodium, potassium and boron content.

TABLE I

COMPARISON BETWEEN CERTAIN PHYSICAL CHARACTERISTICS OF MUD VOLCANOES, COPPER RIVER BASIN, ALASKA

	Mud Volcano	Diagrammatic cross-section N S	Approximate dimension * of cone: Base	Approximate dimension * of cone: Hgt.	Alt. * of crest	Approx. * diam. of "crater"	Surf. water temp., °F.	Est. water disch., gpm.
Drum Group	Shrub		3600 4200	310	2950	120	54	< ¼
	Upper Klawasi	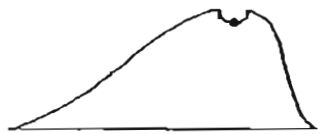	4200 6700	300	3017	150	86.5	2-5
	Lower Klawasi		6000 8200	150	1875	175	82	5-10
Tolsona Group	Nickel Creek		800 1000	60	2025	150	cold	< ¼
	Shepard		1300 1600	25	2172	15	—	—
	Tolsona No. 1		600 900	25	2045	30	38-55	< ¼
	Tolsona No. 2		2000 2300	40	2085	150	40-60	< ¼

* = in feet, • = active spring, ∘ = inactive spring.

(From Nichols and Yehle (1961))

Sulphate is also high at Lower Klawasi. The Tolsona group waters have consistently higher iron and calcium, and chloride is almost their sole anion.

Grantz et al. (1962) have shown that the highly saline waters that reach the surface in a large area of the Copper River Basin at about 1,000-3,000 ft. above sea level (Figure 1) are likely to have originated as connate formation waters in the Upper Cretaceous and older marine sedimentary rocks underlying the basin. They recognized two different types of saline waters: a Na-Ca-Cl or Tolsona type, and a Na-Cl-HCO_3 or Klawasi (Drum group) type, these waters emanating from the two groups of mud volcanoes discussed previously. The Tolsona type is relatively widespread in the basin, but the Klawasi type appears to be confined to the west slope of Mt. Drum.

ORIGIN OF THE MUD VOLCANOES

Abundant, unabraded Upper Cretaceous fossils in the mud at the Tolsona and Klawasi cone vents suggest that part of the cone-building material may have been derived directly from underlying Upper Cretaceous marine sediments at depth. Foresman (1970) has pointed out that the Tolsona and Klawasi cone deposits contain about 12 species which are also found in the Upper Cretaceous sections of two wells drilled in the basin.

In addition to the paleontologic data, Foresman (1970) has compared the water chemistry of the mud volcanoes with analysis of formation waters that flowed from a highly overpressured zone below 5,200 ft. depth in the Lower Cretaceous section of the Pan American Moose Creek Unit No. 1 well, located about four miles east of the Tolsona group of mud volcanoes. Figure 2 is a plot of pressure vs. depth in this well.

Tables 2 and 3 compare the chemistry of water from 6,074 ft. depth in the Moose Creek well with water from the mud volcanoes and with oil field brines.

The different chemistries of the two mud volcano groups suggest that they are composed, at least in part, of water of different origin. The Tolsona springs and the water from the Moose Creek well are very similar and lie in the middle range of oil field brines (Foresman, 1970). Foresman argues that the water chemistry similarities and the occurrence of the same fossils indicate that the Copper River Basin mud volcanoes are directly related to the abnormal pressures encountered at depth in the Moose Creek well. The Upper Cretaceous age of the fossils mantling the mud volcanoes vs. the Lower Cretaceous age of the strate of the overpressured zone in the Moose Creek well presumably suggests that these fossils were derived from overlying, younger strata by upward movement of mud from the underlying overpressured zone. He speculates that the zone of high pressure in the Cretaceous basin strata is a result of loading by the relatively young 12-16,000 ft. thick volcanic massif of the Wrangell Mountains. These relationships are shown diagramatically in Figure 3, a hypothetical cross section along line A-A^1 of Figure 1.

Foresman further speculates that the very large areal salinity anomaly in the basin (Figure 1) is caused by abnormal pressure forcing connate water from underlying marine sediments upward into the ground water table.

Foresman's arguments appear convincing for the origin of the Tolsona group of mud volcanoes, and may also, by analogy, explain the origin of the Drum group, although the data are not as convincing for the latter. Foresman does not discuss the effect of the loading of glacial ice (thickness ~ 1000 ft.) and the large pro-glacial ice lake that filled the Copper River Lowland during the last major glacial advance. Grantz et al. (1962) have suggested that the increased lithostatic pressure due to the weight of the ice and the

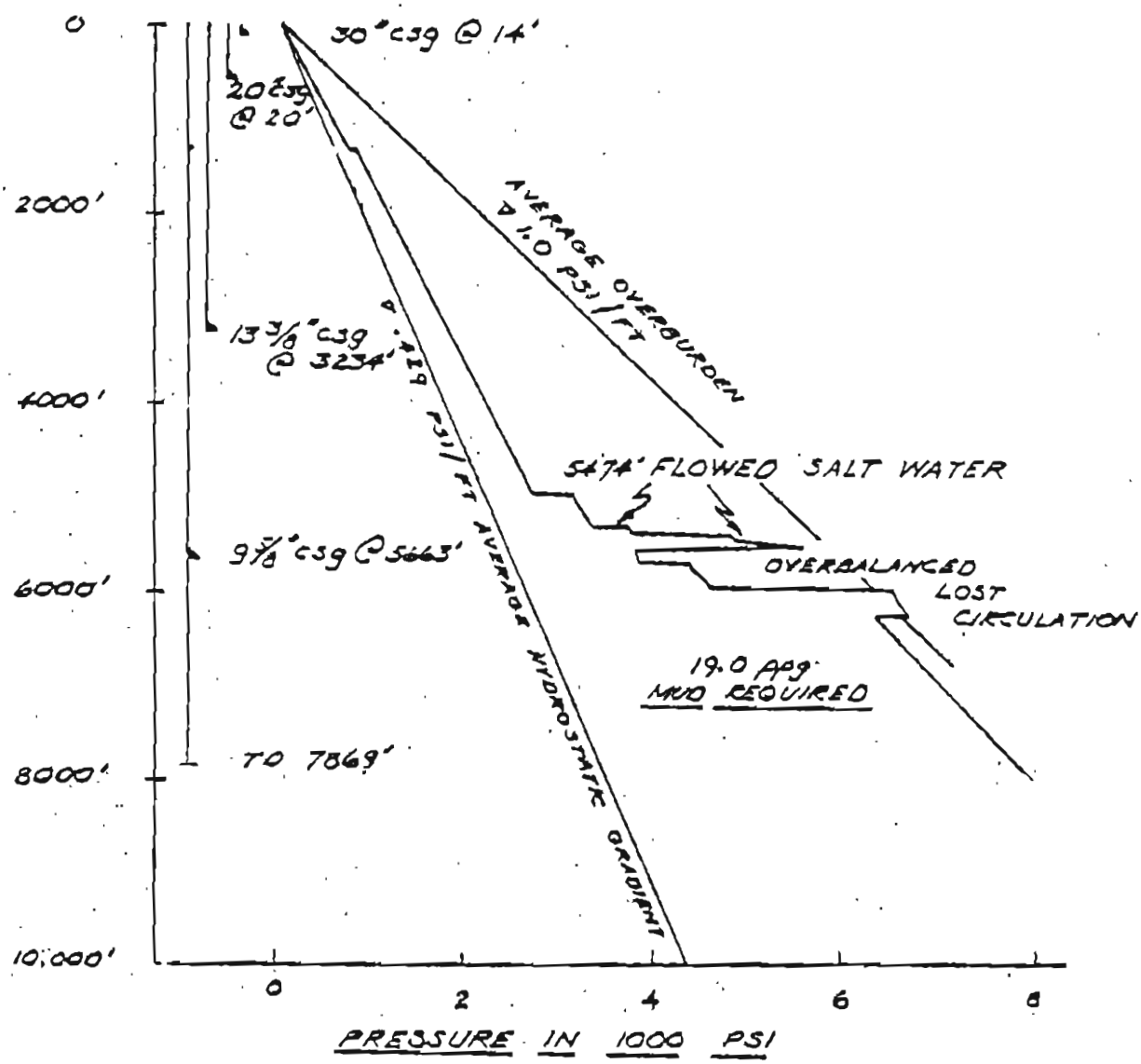

Figure 1-2. Pressure depth of Pan American 1 Moose Creek indicates top of abnormal pressures at 5200'. Pressures estimated to be 5750-6100 psi (Foresman, 1970).

TABLE 2. COMPARISON OF MUD VOLCANO AND GROUND WATER WITH FLUIDS ANALYZED AT 6075' IN THE MOOSE CREEK I, COPPER RIVER BASIN, ALASKA (Foresman, 1970)
(Chemical concentrations in parts per million)

	Klawasi Group			Tolsona Group		Ground Water			Moose Creek
Constituent	Shrub	Lower Klawasi	Nickel Creek	Tolsona No. 1	Tolsona No. 2	354-foot Well	Copper River Seep	Pan Am. I Inital Flow	Two Days after IF
SiO_2	65.00	132.00	10.00	16.00	7.10	19.00	-	-	-
Fe	0.04	0.03	0.67	0.26	-	2.20	-	-	-
Al	-	-	-	0.16	-	-	-	-	-
Ca	94.00	119.00	2,760.00	787.00	1,580.00	1,900.00	2,080.00	1,782.00	2,603.00
Mg	502.00	130.00	65.00	111.00	94.00	520.00	392.00	24.00	12.00
Na	9,390.00	10,400.00	2,600.00	4,600.00	4,000.00	1,150.00	670.00	4,059.00	3,871.00
K	275.00	433.00	24.00	60.00	26.00	44.00	-	-	-
Ba	-	-	-	-	14.00	-	-	-	-
Li	-	-	8.00	-	-	-	-	-	-
Mn	-	-	0.97	-	0.02	-	-	-	-
NH_4	11.00	-	-	5.60	-	-	-	-	-
Zn	-	-	-	0.02	-	-	-	-	-
CO_3	0.00	0.00	-	0.00	-	0.00	0.00	-	0.00
HCO_3	7,350.00	7,290.00	90.00	143.00	48.00	53.00	226.00	268.00	525.00
SO_4	0.00	666.00	230.00	0.00	5.50	0.00	60.00	378.00	742.00
Cl	12,000.00	12,500.00	9,100.00	8,870.00	9,450.00	6,470.00	5,680.00	9,042.00	9,752.00
F	0.40	-	0.40	0.30	-	-	-	-	-
Br	-	-	17.00	17.00	-	-	-	-	-
I	-	-	2.20	3.70	-	-	-	-	-
NO_3	5.50	-	-	0.70	-	-	-	-	-
B	120.00	-	-	35.00	-	-	-	-	-
PO_4	-	-	0.16	-	-	-	-	-	-
Dissolved solids	26,100.00	28,000.00	14,900.00	14,600.00	15,200.00	10,200.00	8,990.00	15,533.00	18,332.00
Hardness:									
Non carb.	0.00	0.00	7,080.00	2,310.00	4,280.00	6,840.00	6,620.00	-	-
Total	2,300.00	832.00	7,150.00	2,430.00	4,330.00	6,880.00	6,800.00	-	-

TABLE 3. COMPARISON OF CHEMICAL CONSTITUENT RATIOS OF WATER FROM THE COPPER RIVER BASIN (Foresman, 1970)

Ratios	Klawasi Group		Tolsona Group			Ground Water		Pan Am. I Moose Creek		Oil-field Brines Approx. Range
	Shrub	Lower Klawasi	Nickel Creek	Tolsona No. 1	Tolsona No. 2	354-foot Well	Copper R. Seep	Initial flow	Two days after IF	
HCo_3/Cl	0.6125	0.5832	0.00989	0.01612	0.00508	0.0082	0.0400	0.02964	0.05384	0.0001 -1.0
SO_4/Cl	0.00	0.05328	0.02527	0.00	0.000582	0.00	0.0106	0.41805	0.07609	0.00 -1.0
F/Cl	0.000033	-	0.000044	0.000034	-	-	-	-	-	0.00001-0.001
Br/Cl	-	-	0.001868	0.001916	-	-	-	-	-	0.0001 -0.01
I/Cl	-	-	0.000242	0.000417	-	-	-	-	-	0.00003-0.02
B/Cl	0.01	-	-	0.003945	-	-	-	-	-	0.00001-0.02
K/Na	0.0293	0.0416	0.00923	0.01288	0.0065	0.038	-	-	-	0.001 -0.003
Li/Na	-	-	0.00308	-	-	-	-	-	-	0.0001 -0.003
$\frac{Ca + Mg}{Na + K}$	0.0617	0.02299	1.0766	0.19025	0.4158	2.027	3.70	0.4494	0.6756	0.01 -5.0

lake may have increased the discharge of water and gas in the springs that build the mud volcanoes. These authors point out that the present cones may have attained most of their bulk during the later stages of the advance when the ice over these sites was relatively thin or gone, but while the Lowland was still subjected to the load of some ice and a large lake.

It appears that there are thus two plausible mechanisms for loading the Cretaceous sediments in the basin to produce an overpressured zone which may have given rise to the mud volcanoes - loading by the young Wrangell volcanic massif and loading by thick glacial ice and lake water. It is possible that either mechanism acting separately, or both acting together could have produced the mud volcanoes.

IMPLICATIONS OF THE MUD VOLCANOES FOR GEOTHERMAL EXPLORATION

Neither of the above mechanisms require a thermal drive to produce the mud volcanoes. It is therefore by no means certain that any of the mud volcanoes represent a good target for geothermal energy exploration. However, the existence of significant helium anomalies at both groups and the preliminary geothermometry from Lower Klawasi (Motyka, in prep.) indicate a reasonable possibility that this mud volcano may possibly overlie a geothermal reservoir.

In our preliminary report on the Copper River Basin, we recommended that adequate geophysical and geochemical surveys be carried out at Lower Klawasi to ascertain whether or not it represents a geothermal anomaly. We further recommended that a regional reconnaissance Helium soil gas survey be carried out on the east side of the basin in order to ascertain whether of not significant helium anomalies are present in areas beyond the mud volcanoes (Turner et al., 1982). Helium anomalies can help to define target areas for

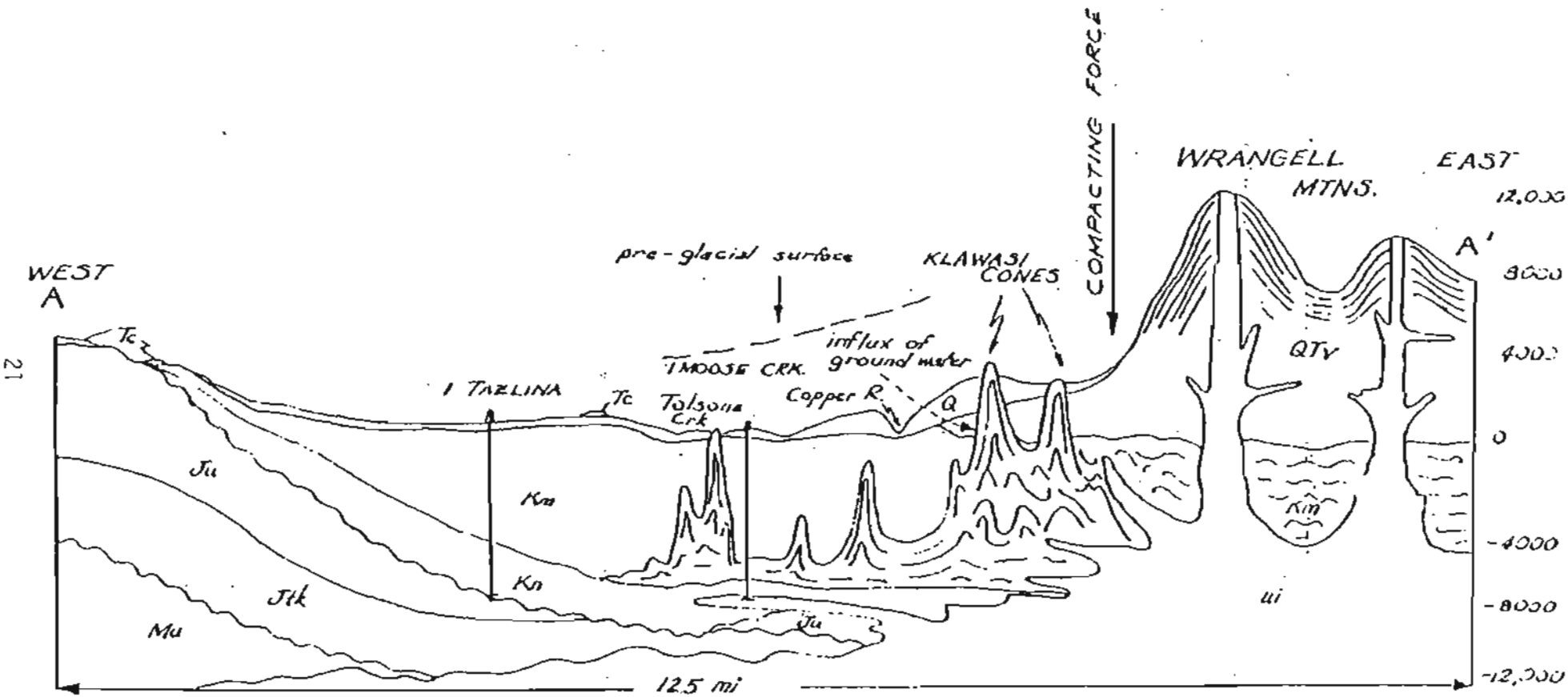

Figure 1-3. Diagrammatic cross section of the Copper River Basin showing the stratigraphy and the relationship of high pressure and mud volcanoes to compacting force. Vertical exaggeration by about 10X. (Foresman, 1970).

additional geophysical and geochemical work aimed at discovering geothermal reservoirs.

PREVIOUS GEOPHYSICAL AND GEOCHEMICAL SURVEYS

The Copper River Basin has been the subject of geophysical surveys by various oil companies, but these data are proprietary and not available to us.

The basin has been partially covered by aeromagnetic surveys. Andreasen et al. (1958) reported on aeromagnetic coverage north from the Chugach Mountains to 63°00'N with eastern and western boundaries of longitude 145°00'W and 147°20'W respectively. This area includes the Tolsona group and Lower Klawasi. Upper Klawasi and Shrub mud volcanoes are just outside this coverage. Additional aeromagnetic coverage to the south in the Valdez quadrangle is available as a USGS open file report. The USGS aeromagnetic map is printed over a generalized geologic map of the Copper River Basin (Andreasen et al., 1964).

There is a negative 44 gamma anomaly at Lower Klawasi mud volcano, elongated in the direction of Shrub. Although Shrub is off the edge of the aeromagnetic coverage it almost certainly is in an area of steep magnetic gradient. Upper Klawasi on the other hand is in an area of gentle gradient.

The USGS has done gravity mapping in the Copper River Basin. A 5 mgal contour map based on a survey by D.F. Barnes and others in 1958-60 has been published and discussed (Andreasen et al., 1964). A map with additional gravity values has also been supplied to us (D.F. Barnes, personal communication, 1981). There are many gaps in the coverage. B. Isherwood (personal communication, 1981) has made a fairly detailed gravity survey (223 stations) of the Mt. Drum area extending out to include the Klawasi mud

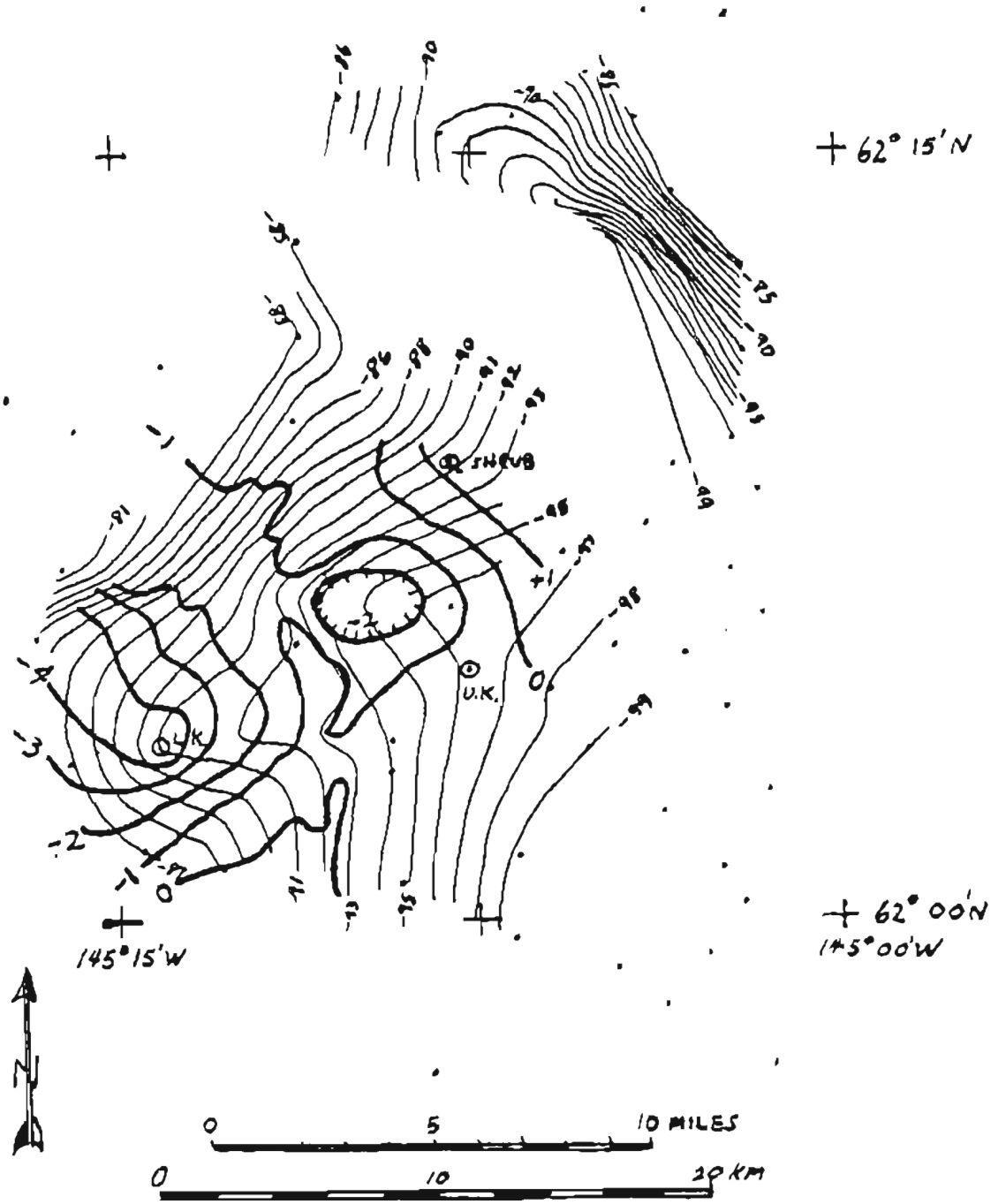

Figure 4. Corrected Bouguer anomaly map from data by B. Isherwood (personal communication, 1981). The thin lines are 1 mgal contours, thick lines are residual gravity after removal of regional gravity. Dots show stations (about one per 12 square miles). Mud volcanoes, Lower Klawasi (L.K.), Upper Klawasi (U.K.) and Shrub are shown. Note the 3-4 mgal negative anomaly at Lower Klawasi and the 2-3 mgal negative anomaly near the center of the L.K., U.K. and Shrub triangle.

volcanoes. The data have been made available to us in the form of computer printouts and 2 mgal simple Bouguer and terrain corrected Bouguer gravity anomaly maps. The station density in the vicinity of the Klawasi mud volcanoes is about one station per seven square miles. Isherwood's corrected Bouguer anomaly values have been plotted and contoured at 1 mgal intervals as shown in Figure 4 for the vicinity of the Klawasi group. There are insufficient stations northeast of Shrub to warrant contouring. There is an obvious regional gradient due to Mt. Drum. The heavy contour lines are the residuals after the regional gradient was removed graphically. There appears to be a negative 3-4 mgal anomaly associated with Lower Klawasi (L.K.) and an interesting negative 2-3 mgal anomaly centered in the triangle formed by Lower Klawasi, Shrub and Upper Klawasi. More detailed gravity surveys at one station per square mile in the area should make the relationship of these anomalies to the mud volcanoes or a geothermal system clearer.

Andreasen et al. (1964) have discussed in detail their geologic interpretation of the magnetic and gravity data in the Copper River Basin. The area including the Klawasi group has been called the Mt. Drum magnetic anomaly pattern. The pattern consists of a fanlike group of magnetic anomalies that project from the east edge of the surveyed area. They interpret the magnetic pattern "to be produced by andesitic lavas from the now extinct and dissected Mt. Drum volcanic cone". They considered the anomalies within the pattern to be unsuitable for quantitative depth analysis, but suggested that steep magnetic gradients in the center near the edge of the surveyed area near and north of Shrub indicate that lavas there are at or near ground surface. They suggest a depth to the lavas of perhaps 500 ft. near the rim of the pattern, e.g. under Gulkana and Gakona. However, volcanic flows were not encountered in the AMOCO Ahtna wells discussed previously.

Andreasen et al. (1964) interpret the gravity anomalies on the simple Bouguer anomaly map of Barnes et al. as suggesting that structures within the basin probably extend under the Wrangell Mountains where they are buried by Cenozoic lavas. All the gravity gradients associated with the Mt. Drum pattern are small, suggesting deep or gently sloping structures.

Andreasen et al. (1964) measured the densities of some Copper River Basin rock units as given in Table 4 below.

Table 4. - Densities of Copper River Basic rock units, in grams per cubic centimeter

Rock Group	Number of specimens	Density Minimum	Density Maximum	Density Average
Carboniferous and older	16	2.61	3.04	2.85
Permian and Triassic	2	2.93	2.98	[1]2.96
Jurassic and older volcanic rocks	38	2.29	2.83	2.64
Jurassic and Cretaceous sedimentary rocks	51	2.29	2.93	2.58
Intrusive rocks	15	2.38	2.76	2.61
Tertiary sedimentary rocks	11	1.90	2.56	2.30
Cenozoic volcanic rocks	2	2.66	2.69	[1]2.67

[1] Average based on only two specimens.

Densities from Amoco well logs are also available for gravity interpretations.

Andreasen et al. (1964) also reported on a few magnetic properties of hand specimens:

> "Magnetic properties of hand specimens from the Copper River Basin were examined qualitatively by placing them in the field of a Schmidt vertical magnetometer according to a modification of the method of Hyslop (1945). The induced magnetization exceeded the remanent magnetization of all except a few specimens of Jurassic and Carboniferous volcanic rocks and of Middle Murassic sandstone containing local concentrations of magnatite. Strong remanent magnetism is present in more parts of the Talkeetna Formation than in any other rock in the surveyed area, and magnetic susceptibility measurements for this formation also showed a wide range (from less than 0.0001 to more than 0.01 cgs unit). However, high values

and a wide range of magnetic susceptibility are also found in many specimens of Paleozoic volcanic rocks, intrusive rocks, and Tertiary volcanic rocks. Almost all specimens of Jurassic and Cretaceous marine and Tertiary continental sedimentary rocks have susceptibilities below 0.005 and values below 0.001 predominate."

More samples measured quantitatively are needed to make model calculations of the magnetic anomalies.

Well logs of various sorts are available from the petroleum and gas exploration wells which have been drilled on public land in the basin, as discussed under "Stratigraphy". The well logs and drillers log from Pan American Petroleum Corp. Moose Creek No.1 well Sec 29, T4N, R3W CR meridian are most informative. From 5277 ft. to 5517 ft. they encountered a high pressured zone which yielded artesian salt water and methane gas. There were also indications of tar in the section. As discussed by Foresman (1970), this overpressured zone is proposed as the source of the mud volcanoes. The theory appears to be most appropriate for the Tolsona group which lie about four miles west of the well.

The gases emanating from the Tolsona group are rich in methane (Reitsema, 1979). He suggests the Cretaceous Nelchina Formation as the likely source of the methane. This is consistent with the overpressured zone providing the energy for the eruptions. No source of heat is required to drive them. This explanation would also fit the Nickel Creek mud volcano and a spring 7.5 km SSW of Lower Klawasi mud volcano.

The gas from Tolsona group of mud volcanoes is also anomalously high in helium, ranging from 612 to 1,775 ppm. If the source of the methane is the overpressured zone in the Nelchina Formation, the gas reservoir might also serve as a trap for helium as well. The logs indicate a thick section of shale overlying the overpressured zone which might serve as an effective cap

for both methane and helium. If so, the high helium might not indicate a geothermal source for the water flowing from these cones.

The Klawasi group, however, are quite different. The gases are about 99.5% CO_2 with a helium content of 97 to 258 ppm. The helium content is anomalous with respect to the atmospheric value of 5.24 ppm but the significant parameter of the flux of helium through the soil is unknown for comparison with known geothermal areas. Soil gas measurements as a function of distance from the mud volcanoes will allow an assessment of the importance of helium concentration as an indicator of geothermal resources.

FIELD WORK PLAN

Field work was begun on June 15, 1982 and continued for two weeks with helicopter support. We conducted ground measurements of gravity, total magnetic field, self-potential profiles and helium soil gas concentrations. A contracted aeromagnetic survey was also flown.

Based upon our study of the existing data we believe that the western or Tolsona group of mud volcanoes are probably driven by an overpressured zone found near 5,500 ft. depth in Pan American Moose Creek #1 well. The zone produced methane which is the principal gas coming out of the Tolsona gorup. The eastern or Klawasi group of mud volcanoes have different water and gas chemistry, and may be driven by an overpressured zone or perhaps by a heat source. Previous gravity and magnetic data suggest the Klawasi group are underlain by volcanic flows and intrusives interbedded with and overlying sediments. Since the geothermometry of the Klawasi group is subject to different interpretations, we conducted a wider-ranging helium survey to look for evidence of geothermal areas beyond the mud volcanoes while still making detailed helium studies around the mud volcanoes, Lower Klawasi in particular.

GRAVITY

Two sets of gravity data are available from the USGS at this time. One set covers the eastern portion of the basin in detail to 2 mgal contours and includes the Lower and Upper Klawasi and Shrub mud volcano areas at about one station per 12 square miles. We have made extensive gravity measurements in the vicinity of the Klawasi mud volcanoes at about 1-2 stations per square mile to look for gravity anomalies. The second data set covers the whole basin, with less complete coverage. We have filled in many of the gaps with

our present survey. We have also collected hand samples for density measurements of Mt. Drum volcanics.

MAGNETICS

In 1982, DGGS contracted for an aeromagnetic survey of the area surrounding the Drum group of mud volcanoes and overlapping the previous coverage. We have completed a preliminary analysis of the data.

In addition, we made detailed ground magnetometer surveys of Lower Klawasi mud volcano. We also collected hand samples of representative Copper River Basin rock types for magnetic susceptibility measurements.

SELF-POTENTIAL SURVEY

Self-potential anomalies that appear to be related to geothermal activity have been reported from a considerable number of geothermal areas. Corwin and Hoover (1979) have reviewed case histories, theoretical and model studies and conclude that self-potential anomalies of 50 mV to over 2 V in amplitude may be generated by electrokinetic and thermoelectric coupling. We have run long self-potential survey lines to look for long period self-potential anomalies associated with geothermal resources. Expected anomalies due to streaming potentials generated by a mud volcano can, in theory, be modeled and differentiated from geothermal sources. Self-potential surveys are more likely to locate geothermal areas than the previously proposed transient electromagnetic technique research (Turner et al., 1982).

HELIUM SOIL GAS SURVEYS

Helium in soil gas has been shown to be an effective geothermal indicator in several regions of Alaska. Helium is also known to be present in the gases

emanating from the mud volcanoes. We have conducted Helium soil sample surveys in the vicinity of the mud volcanoes and a general reconnaissance survey of the eastern basin area to search for patterns of anomalies related to geothermal resources.

COPPER RIVER BASIN BIBLIOGRAPHY

Ager and Sims, 1981, Holocene pollen and sediment record from the Tangle Lakes area, central Alaska, Palynology, Alaska Glacial Map, 5:85-98.

Aliev, A.A., and Buniat-Zade, Z.A., 1966, Chemical composition of waters from the mud volcanoes of the Kyurovdag-Babazanan-Neftechalinsk anticlinal zone (The Prikurinskaya oil-gas province): Dokl. Akad. Nauk Azerbaidzh, S.S.R., v. 22, no. 1, p. 16-20 (In Russian); T. U. abstr. no. 70, 677.

Allen, D. R., 1968, Physical changes of reservoir properties caused by subsidence and repressuring operations: Jour. Petrol Tech. (Jan.) p. 23-29.

Andreasen, G. E., W. J. Dempsen, J. R. Henderson, F. P. Gilbert, 1958, Aeromagnetic map of the Copper River Basin, Alaska, U. S. Geol. Surv., Geophys. Investigations Map GP-156.

Andreasen, G. E., Grantz, A., Zietz, I., Barnes, D. F., 1964 Geologic interpretation of magnetic and gravity data in the Copper River Basin, Alaska: U. S. Geol. Survey Prof. Paper 316-H, 135-153 p.

Arnold, R., 1912, A petroleum gas volcano; the upheaval of an island off the coast of Trinidad: Petrol. World, London, 9, p. 129-131.

Arnold, R., and Macready, G. A., 1956, Island-forming a mud volcano in Trinidad, British West Indies: Am. Assoc. Petroleum Geologists Bull., v. 40, no. 11, p. 2748-2758.

Atwater, G. I., 1967, Origin of diapiric shale structures of South Louisiana (abs): Am. Assoc. Petroleum Geologists Bull., v. 51, no. 3, pt. 1, p. 452.

Athy, L. F., 1930, Denisty, Porosity and Compaction of Sedimentary Rocks: Am. Assoc. Petroleum Geologists Bull, v. 14, no. 1, p. 1-24.

Barnes, D., 1977, Preliminary Bouguer gravity map of Central Alaska: U. S. Geological Survey, open file report 77-168A.

Bell, J. S., and Shepherd, J. M., 1962, Pressure behavior in the Woodbine Sand in field case histories: Oil reservoirs, no. 4, Soc. Petr. Eng., A.I.M.E., p. 113-122.

Birchwood, K. M., 1965, Mud volcanoes in Trinidad: London, Inst. Petrol. Review, v. 19, no. 221, p. 164-167.

Boatman, W. A., Jr., 1967, Measuring and using shale density to aid in drilling wells in high-pressure areas: Journ. Petr. Tech., p. 1423-1429.

Bosworth, T. O., 1912, Birth of an island near the coast of Trinidad: Geological Mag., p. 159-163.

Bower, T. H., 1951, Mud flow occurrence in Trinidad, B.W.I.: Am. Assoc. Petroleum Geologists Bull., v. 35, no. 4, p. 908-912.

Cannon, G. E. and Craze, R. C., 1938, Excessive pressures and pressure variation with depth of petroleum reservoirs in the Gulf Coast region of Texas and Louisiana: Trans. A.I.M.E., v. 127, p. 31-38.

Chibber, H. L., 1943, Mud volcanoes, in Geology of Burma, Macmillan & Co., London, p. 79-86.

Corwin, R. F., and Hoover, D. B., 1979, The self-potential method in geothermal exploration, Geophysics, vol. 44 (2), p. 226-245.

Coulter, H. W., and Coulter, E. B., 1962, Preliminary geologic map of the Valdez-Tiekel belt, Alaska: U. S. Geological Survey Miscellaneous Geologic Investigations Map I-356, 1 sheet, scale 1: 96,000.

Dadashev, F. G., and Kravchinskii, Z. Ya., 1966, Concerning the geochemistry of the mud volcanic gases in the South Caspian Basin: Dokl. Akad. Nauk S.S.R., v. 167, no. 4, p. 906-909, (In Russian) T. U. abstr. no. 69, 184.

Dickey, P. A., Shriam, C. R., and Paine, W. R., (1968). Abnormal pressure in deep wells of southwestern Louisiana: Science, v. 160, no. 3828, p. 609-615.

Dickenson, G., 1953, Geological aspects of abnormal reservoir pressures in the gulf coastal region of Louisiana: A.A.P.G. Bull., v. 37, p. 410-432 (Orig. Publ. in Proceedings of Third World Petroleum Congress, The Hague, 1951).

von Engelhardt, W., and Gaida, K. H., 1963, Concenetration changes of pore solutions during the compaction of clay sediments: Jour. of Sed. Petr., v. 33, no. 4, p. 919-930.

Ferrians, O. J., Jr., 1963, Glaciolacustrine diamicton deposits in the Copper River Basin, Alaska, in Short Papers in Geology and Hydrology, 1963: U. S. Geological Survey professional Paper 475-C, p. C121-C125.

Ferrians, O. J., Jr., 1963, Till-like glaciolacustrine deposits in the Copper River Basin, Alaska (abs.): Geological Society of America Special Paper 73, p. 151.

Ferrians, O. J., Jr., 1965, Permafrost map of Alaska: U. S. Geological Survey Miscellaneous Geologic Investigations Map I-445, scale, 1:2,500,000.

Ferrians, O. J, Jr., 1966, Effects of the earthquake of March 27, 1964, in the Copper River Basin area, Alaska: U. S. Geological Survey Professional Paper 543-E, p. E1-E28.

Ferrians, O. J., Jr., 1971, Preliminary engineering geologic maps of the proposed Trans-Alaska Pipeline route, Gulkana quadrangle: U. S. Geological Survey open-file report, 2 sheets, scale 1:125,000.

Ferrians, O. J., Jr., 1971, Preliminary engineering geologic maps of the proposed Trans-Alaska Pipeline route, Valdez quadrangle: U. S. Geological Survey open-file report, 2 sheets, scale 1:125,000.

Ferrians, O. J., Jr., Kachadoorian, R., and Greene, G. W., 1969, Permafrost and related engineering problems in Alaska, U. S. Geological Survey Professional Paper 678, 37 p.

Ferrians, O. J., Jr., and Nichols, D. R., 1965, Copper River Basin, in Schultz, C. B., and Smith, H. T. U. (eds.), Guidebook for Field Conference F, Central and South-central Alaska: International Association for Quaternary Research, VII Congress, Lincoln, Nebraska Academy of Science, p. 93-114.

Ferrians, O. J., Jr., Nichols, D. R., and Schmoll, H. R., 1958, Pleistocene volcanic mudflow in the Copper River Basin, Alaska (abs.): Geological Society of America Bulletin, v. 69, p. 1563.

Ferrians, O. J., Jr., and Schmoll, H. R., 1957, Extensive proglacial lake of Wisconsin age in the Copper River Basin, Alaska (abs.): Geological Society of America Bulletin, v. 68, p. 1726.

Foresman, J. B., 1968, Photogeologic and geomorphic study of the Copper River Basin, Alaska, Surface Projects Section, Confidential report, Phillips Petrol. Co., Job. No. P-2094.

Foresman, J. B., 1970, Mud volcanoes and abnormal pressure Copper River Basin, Alaska, Thesis, University of Tulsa.

Foster, J. B. and Whalen, H. E., 1966, Estimation of formation pressures from electrical surveys -- offshore Louisiana: Jour. Petr. Tech., p. 165-171.

Frederick, W. S., 1978, Planning a must in abnormally pressured areas: World Oil, v. 164, no. 4 (March), p. 73-77.

Freeman, P. S., 1966, Extrusive shale masses: new Gulf Coast exploration frontier: 16th Ann. Gulf Coast Assoc. Geol. Soc. & Reg. A.A.P.G. Mtg. Paper, Abstr.: Bull, Amer. Assoc. Petrol. Geol., v. 50, no. 10, p. 2324-2325.

Freeman, P. S., 1968, Exposed middle Tertiary mud diapirs and related features in south Texas, in Diapirism and diapirs - Mem. 8, Am. Assoc. Petrol. Geologists, p. 162-182.

Gerdine, T. G., Copper and upper Chistochina rivers: scale, 1:250,000. Contained in "A geology of the central Copper River basin." Professional Paper No. 41.

Gerdine, T. G., and Witherspoon, D.C., Chitina and lower Copper River region; scale, 1:250,000. Contained in "The geology and mineral resources of a portion of the Copper River district, Alaska" Special publication of the U. S. Geol. Survey, Washington, Government Printing Office, 1901.

Gilbreath, J. A., 1968, Electric log characteristics of diapiric shale in Diapirism and diapirs - Mem. 8, Am. Assoc. Petroleum Geologists, p. 137-144.

Gorin, V. A., and Buniat-Zade, Z. A., 1967, Mechanism of formation of the south Caspian depression oil and gas deposits: U.S.S.R. All-Union Oil & Gas Genesis Symp. (Moscow) Proc. p. 539-544, (In Russian): T. U. abstr. no. 90,881.

Gorkun, V. N., and Siryk, I. M., 1967, Calculation of depth and volume of released gas during the eruption of mud volcanoes in southern Sakhalin: Geol. Geofiz. no. 2, p. 30-42, (In Russian): T. U. Abstr. no. 86,802.

Grantz, A., 1956, Possible origin of the placer gold deposits of the Nelchina area, Alaska (abs.): Geological Society of America Bulletin, v. 67, no. 12, pt. 2, p. 1807.

Grantz, A., White, D. E., Whitehead, H. C., and Tagg, A. R., 1962, Saline springs, Copper River lowland, Alaska: Amer. Assoc. Petroleum Geologists Bull., v. 46, no. 11, p. 1990-2002.

Handin, J., Hager, R. V., Jr., Friedman, M., and Feather, J. N., 1963, Experimental deformation of sedimentary rocks under confining pressure: Pore Pressure Tests, Am. Assoc. Petroleum Geologists Bull., v. 47, no. 5, p. 717-755.

Hedberg, H. D., 1936, Gravitational compaction of clays and shales: Amer. Jour. Sci. 5th Series, v. 31, no. 184, p. 241-287.

Higgins, G. E., 1959, Geophysics, Seismic velocity from Trinidad, B.W.I., and comparison with the Caribbean area, vol. XXIV, no. 3, p. 580-597.

Higgins, G. E., and Saunders, J. B., 1967, Report on 1964 Chatham mud island, Erin Bay, Trinidad, West Indies: Amer. Assoc. Petroleum Geologists Bull., v. 51, no. 1, p. 55-64.

Hill, G. A., Colburn, W. A., and Knight, J. W., 1961, Reducting oil finding costs by use of hydrodynamic evaluations: Economics of Petroleum Exploration, Development and Property Evaluation, Interntional Oil and Gas Educational Center, Southwest Legal Foundation, Prentice-Hall, Inc., p. 38-69.

Hottman, E. C., and Johnson, R. K., 1965, Estimation of formation pressure from log-derived shale properties: Jour. Petrol. Tech., p. 717-722.

Hyslop, R.C., 1945, A field method for determining the magnetic susceptibility of rocks: Am. Inst. Mining, Metall. Engineers Trans., v. 164, p. 242-246.

Jones, D.L., N.J. Solberling, and J. Hillhouse, 1977, Wrangellia - a displaced terraine in northwestern North America, Can. J. Earth Sci., V. 14, No. 11, p. 2565-2577.

Kachadoorian, R., Hopkins, D. M., and Nichols, D. R., 1955, A preliminary report of geologic factors affecting highway construction in the area between the Susitna and Maclaren Rivers, Alaska: U. S. Geological Survey open-file report, 74 p. (Administrative report, 1954, to Alaska Road Commission).

Kalinko, M. K., 1967, Mud volcanoes as a source of information on the composition of hydrocarbons, their quantity, and conditions of occurrence: Soviet. Geol., no. 7, p. 86-96, (In Russian); T. U. abstr. no. 96,201.

Karlstrom, T. N. V., and others, 1963, Surficial deposits of Alaska: U. S. Geological Survey Miscellaneous Geologic Investigations Map I-357, 2 sheets, scale 1:1,584,000.

Kubota, J., 1953, Reconnaissance soil survey of the Nelchina-Tazlina District, Alaska, a preliminary report: Unpublished manuscript in files of U. S. Geological Survey, 54 p. typescript, 17 figs., tables.

Kugler, H. G., 1933, Contribution to the knowledge of sedimentary volcanism in Trinidad: Jour. Inst. Petrol., Tech., v. 19, no. 119, p. 743-772.

Kugler, H. G., 1938, Nature and significance of sedimentary volcanism: Sci. of Petrol., v. 1, Oxford Univ. Press, p. 297-299.

Landes, K. K., 1959, Surface observations, seeps, in Petroleum Geology, 2nd ed., New York, John Wiley & Sons, p. 48.

Levorsen, A. I., 1954, The occurrence of petroleum; mud volcanoes, in Geology of Petroleum, San Francisco, W. H. Freeman Co., p. 19-23.

Link, W. K., 1952, Significance of oil and gas seeps in the world oil exploration: Am. Assoc. Petroleum Geologists Bull., v. 36, no. 8, p. 1505-1540.

Lowe, P. G., Mahlo, E., and Schrader, E. C., Copper River region; scale, 1:376,000. Contained in "A reconnaissance of a part of Prince William Sound and the Copper River district, Alaska, in 1898." Twentieth Ann. Rept., pt. 7, 1900, pp. 341-423.

MacGregor, J. R., 1965, Quantitative determination of reservoir pressures from conductivity log: Am. Assoc. Petroleum Geologists Bull., v. 19, no. 9, p. 1502-1511.

Mahlo, E., and Schrader, F. C., Prince William Sound, sketch map of; scale 1:376,000. Contained in "The geology and mineral resources of a portion of the Copper River district, Alaska."

Mamedov, A. M., 1967, On the origin of mud volcanoes: Dokl. Akad. Nauk Azerbaidzh. S.S.R., v. 23, no. 8, p. 47-53, (In Russian) T. U. abstr. no. 99433.

Mendenhall, W. C., 1903, The Chistochina gold field, Alaska. In Bull. No. 213, pp. 71-75.

Mendenhall, W. C., 1903, The mineral resources of the Mount Wrangell district, Alaska. Professional paper no. 15, pp. 1 71.

Mendenhall, W. C., 1905, Geology of the central Copper River region, Alaska, U. S. Geol. Surv. Prof. Paper 41, 133 p.

Mendenhall, W. C., and Schrader, F. C., 1903, Copper deposits of Mount Wrangell region, Alaska. In Bull. No. 213, pp. 141-148.

Military Geology Branch, U. S. Geological Survey, 1959, Terrain study of the Exercise Little Bear area, central Copper River Basin, Alaska: Office of the Chief of Engineers, U. S. Army, Engineer Intelligence Study 258, 50 p., 45 figs., 27 pls, scales 1:50,000 and 1:250,000 (Williams and others).

Military Geology Branch, U. S. Geological Survey, 1959, Terrain and construction materials, Denali area, Alaska: Office of the Chief of Engineers, U. S. Army, Engineer Intelligence Study 248, 56 p., 34 figs., 3 pls., scale 1:50,000 (Nichols and others).

Military Geology Branch, U. S. Geological Survey, 1959, Certain aspects of the engineering geology along the Glenn and Richardson Highways, Copper River Basin, Alaska: Office of the Chief of Engineers, U. S. Army, Engineer Intelligence Study 190, 20 p., 18 pls., scale 1:50,000 (Williams and others).

Military Geology Branch, U.S. Geological Survey, 1960, Terrain study of Delta River Region, Alaska: Office of the Chief of Engineers, U. S. Army, Engineer Intelligence Study 264, 46 p., 37 figs., 22 pls., scales 1:50,000 and 1:250,000 (Pewe).

Military Geology Branch, U. S. Geological Survey, 1960, Terrain study of the Exercise Willow Freeze area, Alaska: Office of the Chief of Engineers, U. S. Army, Engineer Intelligence Study 292 g 87 p., 61 figs., 21 pls., scales 1:50,000 and 1:250,000 (Ferrians and others).

Military Geology Branch, U. S. Geological Survey, 1961, Terrain study of Alaska: Office of the Chief of Engineers, U. S. Army, Engineer Intelligence Study 301, 12 maps, 12 tables on following subjects: climate, physiographic regions, soils, rock types, vegetation, water resources, state of ground, permafrost, cross-country movement, airfield and road construction, airborne operations, and terrain summary. Scale 1:2,500.000.

Military Geology Branch, U. S. Geological Survey, 1963, Basic terrain study, Gulkana, Alaska: Prepared for Defense Intelligence Agency, 6 sheets, scale 1:250,000 (Ferrians and others).

Military Geology Branch, U. S. Geological Survey, 1963, Basic terrain study, Valdez, Alaska: Prepared for Defense Intelligence Agency, 6 sheets, scale 1:250,000 (Nichols and others).

Miller, D. J., Payne, T. G., and Gryc, G., 1959, Geology of possible petroleum provinces of Alaska: U. S. Geol. Survey Bull. 1094, 131 p.

Morgan, J. P., Coleman, J. M., Gagliana, S. M., 1968, Mudlumps: diapiric structures in Mississippi delta sediments in Diapirism and diapirs - Mem. 8, Am. Assoc. Petroleum Geologists, p. 145-151.

Motyka, R., MacKeith, P., and Benson, C., 1980, Mt. Wrangell Caldera: Utilization of glacier ice to measure heat flow and infer thermal regime, EOS, V. 61, No. 6, p. 69.

Musgrave, A. W., and Hicks, W. G., 1968, Outlining shale masses by geophysical methods in Diapirism and diapirs - Mem. 8, Am. Assoc. Petroleum Geologists, p. 122-136.

Myers, Robert L., & Van Siclen, Dewitt, C., 1964, Dynamic phenomena of sediment compaction, Matagorda, Co., Texas: Trans. Gulf Coast Assoc. Geol. Soc., v. 14, p. 241-252.

Nichols, D. R., 1956, Permafrost and ground-water conditions in the Glennallen area, Alaska: U. S. Geological Survey open-file report 392, 18 p.

Nichols, D. R., 1960, Reconnaissance geologice strip map along part of Edgerton Highway, Valdez C-2 quandrangle, Alaska: Prepared for Bureau of Public Roads, Anchorage, Alaska.

Nichols, D. R., 1960, Slump structures in Pleistocene lake sediments, Copper River Basin, Alaska, in Short papers in the geological sciences, 1960: U. S. Geological Survey Professional Paper 400-B, p. B353-B354.

Nichols, D. R., 1961b, Analysis of gas and water from two mineral springs in the Copper River Basin, Alaska, in Short papers in the Geologic and Hydrologic Sciences: U. S. Geol. Survey Prof. Paper 424-D, p. 191-194.

Nichols, D. R., 1965, Glacial history of the Copper River Basin, Alaska (abs.): International Association for Quaternary Research, VII Congress, Boulder, Colorado, 1965 (Proceedings, v. 22), p. 360.

Nichols, D. R., 1965, Glacial history of the Copper River Basin, Alaska: Oral presentation before members of Field Trip F, International Association for Quaternary Research, VII Congress, typescript, 36 p.

Nichols, D. R., 1963, Origin of the course of the Copper River, Alaska (abs.): Geological Society of America Special Paper 73, p. 210.

Nichols, D. R., 1966, Permafrost in the Recent Epoch, in Permafrost International Conference, Lafayette, Indiana, 1963, Proceedings: National Academy of Sciences-National Research Council Publication 1287, p. 172-175.

Nichols, D. R., and Watson, J. R., Jr., 1955, Preliminary report on engineering permafrost studies in the Glenallen area, Alaska (abs.), in Science in Alaska, 1955 and 1956, Proceedings of the 6th and 7th Alaska Science Conferences, American Association for Advancement of Scineces, p. 89-90. Repr. in Geological Society of America Bulletin v. 66, p. 1706 (1955).

Nichols, D. R., and Yehle, L. A., 1961, Highway construction and maintenance problems in permafrost regions, in Proceedings 12th Annual Symposium on geology as applied to highway engineering, University of Tennessee Engineering Experiment Station Bulletin 24, p. 19-29.

Nichols, D. R., and Yehle, L. A., 1961, Analyses of gas and water from two mineral springs in the Copper River Basin, Alaska, in Short papers in the geologic and hydrologic sciences, 1961: U. S. Geological Survey Professional Paper 424-D, p. D191-D194.

Nichols, D. R., and Yehle, L. A., 1961, Mud volcanoes in the Copper River Basin, Alaska, in Raasch, G. O. (ed.), Geology of the Arctic: Toronto, University of Toronto Press, v. 2, p. 1063-1087.

Nichols, D. R., and Yehle, L. A., 1969, Engineering geologic map of the southeastern Copper River Basin, Alaska: U. S. Geological Survey Miscellaneous Geologic Investigations Map I-524, scale 1:125,000.

Nichols, D. R., and Yehle, L. A., 1980, Reconnaissance map and description of the Chetaslina volcanic debris flow (new name) SW Copper River Basin and adjacent areas, southcentral Alaska, scale, 1:250,000, Map MF-1209.

Pewe, T. L., 1961, Multiple glaciation in the headwaters area of the Delta River, central Alaska, in Short papers in the geologic and hydrologic sciences, 1961: U. S. Geological Survey Professional Paper 424-D, p. D200-D201.

Pewe, T. L., 1975, Quaternary geology of Alaska: U. S. Geological Survey Professional Paper 835, 145 p., 1 pl.

Reitsema, R. H., 1979, Gases of mud volcanoes in the Copper River Basin, Alaska, Geochimica et Cosmochimica Acta vol. 43, pp. 183-187, Pergamon Press Ltd.

Richter, D. H., Smith, R. L., Yehle, L. A., and Miller, T. P., 1979, Geologic map of the Gulkana A-2 Quadrangle, Alaska, U. S. Geological Survey, G. Q. 1520.

Richter, D. H., Matson, N. A., Jr., and Schmoll, H. R., 1973, Reconnaissance geologic map of the Nabesna A-1 quadrangle, Alaska: U. S. Geological Survey Miscellaneous Geologic Investigations Map I-807, scale 1:63,360.

Richter, D. H., Matson, N. A., Jr., and Schmoll, H. R., 1976, Geologic map of the Nabesna C-4 quadrangle, Alaska: U. S. Geological Survey Geologic Quandrangle Map GQ-1303, scale 1:63,360.

Richter, D. H., and Schmoll, H. R., 1973, Geologic map of the Nabesna C-5 quadrangle, Alaska: U. S. Geological Survey Geologic Survey Geologic Quandrangle Map GQ-1062, scale 1:63,360.

Richter, D. H., Smith, R. L., Yehle, L. A., and Miller, T. P. (in press), Geologic map of the Gulkana A-2 quandrangle, Alaska: U. S. Geological Survey Geologic Quandrangle Map GQ-1520, scale 1:63,360.

Richter, D.H., Smith, R.L., 1976, Geologic map of the Nabesna A-5 quadrangle, Alaska: U.S. Geological Survey Geologic Quadrangle Map GQ-1520, scale 1:63,360.

Ridd, M. F., 1970, Mud volcanoes in New Zealand: Am. Assoc. Petroleum Geologists Bull., v. 54, no. 4, p. 601-616.

Rohn, O., A reconnaissance of the Chitina River and the Skolai Mountains, Alaska. In Twenty-first Ann. Report., pt. 2, 1900, pp. 303-340.

Schmoll, H. R., 1961, Orientation of phenoclasts in laminated glaciolacustrine deposits, Copper River Basin, Alaska, in Geological Survey Research, 1961: U. S. Geological Survey Professional Paper 424-C, p. C192-C195.

Schmoll, H. R., 1963, Geologic strip map along the Slana-Tok Highway, Nabesna C-6 and D-6 quandrangles, Alaska: Prepared for Alaska Department of Highways.

Schrader, F. C., A reconnaissance of a part of Prince William Sound and the Copper River district, Alaska, in 1898. In Twentieth Ann. Rept. pt. 7, 1900, pp. 341-423.

Schrader, F. C., and Spencer. A. C., The geology and mineral resources of a portion of the Copper River district, Alaska. A special publication, Washington, Government Printing Office, 1901, pp. 1-94.

Scrope, G. P., 1872, Mud volcano (definition), in Glossary of Geology, Anmer. Geological Inst. 2nd ed., 1966, p. 194.

Shepherd, F. P., Dill, R. F., and Heezen, B. C., 1968, Diapiric intrusions in foreset slope sediments off Magdalena Delta, Colombia: Amer. Assoc. Petroleum Geologists Bull., v. 52, no. 11, p. 2197-2207.

Smith, R.L. and H.R. Shaw, 1979, Igneous-related geothermal systems, in Muffler, L.J.P., Ed., Assessment of geothermal resources of the United States -- 1978, U.S. Geol. Survey Circular 790, 163 p., p. 12-17.

Snead, R. E., 1964, Active mud volcanoes of Baluchistan, West Pakistan: Geographical Rev., v.14, no. 4, p. 546-560.

Stamp, D. L., 1934, Natural gas fields of Burma: Amer. Assoc. Petrol. Geol. Bull., v. 18, no. 3, p. 315-326.

Suter, H. H., 1952, Colonial geology and mineral resources: v. 3, no. 1, p. 18, Fig. 13.

Suter, H. H., 1960, The general and economic geology of Trinidad, B.W.I., appendix by G. E. Higgins, Her Majesty's Stationery Office, London.

Thompson, A. B., 1916, Oilfield Development and Petroleum Mining, p. 184.

Tkhostov, B. A., 1963, Initial Rock Pressures in Oil and Gas Deposits: Macmillan Co., Tranlated from Russian by R. A. Ledward, 118 p.

Turner, D.L., E.M. Wescott, and C.J. Nye, 1982, Summary of geologic geochemical and geophysical data relevant to geothermal energy exploration in the eastern Copper River Basin, Alaska, prelim. rept. to Ak. Div. of Geol. and Geophys. Surveys for RSA #82-5X-670, 47 p.

U. S. Geological Survey, 1979, Aeromagnetic map of part of Valdez Quadrangle, Alaska, U. S. Geol. Survey open file report 79-381, scale 1:250,000, contour internal 20 gammas.

Wallace, W. E., Jr., 1965, Abnormal pressures measured from conductivity or resistivity logs: S.P.W.L.A., The Log Analyst, v. 5, no. 4, p. 26-38.

Watson, J. R., Jr., and Nichols, D. R., 1955, Preliminary report on engineering permafrost studies in the Glenallen area, Alaska: Interagency Administrative Report to Bureau of Public Roads, Item 11, Research, p. 68-73.

Watts, E. V., 1948, Some aspects of high pressures in the D-7 zone of the Ventura Avenue field: A.I.M.E., Petrol. Trans. v. 174, p. 191-205.

Weeks, W. G., 1929, Notes on a new mud volcano in the see off the coast of Trinidad: Journ. Inst. Petrol. Technol., v. 15, p. 385-391.

Weller, J. Marvin, 1959, Compaction of sediments: Am. Assoc. Petroleum Geologists Bull., v. 43, no 2, p. 273-310.

White, D. E., 1955, Violent mud-volcano eruption of Lake City hot springs, northeastern California: Bull. Geol. Soc. Amer., v. 66, no. 9, p. 1109-1130.

White, D. E., 1957, Magmatic connate and metamorphic waters: Geol. Soc. America Bull., v. 68, p. 1659, 1682.

Williams, J. R., 1962, Field conference, southwestern Copper River Basin, Alaska, July 28-29, 1962: Unpublished field trip guide, 16 p. typescript.

Williams, J. R., 1970, Ground water in the permafrost regions of Alaska: U. S. Geological Survey Professional Paper 696, 83 p.

Williams, J. R., and Ferrians, O. J., Jr., 1958, Late Wisconsin and recent history of the Matanuska Glacier (abs.): Geological Society of American Bulletin, v. 69, no. 12, pt. 2, p. 1757.

Williams, J. R., and Ferrians, O. J., Jr., 1961, Late Wisconisin and recent history of the Matanuska Glacier: Arctic, v. 14, p. 82-90.

Williams, J. R., and Johnson, K. M. (in prep.), Surficial deposits map of the Valdez quadrangel, Alaska, in Albert, N. R. D., and Hudson, Travis (eds.), The United States Geological Survey in Alaska - Accomplishments during 1979: U. S. Geological Survey Circular.

Williams, J. R., and Johnson, K. M. (in compilation), Surficial deposits map of the Valdez quadrangle, Alaska: U. S. Geological Survey open-file report, scale 1:250,000.

Wilson, C. C., and Birchwood, K. M., 1965, The Trinidad mud volcano island of 1964 (Rept. of a demonstration to the Geol. Soc. London on 12 May, 1965): Geol. Soc. London Proc., no. 1626, p. 169-174.

Winkler and others, 1981, Folio of the Valdez quadrangle, Alaska, U. S. Geological Survey open file report 80-892-A, 2 sheets (Bedrock Geologic Map).

Witherspoon, D.C., Copper Nabesna, and Chisana rivers, headwaters of; scale, 1:250,000. Contained in "The geology of the central Copper River Basin." Professional Paper No. 41.

Wright, H. E., 1953, Glacial history of the Mentasta Mountains, southeastern Alaska Range (abs.): Geological Society of America Bulletin, v. 64, p. 1953 (also a typescript report on same subject).

Yehle, L. A., in press, Preliminary surficial geologic map of the Valdez C-1 quadrangle, Alaska: U. S. Geological Survey Miscellaneous Field Studies Map MF-1132, 1 sheet, scale 1:63,360.

Yehle, L. A., 1981, Preliminary surficial geologic map of the Valdez B-1 quadrangle, Alaska: U. S. Geological Survey Map MF-1364, scale 1:63,360.

Yehle, L. A., and Nichols, D. R., 1980, Reconnaissance map and description of the Chetaslina volcanic debris flow (new name), Southeastern Copper River Basin and adjacent areas, south-central Alaska, U. S. Geological Survey May MF-1209.

CHAPTER 2

A Helium Soil Survey in the Eastern Copper River Basin, Alaska

by

Donald L. Turner and Eugene M. Wescott

Characteristics and Sources of Helium

Helium is the second lightest known element with a specific gravity of 0.1381 (hydrogen is 0.0695 and air is 1). It has a molecular and atomic weight of 4 and is an inert, elemental gas with no known chemical compounds. Helium's low solubility in cold water, monatomic molecular structure, low cross-section capture coefficient, extremely light weight, chemical inertness and high diffusivity give it a unique advantage over other geochemical trace elements in that helium will always migrate from its source to the surface of the earth.

Helium is steadily generated by radioactive elements in rocks and minerals. This occurs when alpha particles (released by decay in the uranium and thorium isotope series) capture two electrons to form atoms of inert helium. Other sources of helium on earth, such as those due to primordial accumulations, cosmic radiation, meteorites, radioactive tritium decay, etc., do not contribute significantly to the total annual production.

Helium production differs considerably with respect to rock type due to variable radioactive element content. Anomalous concentrations of helium in soil gases have been found over radioactive ore bodies (Dyck, 1976). This source of surface helium flux non-uniformity is unlikely to be of importance in the Copper River Basin. Helium loss to the atmosphere is only about five percent of its rate of production, indicating that most of the helium produced is trapped within the earth in various ways. Helium movement through the geologic column is a complex combination of

fluid transport and gaseous diffusion. Studies have shown that the distance helium moves by diffusion is several orders of magnitude smaller than the distance moved in equal time by fluid transport.

Most petroleum reservoirs in the United States have significant concentrations of helium - greater than 100 parts per million (Dyck, 1976). Helium tends to migrate into traps that contain natural gas (methane). Leakage of helium from these traps will tend to produce non-uniform distributions of helium flux at the surface. For instance, helium would tend to leak around the edges of an impermeable cap rock and form anomalous concentrations around the cap outline. Permeable faults in proximity to gas traps would also serve as escape routes for helium. These sources of helium anomaly patterns are possible in a sedimentary basin such as the Copper River Basin and must be carefully considered in interpreting the results of our helium survey.

Helium is very unusual in that its solubility in water increases with temperature above 30°C (Figure 2-1 after Mazor, 1972). In a geothermal system, pressurized hot water will therefore be a very efficient scavenger of helium produced by radioactive decay of uranium and thorium contained in the rocks at depth. This scavenged helium will be released as the heated water rises towards the surface, cools and depressurizes. Since helium is highly mobile it will seek faults, fractures and pore spaces to rise to the surface above the geothermal system. Figure 2-2 is a schematic diagram showing how a geothermal reservoir acts as a local source of helium. Figure 2-3 illustrates that faults provide an easy path for helium as well as rising hot water (Figures after Pogorski and Quirt, 1981).

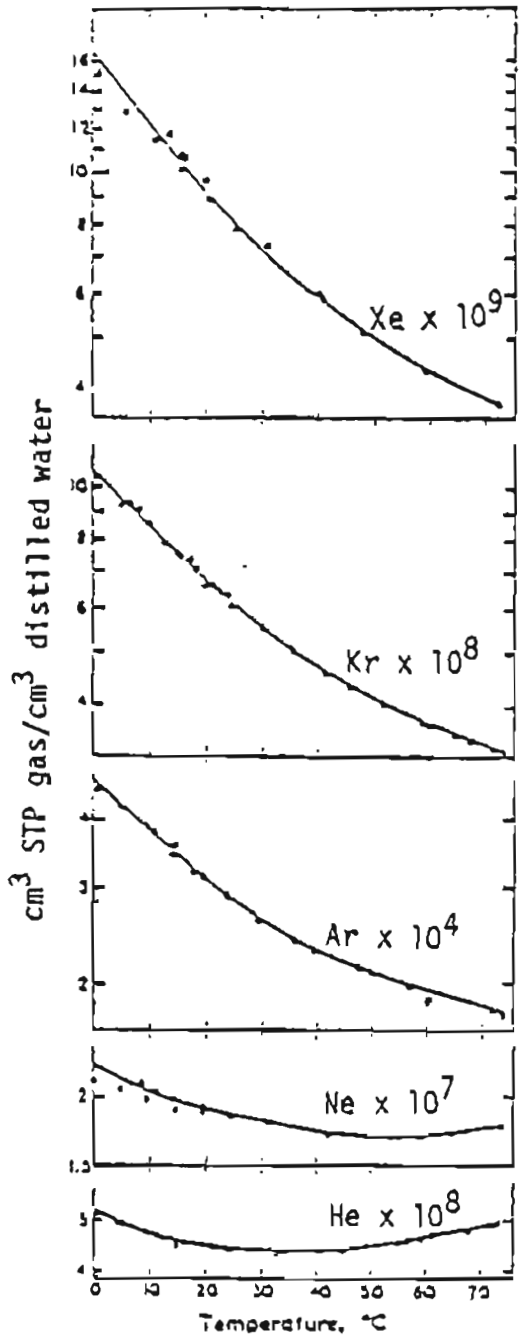

Figure 2-1. Solubility of noble gases in fresh water (after Mazor, 1972).

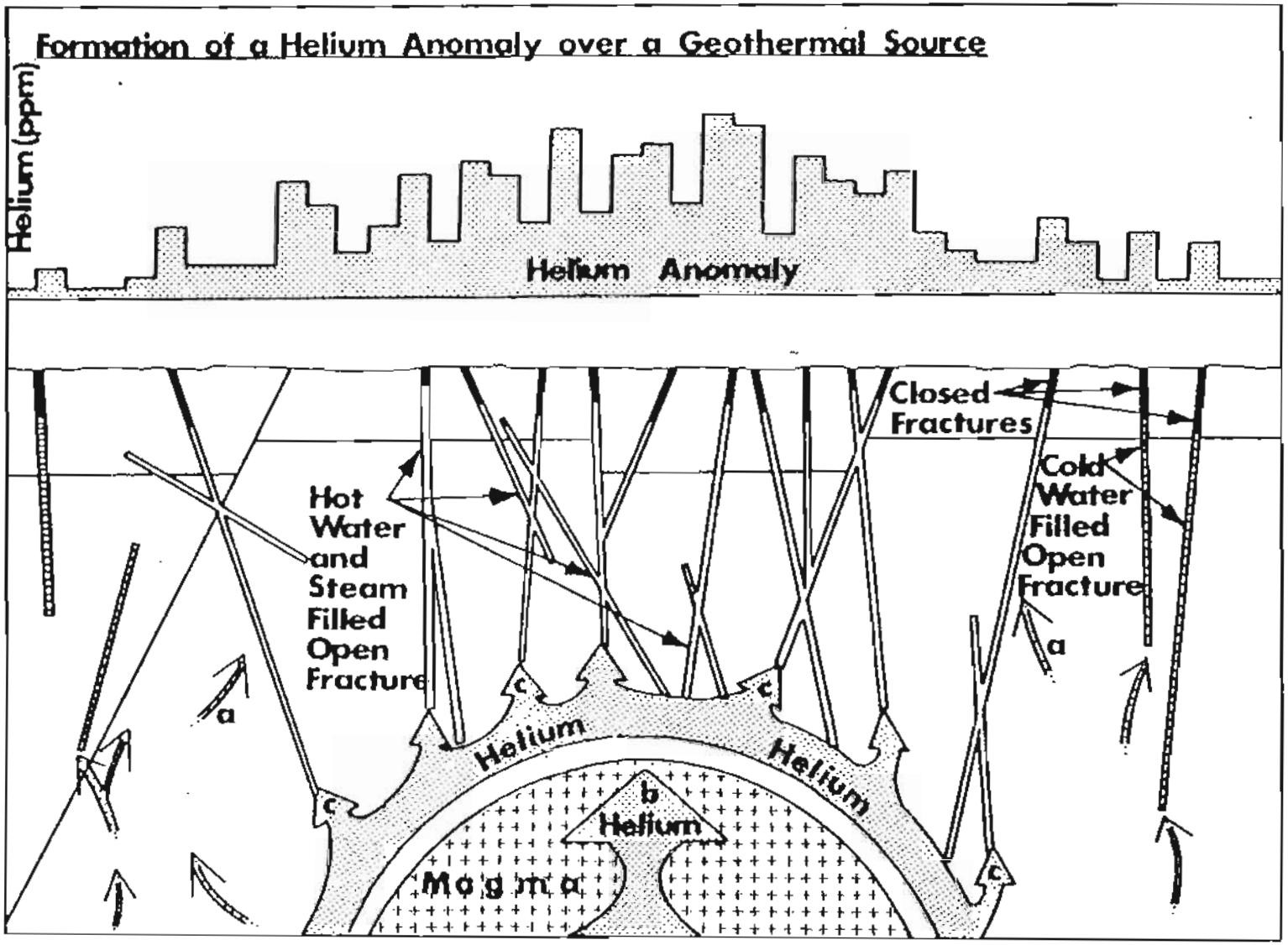

Figure 2-2. A schematic diagram illustrating that a geothermal reservoir acts as a local source of helium. In this diagram there are three sources of helium: (a) helium from the background flux; (b) helium from the magma heat source; and (c) helium scavenged by the hot geothermal waters. From Pogorski and Quirt (1980).

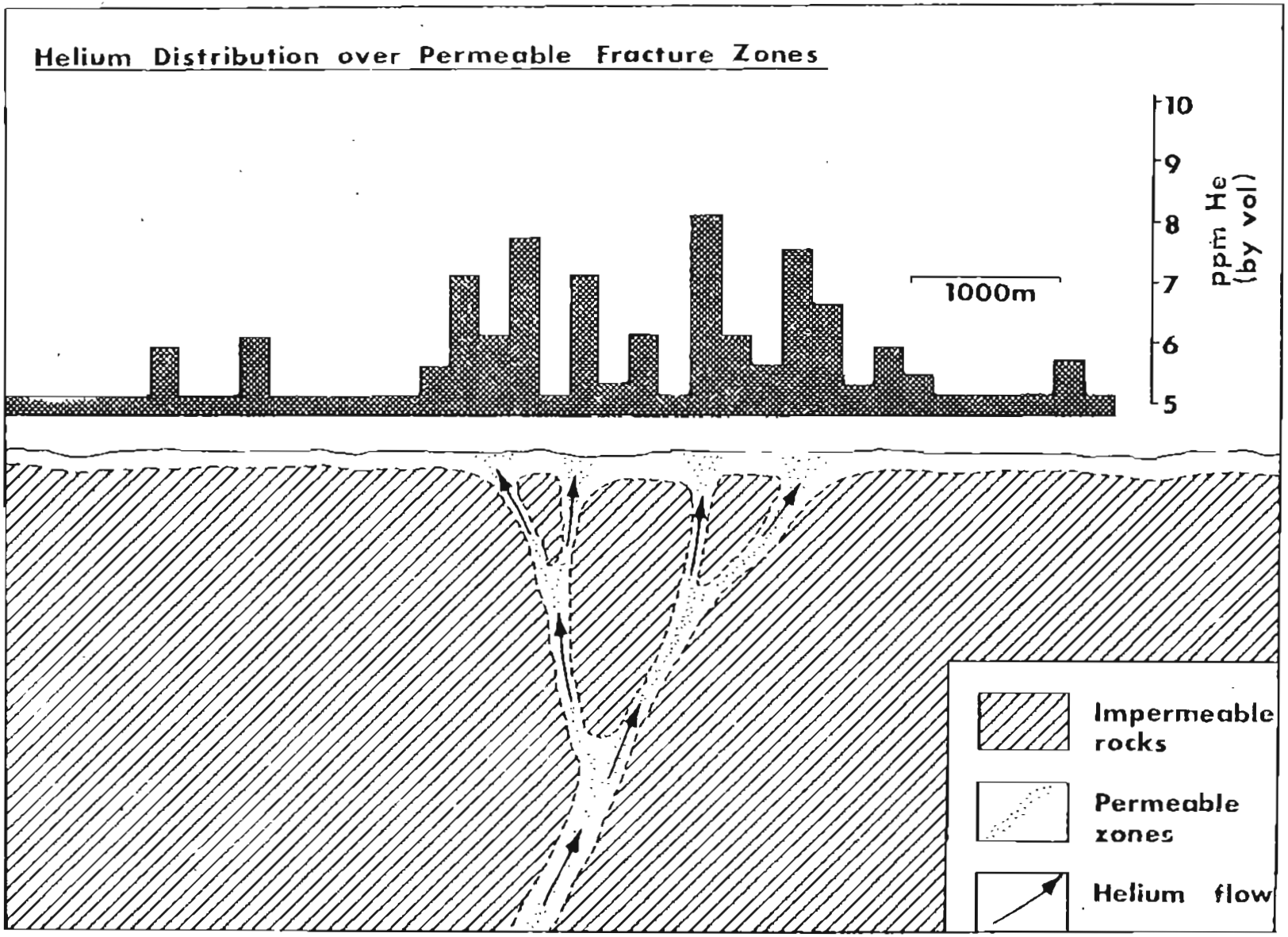

Figure 2-3. A schematic diagram illustrating that faults provide an easy path for helium migration from depth. From Pogorski and Quirt (1980).

The ability of helium to migrate away from its ultimate source of radioactive rocks and to accompany geothermal systems provides a convenient geochemical tracer. In fact it appears that helium might even be considered a direct trace element for geothermal reservoirs since elevated levels of helium are observed at most geothermal sites (Appendices A and B).

Exploration Techniques

Helium surveys have been developed and perfected as a time and cost effective, geothermal exploration method. The ability of helium to migrate long distances through the entire geologic column creates large-halo, helium anomalies which can be defined by water, soil and soil-gas sampling.

In addition to helium, many other techniques are used for outlining geothermal resource areas. The most common and direct approach has been with the use of surface heat flow mapping (not too reliable for deep reservoirs) and borehole temperature probing (expensive). These temperature methods are not generally used in an initial exploration phase, but rather as follow-ups to discoveries of hot springs, volcanic areas and subsurface (drill hole) temperature anomalies. Other techniques have evolved in the past several years to augment temperature gradient surveys in order to precisely define the ultimate heat source or fracture system. These include the usual literature search, photogeology and imagery, as well as isotope ratioing, chemical thermometry, surface/subsurface alteration studies, microearthquake monitoring, electrical surveying (e.g., resistivity and self-potential) and various other geophysical and geochemical methods.

However, when the heat source is deeply buried, as perhaps in the case of broad sedimentary basins with insulating rock layers, then many of these exploration methods can be costly and prohibitively time consuming.

Helium surveys provide a rapid sampling technique that can be used with minimum effort and at a very low cost. Samples can be collected as water, soil or soil gas and then analyzed for helium concentrations to better than 10 parts per billion in the gaseous sample by mass spectrometry. It is this precise analytic capability that only recently has permitted helium to be utilized as an effective trace element in geothermal exploration.

Due to helium's ability to escape from the geothermal system at depth, anomalies will be noted above fractures connected to the geothermal reservoir. This may be the only identifiable tracer, since precipitated calcite and silica may have effectively sealed the reservoir and prevented heavier elements from reaching the surface. Similarly, although there may be an active reservoir at depth, near surface temperature anomalies may be slight or even non-existent.

In the event that temperature anomalies are positive, they will usually coincide with helium anomalies, although there may be some offset e.g. Appendix A, Figure 1. This is a very significant correlation and gives the geothermal explorationist an additional method with which to define optimum drill sites for reservoir confirmation.

Regional helium surveys generally require a sample density of one to five samples per square mile. Detailed exploration is usually conducted with a 0.1 mile grid spacing, which can be followed up with sample spacing of 50 to 100 feet in the most anomalous zones. If an elongate reservoir is expected (such as a rift or parallel fault/fracture zone) the grid can be modified accordingly.

Sampling Methods

Figure 2-4 (after Pogorshi and Quirt, 1981) illustrates how helium occurs in soil, and indicates how it would be sampled. We sample the soil for

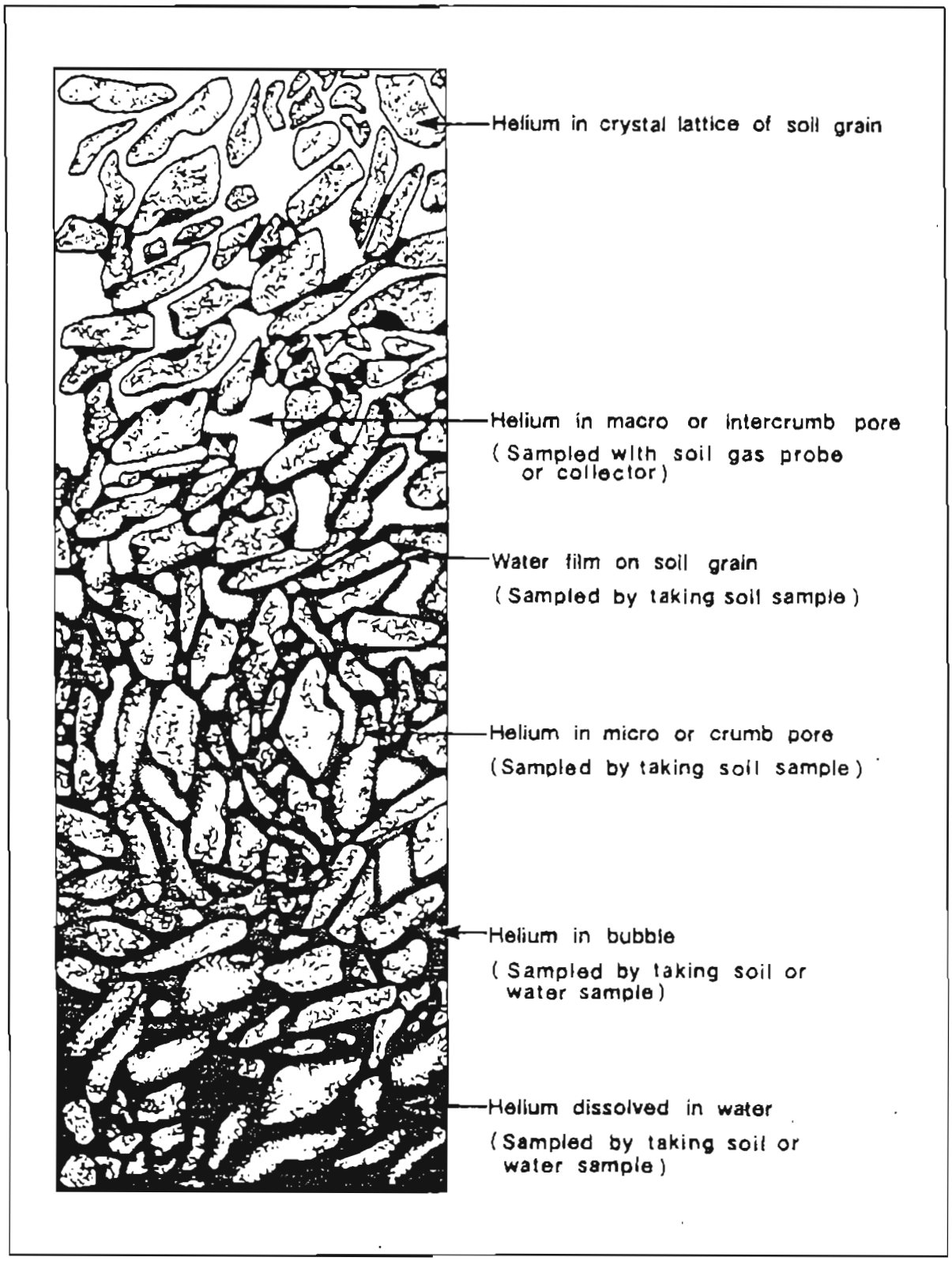

Figure 2-4. A schematic diagram showing how helium occurs in soil. From Pogorski and Quirt (1980).

helium in two ways: when the soil is dry and permeable, we drive a probe 3 feet into the ground and draw off a soil gas sample which is then inserted into a small evacuated steel ampule with a syringe and sealed for later analysis. This method does not work well in wet soil or where the soil is rocky or frozen. In such conditions we use a soil auger to drill a hole as close to 3 ft. depth as possible. The soil core from the bottom of the hole is then quickly placed in a steel can and sealed with a portable canner. Water in lakes and ponds below the thermocline can also be sampled for helium by collecting the water in a special bottle with a known fraction of air, shaking the sealed bottle to exsolve the helium, and drawing off a gas sample with a syringe. The gas in the syringe is then inserted into the same evacuated ampules used for soil gas, as described above. Normal atmospheric He concentration is 5.24 ppm, and any significant soil concentration above this represents an anomaly.

Hexco International, of Morrison, Colorado, performs the mass spectrometric helium analyses to a precision of 10 parts per billion. Hexco has provided us with very rapid analysis of samples mailed from the field site, with results often made available within one week of actual sample collection. This has allowed us to plan the second half of our field sampling program based on the results from the first half, and has resulted in the confirmation and extension of several anomaly areas which might have otherwise remained speculative.

We attempted to take helium samples on a one mile grid spacing, but lack of helicopter landing areas prevented sampling in many locations. Closer spaced sampling was done in areas of special interest, e.g., mud volcanoes and areas where our initial sampling produced positive results.

Results

A total of 144 samples were taken. Of these 113 were soil, 28 were soil gas and 3 were water. Sample locations are shown on Plate 1. Helium values for each sample are given in Table 1.

Permafrost was encountered in a large proportion of the sampling sites and the soil auger could generally not be driven to the desired 3 ft. depth. Because of this problem, frozen soil cores were generally taken from only 1 to 2 ft. depths. However, the many anomalously high helium results from holes ranging in depth from 0.5 to 1.5 ft. (Table 1) indicate that shallow soil cores in permafrost yield acceptable samples for helium analysis. Roberts (1981) also reported on helium surveys in permafrost areas of Alaska's north slope, and found good results sampling the permafrost.

The number of helium anomalies is surprisingly high, with 25% of the samples having > 5.4 ppm. Plate 1 shows several areas of anomalously high helium in the soil. There are definite, intervening areas of normal helium soil gas values (open circles) indicating a non-uniform source of the helium.

A number of helium concentration values below the atmospheric concentration of 5.24 ppm (Table 1) are believed to result from a flow of other gases such as methane and CO_2 diluting the helium gas fraction. In drawing the helium anomaly patterns of Plate 1, we have considered all values less than 5.24 to be equal to 5.24. In fact, some may actually be greater than 5.24 but we cannot determine the anomalous presence of other gases with our present sampling techniques.

We have carefully considered the source of the helium anomalies in the primary survey area (Plate 1). As previously mentioned, helium tends to

be trapped in the same areas as natural gas, and its diffusion from depth produces non-uniform concentrations on the surface. Gases from the Tolsona group of mud volcanoes contain high concentrations of methane and helium. Helium soil samples near the Tolsona mud volcanoes were also anomalously high (up to 9.15 ppm, Table 1). This evidence strongly suggests that the Tolsona group of mud volcanoes are caused by upward migration of mud, gas and water from a deep overpressured layer as discussed by Turner et al., Chapter 1.

However, the Klawasi group of mud volcanoes produce gas which is almost pure CO_2, with low concentrations of helium and methane. Helium is generally at background levels near these mud volcanoes. This argues against the observed anomaly patterns in our primary helium survey area (Plate 1) arising from non-uniform leakage of helium from natural gas traps. A more likely interpretation is that upwelling hot water rising in convection plumes or along faults is carrying the helium.

The several areas of anomalously high helium are consistent with the hypothesis that these areas may be underlain by hot water reservoirs. Although helium anomalies do not in themselves constitute proof that hot water is present, the fact that two of the major anomaly areas (3 and 5) are coincident with other geophysical anomalies strongly suggests a relationship to geothermal sources. This will be discussed more fully in the summary and recommendations chapter. The largest areas of anomalous helium (Anomalies 3 and 5, Plate 1) are on the west flank of Mt. Drum, about six miles east of the Copper River. One or both of these may represent meaningful drilling targets.

Perhaps more interesting in terms of their potential for near-term utilization, however, are the anomalies along the Richardson Highway,

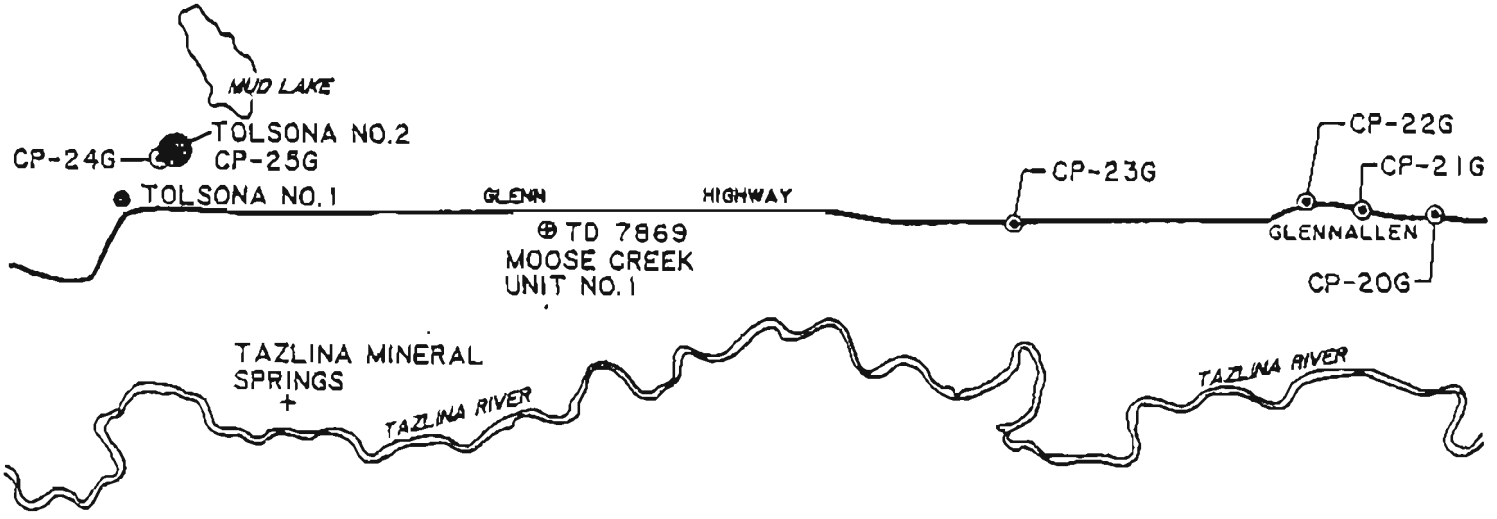

Figure 2-5. Helium soil gas samples along the Glenn Highway. Large black dot = 9.15 ppm. Open circles are normal background values. Samples 20 - 22 G taken in town of Glenallen.

from 4 to 10 miles north of Copper Center. These areas will be far cheaper to explore and develop because of their distribution along a major all-weather highway with an existing population vs. the much higher cost of exploration and development of resources located several miles on the other side of the Copper River. One of these areas (Anomaly 1, Plate 1) has three soil samples with helium values above background and contains the highest helium value in the entire area of the figure (6.15 ppm). The fairly extensive number of normal background value soil samples surrounding this anomaly area indicate that it does not extend significantly north or south, but it could possibly extend further to the east and west. The other two anomaly areas along the highway consist of single samples only, but are also encouraging sites for future study.

Reconnaissance helium surveying was continued along the highway to about 3 miles north of the Gulkana airport, but no additional positive anomalies were found. We also took three soil gas samples at Glenallen and one near Glenallen Lodge (Figure 2-5) with negative results. A significant helium soil gas anomaly was found at the Tolsonal No. 2 mud volcano (Figure 2-5), consistent with the high helium flux reported by previous workers and discussed by Turner et al. in Chapter 1.

Three hypothetical linear distributions of helium anomaly areas, labelled Lin. 1, 2 and 3, are shown on Plate 1. These hypothetical linears may be significant in that they appear to connect nearly all of the helium anomalies in the area, as well as the mud volcanoes and a mineral spring. One reasonable working hypothesis is that one or more of these linears may represent subsurface faults which serve as conduits for upwelling warm water and mud along portions of their lengths. The apparent distribution of anomalous features along these linears could

also be coincidental, but the linear distribution appears adequate to support the above hypothesis to be tested by future work. The proposed linears do not have any known surface expressions. They are, however, parallel to the long gravity trough that extends northeast across the area (see gravity chapter). If fault-controlled conduits are later shown to be present, they would represent important drilling targets to explore for deeper and hotter water than is likely to be present in near-surface reservoirs. This will be discussed more fully in the summary and recommendations chapter.

Table 1. Helium Data from Soil, Soil Gas and Water Samples

SAMPLE NO.	He (PPM)	SAMPLE TYPE	SAMPLE DEPTH (ft.)	SOIL TYPE
CB-3G	5.09	soil-gas	-	-
CB-5G	5.20	soil-gas	-	-
CB-7G	5.28	soil-gas	-	-
CB-13S	5.79	soil	-	-
CB-17G	5.13	soil-gas	-	-
CB-18S	5.20	soil	-	-
CP-1G	5.25	soil-gas	-	-
CP-2G	5.24	soil-gas	-	-
CP-3G	5.25	soil-gas	-	-
CP-4G	5.28	soil-gas	1.5	-
CP-5G	5.24	soil-gas	-	-
CP-6G	5.52	soil-gas	-	-
CP-7G	5.33	soil-gas	-	-
CP-8G	5.27	soil-gas	1.5	-
CP-9G	5.24	soil-gas	-	-
CP-10G	5.27	soil-gas	-	-
CP-11G	5.19	soil-gas	-	-
CP-12G	5.27	soil-gas	2.0	-
CP-13G	5.44	soil-gas	-	-
CP-14G	5.26	soil-gas	-	-
CP-15G	6.15	soil-gas	-	-
CP-16G	5.27	soil-gas	-	-
CP-17G	5.26	soil-gas	-	-
CP-18G	5.11	soil-gas	-	-

SAMPLE NO.	He (PPM)	SAMPLE TYPE	SAMPLE DEPTH (ft.)	SOIL TYPE
CP-20G	5.22	soil-gas	-	-
CP-21G	5.24	soil-gas	-	-
CP-22G	5.23	soil-gas	2.0	-
CP-23G	5.31	soil-gas	2.0	-
CP-24G	5.39	soil-gas	2.5	-
CP-25G	9.15	soil-gas	2.5	-
CP-26G	5.30	soil-gas	2.0	-
CS-1S	5.27	soil	-	clay
CS-2S	5.38	soil	-	clay
CS-3S	5.33	soil	-	mostly frozen
CS-4S	5.30	soil	-	sandy silt
CS-5S	5.29	soil	-	dry, friable
CS-6S	5.23	soil	-	sandy soil
CS-7S	5.30	soil	0.5	pebbly sand
CS-8S	5.43	soil	0.5	sand and rootlets
CS-9S	5.33	soil	-	friable sand
CT-1S	5.00	soil	-	silty clay
CT-2S	4.91	soil	-	silty clay
CT-3W	5.95	water	-	-
CT-4S	5.82	soil	-	silty clay
CT-5G	5.27	soil-gas	-	silty clay
CT-6S	5.07	soil	-	silty clay
CT-7S	4.54	soil	-	silty clay
CT-8S	4.95	soil	-	silty clay
CT-9S	4.97	soil	-	silty clay
CT-10S	5.15	soil	-	silty clay

SAMPLE NO.	He (PPM)	SAMPLE TYPE	SAMPLE DEPTH (ft.)	SOIL TYPE
CT-11S	5.15	soil	-	permafrost
CT-12S	5.66	soil	-	permafrost
CT-14S	5.27	soil	-	sandy soil
CT-16S	5.22	soil	-	-
CT-18S	5.26	soil	1.5	permafrost
CT-20S	5.28	soil	-	pebbly and sandy permafrost
CT-22S	5.66	soil	1.5	permafrost
CT-24S	5.21	soil	1.5	permafrost
CT-26S	5.20	soil	1.3	permafrost
CT-28AS	5.76	soil	-	clay
CT-28BS	5.05	soil	-	-
CT-30S	4.85	soil	-	pebbly and sandy
CT-32S	5.64	soil	-	-
CT-33S	5.35	soil	1.25	permafrost
CT-34S	5.81	soil	-	-
CT-35S	5.23	soil	-	permafrost
CT-36S	5.04	soil	1.5	permafrost
CT-37S	5.19	soil	2.5	silt
CT-38S	5.49	soil	1.5	clay
CT-39S	5.28	soil	1.0	frozen peat
CT-40S	5.26	soil	1.0	permafrost
CT-41S	5.30	soil	2.0	frozen clay with silt
CT-42S	5.21	soil	2.0	frozen clay with silt
CT-43S	5.39	soil	-	frozen peat
CT-44S	5.39	soil	1.5	silty permafrost
CT-45S	5.69	soil	1.0	frozen silty peat

SAMPLE NO.	He (PPM)	SAMPLE TYPE	SAMPLE DEPTH (ft.)	SOIL TYPE
CT-46S	5.29	soil	1.0	organic-rich silt
CT-47S	5.25	soil	1.25	frozen organic-rich silt
CT-48S	5.47	soil	1.0	frozen peat
CT-49S	5.23	soil	2.0	sand with 20% clay and silt
CT-50S	5.24	soil	1.0	silty permafrost
CT-51S	5.41	soil	1.0	frozen peat
CT-52S	5.22	soil	1.5	sandy silt
CT-54S	5.30	soil	2.0	very sandy
CT-55S	5.23	soil	2.0	slightly frozen silt
CT-56S	5.17	soil	2.0	slightly frozen silt with pebbles
CT-57S	5.16	soil	2.25	sandy silt
CT-59S	5.41	soil	1.0	frozen organic silt
CT-60S	5.23	soil	1.0	frozen organic silt
CT-61S	5.65	soil	0.84	frozen peat
CT-62S	5.73	soil	1.5	silty clay
CT-64S	5.27	soil	1.0	clayey silt
CT-65S	5.31	soil	1.0	silt
CT-66S	5.04	soil	2.0	silty sand with clay
CT-68S	5.61	soil	1.0	frozen organic mud
CT-69S	5.28	soil	1.25	partly frozen clayey silt
CT-70S	5.48	soil	1.5	dry clayey silt
CT-71S	5.64	soil	1.0	frozen organic-rich silt
CT-72S	5.16	soil	2.0	frozen clayey silt
CT-74S	5.69	soil	1.0	silty, sandy soil
CT-75S	5.57	soil	-	frozen organic muck
CT-76S	5.24	soil	0.84	frozen organic-rich silt

SAMPLE NO.	He (PPM)	SAMPLE TYPE	SAMPLE DEPTH (ft.)	SOIL TYPE
CT-78S	5.41	soil	2.75	sandy, clayey silt
CT-79S	5.03	soil	2.25	frozen clayey silt
CT-80S	5.37	soil	2.0	clayey silt
CT-81S	5.79	soil	1.5	frozen organic-rich silt
CT-82S	5.32	soil	1.5	sandy soil
CT-83S	5.76	soil	2.5	wet silty sand
CT-84S	5.60	soil	1.0	frozen silty peat
CT-86S	5.57	soil	1.0	frozen organic-rich silt
CT-87S	5.69	soil	0.84	frozen organic-rich silt
CT-88S	5.29	soil	1.5	barely frozen silt
CT-89S	5.05	soil	1.0	frozen silty clay
CT-90S	5.31	soil	2.5	clay
CT-91S	5.50	soil	1.5	frozen silt
CT-92S	5.31	soil	1.0	frozen silt
CT-93S	5.45	soil	1.25	dry sandy silt
CT-94S	5.19	soil	3.0	clayey silt
CT-95S	5.33	soil	1.0	wet silty sand
CT-96S	5.24	soil	2.0	wet sand with minor silt
CT-97S	5.94	soil	1.0	frozen sandy organic soil
CT-98S	5.35	soil	2.5	wet clayey silt
CT-99S	5.77	soil	2.0	wet sandy silt
CT-100S	5.31	soil	2.5	sand and silt
CT-101S	5.26	soil	2.5	clayey silt
CT-102S	4.94	soil	2.25	clay
CT-103S	4.72	soil	1.0	frozen silt
CT-104S	5.35	soil	1.0	clayey silt

SAMPLE NO.	He (PPM)	SAMPLE TYPE	SAMPLE DEPTH (ft.)	SOIL TYPE
CT-105S	5.26	soil	1.0	frozen silty peat
CT-106S	5.24	soil	2.5	sandy silt
CT-107S	5.37	soil	1.25	frozen organic silt
CT-110W	3.24	water	-	-
CW-1S	5.28	soil	-	-
CW-2W	3.00	water	-	-
CW-13S	5.21	soil	3.0	clay
CW-15S	5.23	soil	1.0	permafrost
CW-17S	5.45	soil	1.0	permafrost
CW-19S	5.28	soil	1.0	frozen silt
CW-21S	5.15	soil	0.5	frozen clayey silt
CW-23S	5.15	soil	-	clay
CW-25S	4.61	soil	-	partially frozen silt
CW-27S	5.28	soil	2.0	silt
CW-29S	5.20	soil	3.0	silt
CW-31S	5.27	soil	-	silty soil

APPENDIX B

References on the Use of Helium in Geochemical Exploration

Bagirov, V. I. et al. 1976, Developing Geochemical Methods for Marine Exploration of Oil and Gas: International Geology Review, v. 18, no. 5, pp. 560-562.

Ball, L. et al. 1979, The National Geothermal Exploration Technology Program: Geophysics, v. 44, no. 10, pp. 1721-1737.

Ball, N. L. and Snowdon, L. R., 1973, A Preliminary Evaluation of the Applicability of the Helium Survey Technique to Prospecting for Petroleum: Geological Survey of Canada, paper 73-18, pp. 199-202.

Bergquist, L. E., 1980. Helium Emanometry, an Energy Exploration Guide: Fiftieth Annual International Meeting and Exposition, Society of Exploration Geophysicists, Houston, Technical Papers, v. 5, pp. 2567-2578.

Bergquist, L. E., 1979, Helium, an Exploration Tool for Geothermal Sites: Transactions, Geothermal Resources Council, v. 3, pp. 59-60.

Bulashevich, Y. P. and Bashorin, V. N., 1973, On the Detection of Faults Along the Sverdlovsk DDS Profile from High Concentrations of Helium in Underground Water: IZV, Earth Physics, No. 3, 1973, pp. 185-189.

Cook, E., 1979, The Helium Question: Science, v. 206, no. 4423, pp. 1141-1147.

Craig, H. et al. 1978, Helium Isotope Ratios in Yellowstone and Lassen Park Volcanic Gases: Geophysical Research Letters, v. 5, no. 11, pp. 897-900.

Denton, E. H., 1977, Helium Sniffer Field Test, Roosevelt Hot Springs, Utah: U.S. Geological Survey, Open-File Report 77-606, 6 p.

Denton, E. H., 1976, Helium Sniffer Field Test, Newcastle, Utah, 10-26 March, 1976: U.S. Geological Survey, Open-File Report 76-421, 4 p.

Dyck, W., 1976, The Use of Helium in Mineral Exploration: Journal of Geochemical Exploration, v. 5, no. 1, pp. 3-20.

Golubev, V. S. et al. 1970, Some Characteristics of Migration of Helium in the Permeable Systems of the Upper Part of the Earth's Crust: Translated from Geokhimiya, in Geochemistry International, 1970, pp. 943-950.

Gutsalo, L. K., 1976, On the Sources and Distribution of Helium and Argon Isotopes in the Thermal Waters of the Kurile Islands and Kamchatka: Translated from Geokhimiya, no. 6, in Geochemistry International, v. 13, no. 3, pp. 167-175.

Gutsalo, L. K., 1976, On the Sources and Distribution of Helium and Argon Isotopes in the Thermal Waters of the Kurile Islands and Kamchatka: Geochemistry International, v. 13, no. 3, pp. 167-175.

Gutsalo, L. K., 1966, Importance of Groundwater Helium Saturation in Oil and Gas Prospecting: Translated (1970) from Izvestiya AN SSS$, Ser. Geologicheskaya, 31 (9) 111-116 (1966), through University of California, UCRL-Trans-10483.

Hinkle, M. E., 1978, Helium, Mercury, Sulfur Compounds, and Carbon Dioxide in Soil Gases of the Puhimau Thermal Area, Hawaii: U.S. Geological Survey, Open-File Report 78-246, 14 p.

Hinkle, M. E. et al. 1978, Helium in Soil Gases of the Roosevelt Hot Springs Known Geothermal Resource Area, Beaver County, Utah: Journal Research, U.S. Geological Survey, v. 6, no. 5, pp. 563-570.

Holland, P. W. and Emerson, D. E., 1979, Helium in Ground Water and Soil Gas in the Vicinity of Bush Dome Reservoir, Cliffside Field, Potter County, Texas: U.S. Department of the Interior, Bureau of Mines Information Circular IC 8807, 22 p. (A Case History).

Hunt, J. M., 1979, Petroleum Geochemistry and Geology, Published by W. H. Freeman and Company, San Francisco, Calif., 617 p.

Levinson, A. A., 1974, Introduction to Exploration Geochemistry, Published by Applied Pub. Co., Wilmette, Ill., 924 p.

Mast, R. F., 1978, U.S. Geological Survey Oil and Gas Resource Investigations Program, U.S. Geological Survey, Open-File Report 78-303, 81 p.

Mazor, E., 1977, Geothermal Tracing with Atmospheric and Radiogenic Noble Gases: Geothermics, v. 5, pp. 21-36.

Mazor, E. and Verhagen, B., 1976, Hot Springs of Rhodesia, Their Noble Gases, Isotopic and Chemical Composition: Journal of Hydrology, v. 28, pp. 29-43.

Mazor, E., 1975, Atmospheric and Radiogenic Noble Gases in Thermal Waters; Their Potential Application to Prospecting and Steam Production Studies: Proceedings, Second United Nations Symposium on the Development and Use of Geothermal Resources, pp. 793-802.

Mazor, E. and Fournier, R. O., 1973, More on Noble Gases in Yellowstone National Park Hot Waters: Geochimica et Cosmochimica Acta, v. 37, pp. 515-525.

Mazor, E., 1972, Paleotemperatures and Other Hydrological Parameters Deduced from Noble Gases Dissolved in Groundwaters; Jordan Rift Valley, Israel: Geochimica et Cosmochimica Acta, v. 36, pp. 1321-1336.

Moore, C. A. and Esfandiari, B., 1971, Geochemistry and Geology of Helium: in Advances in Geophysics, v. 15, pp. 1-57.

Naughton, J. J. et al. 1973, Helium Flux from the Earth's Mantle as Estimated from Hawaiian Fumerolic Degassing: Science, v. 180, pp. 55-57.

Nikonov, V. F., 1972, Formation of Helium - Bearing Gases and Trends in Prospecting for Them: Translated in International Geology Review (1973), v. 15, pp. 534-541.

Newton, R. and Round, G. F., 1961, The Diffusion of Helium through Sedimentary Rocks: Geochimica et Cosmochimica Acta, v. 22, pp. 106-132.

Palacas, J. P. and Roberts, A. A., 1980, Helium Anomaly in Surficial Deposits of South Florida, Possible Indicator of Deep Subsurface Petroleum or Shallow Uranium-Associated Phosphate Deposits: U.S. Geological Survey, Open-File Report 80-91, 14 p. (A Case History).

Panchenko, A. S., 1974, Positive and Negative Gas Hydrochemical Halos and Their Significance for Oil and Gas Prospecting: Translated from Izvestiya AN SSSR, in International Geology Review, v. 16, no. 3, pp. 259-262.

Pierce, A. P. et al. 1964, Uranium and Helium in the Panhandle Gas Field, Texas and Adjacent Areas: U.S. Geological Survey, Professional Paper 454-G, 56 p.

Pierce, A. P., 1960, Studies of Helium and Associated Natural Gases: U.S. Geological Survey Professional Paper 400-B, pp. 877-879.

Pierce, A. P., 1955, Radon and Helium Studies: Geologic Investigations of Radioactive Deposits, Semi-Annual Progress Report, U.S. Department of the Interior, TE1-540, pp. 233-237.

Pirson, S. J., 1969, Geological, Geophysical and Chemical Modifications of Sediments in the Environment of Oil Fields: in Unconventional Methods in Exploration for Petroleum and Natural Gas, Published by Southern Methodist University Press, Dallas, Texas, pp. 159-186.

Pogorski, L. A., and Quirt, G. S., 1981, Helium Emanometry for Hydrocarbons, Part I, in Unconventional Techniques in Exploration for Petroleum and Natural Gas, Southern University Press, Dallas, Texas, pp. 124-135.

Pray, H. A. et al. 1952, Solubility of Hydrogen, Oxygen, Nitrogen and Helium in Water at Elevated Temperatures: Industrial and Engineering Chemistry, v. 44, no. 5, pp. 1146-1151.

Reimer, G. M. et al. 1980, Helium Soil Gas Concentrations in the Torrington, Newcastle, Gillette (Wyoming) and Ekalaka (Montana) 1° x 2° Quadrangles; Data from a Reconnaissance Survey: U.S. Geological Survey, Open-File Report 80-452, 14 p. plus 4 plates. (A Case History).

Riley, G. H., 1979, Helium Isotopes in Energy Exploration: Bulleton, Australia Society of Exploration Geophysicists, v. 10, no. 3, pp. 234-236.

Roberts, A. A., 1979, Helium Emanometry for Hydrocarbons, II: in Unconventional Techniques in Exploration for Petroleum and Natural Gas, Southern Methodist University Press, Dallas, Texas. (A Case History), pp. 135-149.

Roberts, A. A. and Dalziel, M., 1976, A Possible Petroleum Related Helium Anomaly in Soil Gas, Boulder and Counties, Colorado: U.S. Geological Survey, Open-File Report 76-544, 7 p. plus 3 plates. (A Case History),

Roberts, A. A. et al. 1975, Helium Survey, a Possible Technique for Locating Geothermal Reservoirs: Geophysical Research Letters, v. 2, no. 6, pp. 209-210.

Roberts, A. A. 1975, Helium Surveys Over Known Geothermal Resource Areas in the Imperial Valley, California: U.S. Geological Survey, Open-File Report 75-427, 6 p.

Rosler, H. J. et al. 1977, Integrated Geochemical Exploration for Deep-Seated Solid and Gaseous Mineral Resources: Journal of Geochemical Exploration, v. 8, no. 1 & 2, pp. 415-429.

Thomas, D. M. and Naughton, J. J., 1979, Helium/Carbon Dioxide Ratios as Premonitors of Volcanic Activity: Science, v. 204, pp. 1195-1196.

Tiratsoo, E. N., 1967, Natural Gas, a Study: Scientific Press, London, pp. 32-36.

Tissot, B. P. and Welte, D. H., 1978, Petroleum Formation and Occurrence, a New Approach to Oil and Gas Exploration, Published by Springer-Verlag, Berlin, 538 p.

Tongish, C. A., 1980, Helium - Its Relationship to Geologic Systems and Its Occurrence with the Natural Gases, Nitrogen, Carbon Dioxide, and Argon: U.S. Department of the Interior, Bureau of Mines, Report of Investigations 8444, 176 p.

Weiss, R. F., 1971, Solubility of Helium and Neon in Water and Seawater: Journal of Chemical and Engineering Data, v. 16, no. 2, pp. 235-241.

Welhan, J. A. et al. 1977, Gas Chemistry and Helium Isotopes at Cerro Prieto, Scripps Institution of Oceanography, La Jolla, California.

Wescott, E. and Turner, D. (Editors), 1981, Geological and Geophysical Study of the Chena Hot Springs Geothermal Area, Alaska: A geothermal resource investigation by the Geophysical Institute, University of Alaska for the U.S. Department of Energy, Division of Geothermal Energy, 65 p., plus plates.

Yakutseni et al. 1969, Distribution of Helium in the Sedimentary Mantle and the Conditions of Formation of Economic Helium Deposits: Geokhimiya, no. 2, pp. 76-90.

Zarella, W. M., 1969, Applications of Geochemistry to Petroleum Exploration: in Unconventional Methods in Exploration for Petroleum and Natural Gas, Pub. by Southern Methodist Univ. Press, Dallas, Texas, pp. 29-41.

CHAPTER 3

Mercury Soil Sampling in the Eastern Copper River Basin, Alaska

by

Eugene M. Wescott

Introduction

Mercury content in soils has been reported as a possible geothermal resource indicator by Matlick and Buseck (1975). They confirmed a strong association of mercury (Hg) with geothermal activity in three of four areas tested (Long Valley, California; Summer Lake and Klamath Falls, Oregon). Mercury deposits often occur in regions containing evidence of hydrothermal activity, such as hot springs (White, 1967).

Mercury is highly volatile. Its high vapor pressure makes it extremely mobile, and the elevated temperatures near a geothermal reservoir tend to increase this mobility. The Hg migrates upward and outward away from the geothermal reservoir, creating an aureole of enriched Hg in the soil above a geothermal reservoir. Such aureoles are typically much larger in area than a corresponding helium anomaly.

Results

It was our original intention to test all the helium survey soil samples sent to Hexco International for mercury content. However, nearly all of these samples were lost in the mail on the return to Alaska. Only nine samples taken after the main field season in the area of helium anomaly #1 (Plate 1) west of the Copper River were returned. We tested those samples, as well as a sample of lower Klawasi mud, for Hg content as shown in Table 1. A Jerome Instruments gold foil mercury detector was used to analyze the soil samples.

There is no standard background level for mercury in soils. This must be established for an area independently. The average of the ten

samples was 31.2 parts per billion (ppb). Three samples were well above average, three were near average, and three were well below average. Figure 3-1 shows the area of helium anomaly #1 with the sample locations and symbols showing the relative Hg values.

The three above-average samples are located in line with and west of the helium anomaly. The sample of lower Klawasi mud was about average at 30.8 ppb. It appears from our small number of samples that there may be significant mercury variations, but the background level may be actually lower or higher than the average of 33.9 ppb. These samples are too few in number to allow firm conclusions to be drawn.

Table 1

Mercury Values

Sample #	Hg (ppb)
CS 1S	67.0
CS 2S	37.0
CS 3S	42.0
CS 4S	21.4
CS 5S	10.7
CS 6S	30.8
CS 7S	16.1
CS 8S	29.5
CS 9S	26.8
L. Klawasi	30.8
Average	31.2

Figure 3-1. Mercury soil concentrations in the vicinity of helium anomaly area #1. Helium values are shown by open circles (background) small solid circles (greater than 5.4 ppm) large solid circles (greater than 6 ppm). Mercury values are shown by small x's (less than average) and by large x's (greater than average).

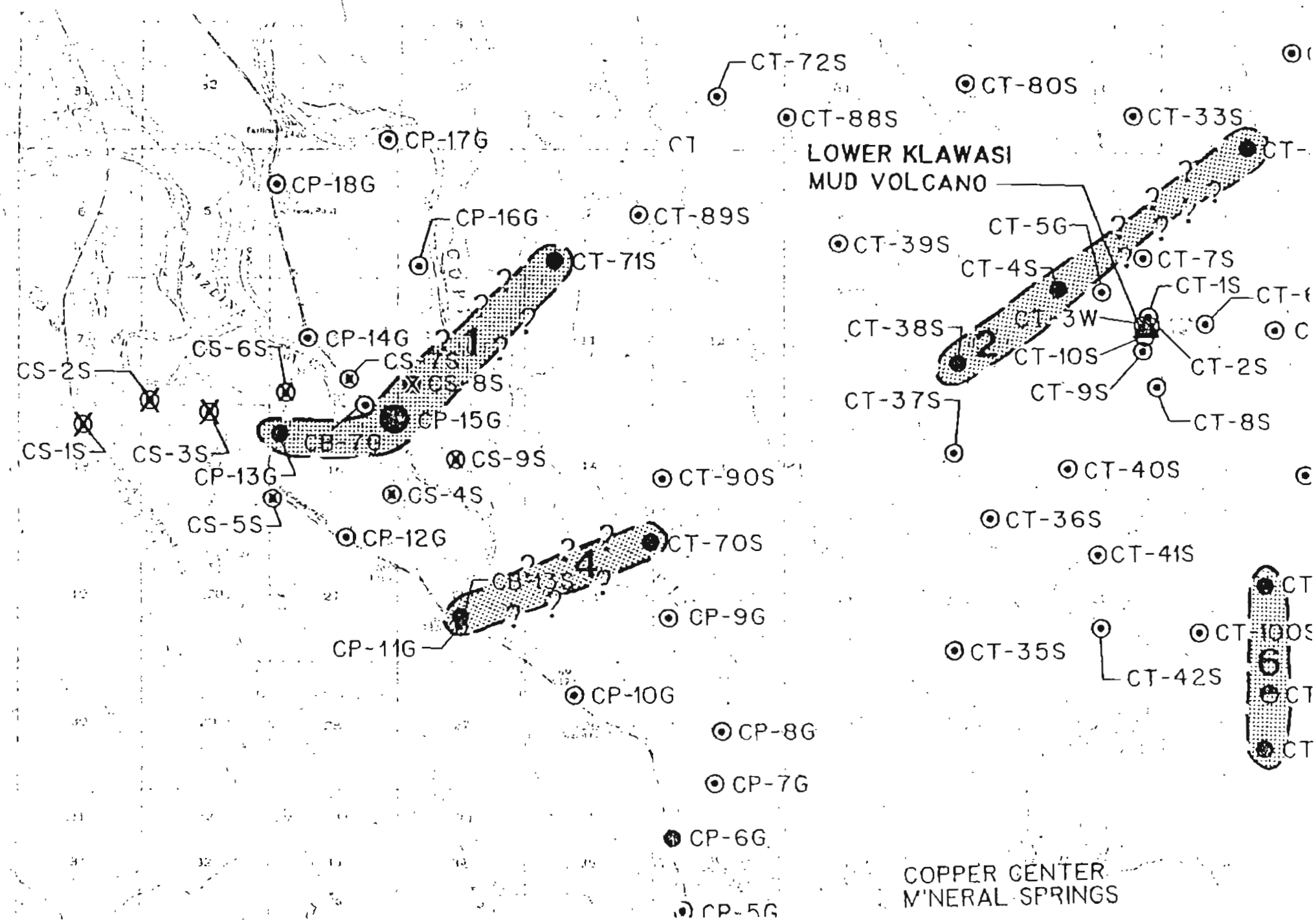

CHAPTER 4

A Gravity Survey of Part of the Eastern Copper River Basin, Alaska

by

Eugene M. Wescott, Becky Petzinger,
Gary Bender, William Witte and Donald L. Turner

Introduction

A regional gravity survey (Barnes, personal communication, 1982) and a more detailed survey by Isherwood (personal communication, 1982) indicated possible structures associated with the Klawasi mud volcanoes. The Isherwood data contoured at 1 mgal intervals (Figure 1-4, Turner et al., Chapter 1) show a low associated with lower Klawasi and several other features. These data, however, are not sufficient to make definitive models.

A more detailed gravity survey, with a station density of about 1 station per square mile was planned for the area of the eastern Copper River Basin. A gravity survey in itself cannot provide direct evidence of geothermal resources. However, in conjuction with other measurements, gravity maps are useful in interpreting structures which may be related to geothermal resources.

After variations in gravity due to latitude and altitude are removed, the variation of the densities of the rocks and their configuration produce the remaining anomalies of interest. The density of rocks depends upon their mineral composition, porosity and age to some degree. In general the most recent sediments tend to have the lowest densities while older, more deeply buried sediments are more dense. Crystalline basement rocks and intrusives tend to have even greater densities. An excess of mass beneath the surface will produce a gravity high while a greater thickness

of low density rocks will produce a gravity low.

Physical Property Measurements

A number of rock samples from volcanic formations on Mt. Drum and greenstone units near Chitna were collected and measured for density and magnetic susceptibility. The volcanic rocks varied considerably in density, from 2.43 to 3.08 gm/cc, with an average value of 2.61. The greenstones had an average density of 2.98 gm/cc. In contrast, the surface mud from upper and lower Klawasi mud volcanoes averaged 1.80 gm/cc. The values which are given in Table 1 can be compared with the previously published values in Chapter 1 (Andreasen et al., 1964).

Gravity Survey

The gravity survey was made using a Worden gravity meter no. 491 with a sensitivity of 0.10078 mgals per scale division. The gravity data are given in Table 2. We used a gravity base station on a concrete gasoline pump pedestal across the road from the Copper Center Lodge, with a given value of 981,931.85 mgals and an altitude of 1015 feet (Barnes, personal communication, 1982). Wherever possible gravity was read at bench marks and VABM stations. At most of the stations, however, altitude control was provided by up to four American Paulin System Altimeters. Unfortunately all were found to have independent drifts. After careful calibration at bench marks and use of temperature corrections, two altimeters were chosen which gave the least and most consistent drifts. One was used as a base station for barometric correction and the other was carried in the helicopter. Temperature and barometric records from the FAA station at the Gulkana airport were also used in calculating corrections for the altimeter readings.

The 1:63,360 scale topographic maps of the area were found to have many errors in topographic features, and were used only generally to check on the accuracy of the altimeter readings. Station locations were determined from air photos and later placed on the maps.

Plate 2 shows the corrected Bouguer anomaly contours based upon our stations (solid circles), the survey stations of Isherwood (crosses, personal communication, 1981) and stations by Barnes (open circles, personal communication, 1982). For the Bouguer correction we used the commonly used density value of 2.67 gm/cc (correction to a sea level datum surface). However, inspection of the density log of the Amoco Ahtna A-1 well shows that this value is too high. A density of 2.4 is appropriate to a depth of 3500 ft. Therefore, another corrected Bouguer anomaly map was prepared using the 2.4 value. The effect of the density change was to reduce the regional west-to-east gradient. The important shorter wavelength anomalies are similar on both versions. The terrain-corrected Bouguer anomaly map (Plate 2) shows three large scale features. There is an almost semi-circular negative pattern in the eastern half of the map, which appears to be related to the large negative Bouguer anomaly of Mt. Drum, about 8 miles east of the edge of the map. In the northwest quadrant of the map there is a positive anomaly of about 18 mgals, which is probably indicative of a structural high in the crystalline basement rocks. South of the positive anomaly is an east-west-trending negative trough.

There are a number of interesting smaller scale features superposed on the Mt. Drum negative regional trend. A negative anomaly of 2 mgals is centered over Mineral Springs (lower Klawasi mud volcano). There are also negative anomalies of the order of 1 mgal 2 miles south, and 3 and 5 miles northeast of lower Klawasi mud volcano.

A positive closed anomaly is located about half way between upper and lower Klawasi mud volcanoes. This area is of considerable interest because it coincides exactly with helium anomaly no. 5 (Plate 1, Turner and Wescott, Chapter 2).

In order to isolate the smaller scale anomalies, the regional trend due to Mt. Drum was removed by subtracting a third degree trend surface from the $\sigma = 2.4$ corrected Bouguer anomaly map. The results are shown in Plate 3. The most prominent feature revealed by removing the regional trend due to Mt. Drum is a northeast-trending trough from lower Klawasi to Shrub mud volcano. At lower Klawasi the trough either bends westward or intersects another linear trough. There are several lows along and adjacent to the trough. It is possible that the trough delineates an old fault which has been buried by glacial lake sediments. It is also possible that this zone of weakness has allowed over-pressured mud to push up along the fault, and in adjacent places to form mud diapirs, and also to occasionally reach the surface as mud volcanoes. However, these hypothetical diapirs would have to be broad and very long. Another, perhaps more likely model for the trough is a sediment-filled valley in the dense basement rocks. Figure 1 shows a generalized NW to SE gravity profile across the trough and a two-dimensional model which fits the data. The model incorporates a mile-wide depression in the greenstone basement 1000 ft. in depth. This could be interpreted as a graben.

The isolated gravity high between lower Klawasi and upper Klawasi mud volcanoes lies at the end of a gravity ridge in line with the east-west gravity trough. This isolated high can be modelled as a dense intrusive, perhaps a dacite dike. Figure 2 shows a cross section model using a density contrast + 0.3 gm/cc which fits the data well. Model A is an

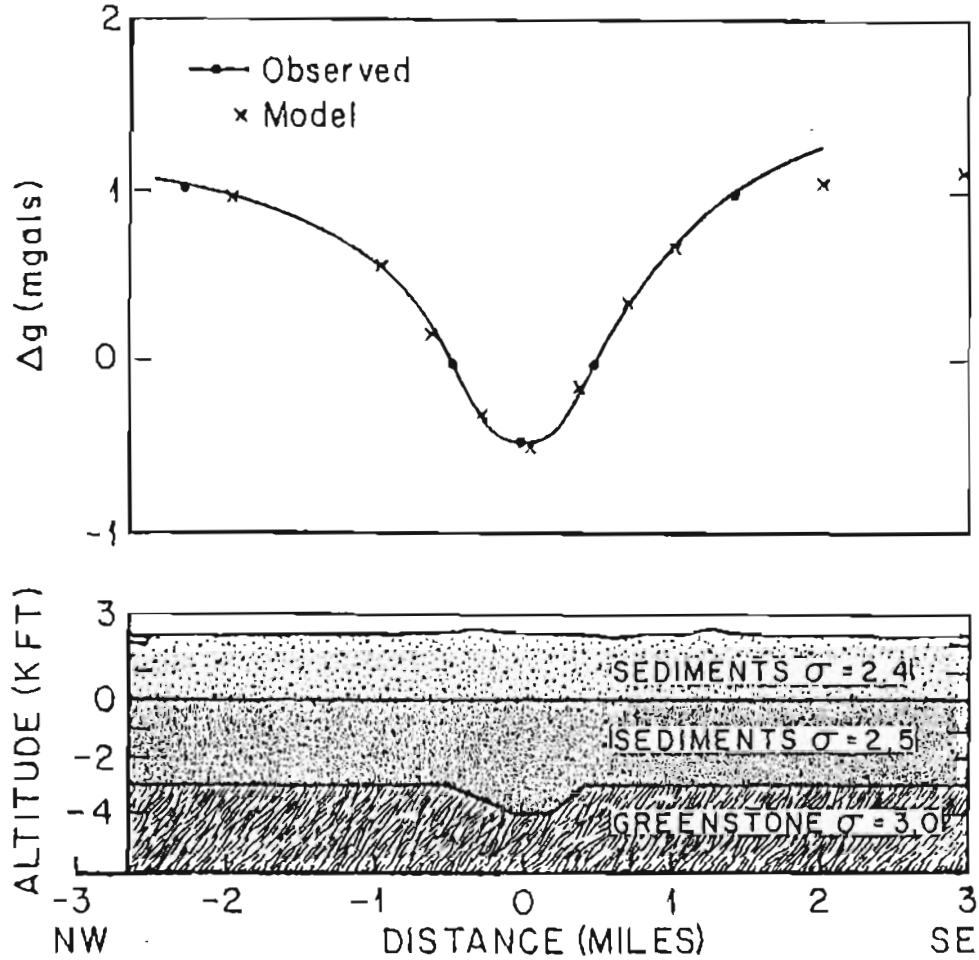

Figure 4-1. Top: Gravity anomaly profile NW-SE across the gravity trough running generally between Lower Klawasi and Shrub mud volcanoes - solid line. Bottom: Model cross section, no vertical exaggeration, of a bedrock valley or graben structure which would explain the anomaly. Model values are shown on profile by x's.

Figure 4-2. Top: N-S gravity profiles across positive gravity anomaly at helium anomaly #5. Solid line - observed, dashed line - model A, dotted line - model B. Bottom: Cross section of models, A - deep intrusive, B - shallow lacolith intrusive.

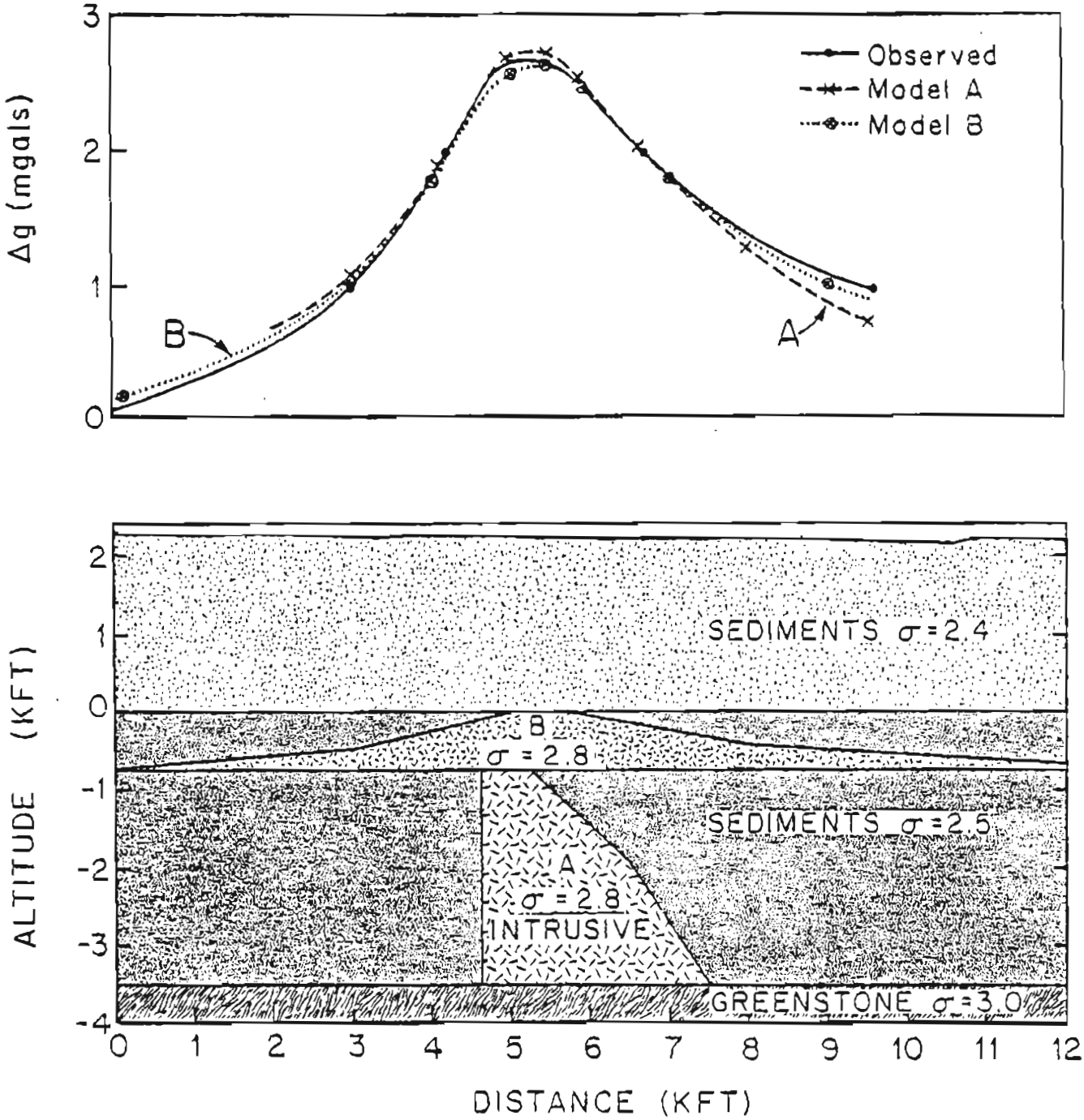

ellipsoidal intrusive about 3X as wide as its thickness with a depth to its top of 3000 ft. This model is almost a maximum depth model for a density contrast of 0.3. Model B is a mushroom shaped laccolith at a shallower depth which also gives a close fit to the data.

Without some other type of geophysical data there is no way of determining a unique model for the observed gravity data. The positive gravity anomaly coincides with an area of lower than average total field magnetic anomaly, and is also coincident with helium anomaly area no. 5 (Plate 1). This situation strongly suggests that the area is a geothermal prospect. Geothermal fluids have a tendency to chemically alter magnetite and other magnetic mineral components of rocks to non-magnetic alteration products. In addition to these indicators, self-potential traverse E-E', Figure 5-6 shows a strong positive gradient in the direction of the anomaly, again suggestive of a geothermal resource area.

The gravity low about 8 km NE of lower Klawasi mud volcano is also of considerable interest. It coincides fairly well with the large helium anomaly 3 (Plate 1). This negative gravity anomaly also corresponds with an east-west negative trend in the magnetic maps, possibly suggesting geothermal alteration of magnetic minerals.

Table 4-1

Physical Property Determinations

Sample No.	Description	Magnetic Susceptibility (cgs units x 10^{-6})	Density (gm/cc)
DT82-1A	hornblende plagioclase andesite Porphyritic	1765	2.57
DT82-1B	"	680	2.54
DT82-2A	"	1254	2.43
DT82-2B	Fine-grained, vesicular, non-porphyritic basalt	1326	2.47
DT82-4	"	622	3.08
DT82-3	"	1299	2.58
DT82-5	"	1231	2.54
DT82-6A	Porphyritic pyroxene - plagioclase andesite	1730	2.64
DT82-6B	"	1475	2.57
DT82-7A	"	1219	2.62
DT82-7B	"	1102	2.67
A	Greenstone - probably meta-basalt	7613	2.93
B	"	1319	3.01
C	"	5700	3.00
Upper Klawasi mud	light gray mud, mostly clay size	48	1.82
Lower Klawasi mud	"	46	1.78

Table 4.2. Copper River Basin Gravity Stations

Station	Latitude	Longitude	Elevation (ft.)	FAA	6 = 2.67 SBA	6 = 2.67 CBA	6 = 2.4 CBA
CUCE	61° 57' 17"	145° 17' 07"	1015.0	-40.01	-74.62	-74.62	-71.06
GM1	62° 03' 31"	145° 13' 22"	1856.6	-27.89	-91.19	-91.01	-84.62
GM2	62° 03' 29"	145° 13' 17"	1860.0	-28.03	-91.45	-91.27	-84.87
GM4	62° 03' 45"	145° 14' 38"	1745.0	-28.72	-88.22	-88.22	-82.15
GM5	62° 03' 42"	145° 13' 56"	1766.1	-29.48	-89.69	-89.69	-83.57
GM6	62° 03' 29"	145° 12' 31"	1764.0	-28.82	-88.96	-88.96	-82.83
GM7	62° 03' 52"	145° 13' 11"	1778.0	-27.61	-88.23	-88.23	-82.06
GM8	62° 03' 05"	145° 13' 15"	1734.8	-31.22	-90.00	-90.00	-83.95
GM9	62° 03' 19"	145° 13' 26"	1839.0	-27.66	-90.36	-90.36	-83.94
GM11	62° 05' 32"	145° 08' 45"	2228.0	-14.16	-90.12	-90.12	-82.29
GM12	62° 06' 17"	145° 06' 36"	2389.2	-11.14	-92.60	-92.60	-84.32
GM13	62° 05' 46"	145° 03' 37"	2507.0	-10.06	-95.54	-95.54	-86.85
GM15	62° 05' 40"	145° 05' 27"	2421.4	-11.43	-93.99	-93.99	-85.60
GM17	62° 06' 51"	145° 07' 13"	2359.0	-11.44	-91.65	-91.65	-83.13
GM19	62° 07' 47"	145° 10' 38"	2137.7	-11.21	-84.10	-84.10	-76.68
GM21	62° 07' 43"	145° 14' 45"	1805.1	-16.54	-78.09	-78.09	-71.82
GM67 & GM23 Shrub	62° 08' 59"	145° 01' 08"	2943.0	6.25	-94.09	-92.09	-82.47
GM25	62° 07' 07"	145° 03' 43"	2511.3	- 7.03	-92.65	-92.65	-83.96
GM27	62° 07' 28"	145° 00' 23"	2652.0	- 4.04	-94.21	-94.21	-84.87
GM29	62° 04' 16"	145° 07' 52"	2229.0	-16.25	-92.04	-92.04	-84.16
GM31	62° 04' 58"	145° 07' 25"	2245.9	-16.54	-92.87	-92.87	-84.96
G34	61° 59' 26"	145° 16' 23"	1444.3	-30.65	-79.89	-79.62	-74.67
G35	62° 01' 16"	145° 16' 09"	1542.8	-29.81	-82.42	-82.42	-77.06
G36	62° 02' 10"	145° 15' 37"	1594.5	-32.43	-86.79	-86.79	-81.26
G37	62° 02' 38"	145° 16' 09"	1604.8	-32.76	-87.48	-87.48	-81.91
G38	62° 03' 14"	145° 16' 05"	1641.8	-32.68	-88.65	-88.65	-82.96
G39	62° 04' 04"	145° 17' 47"	1571.8	-33.80	-87.39	-87.39	-81.97
G40	62° 02' 32"	145° 14' 32"	1675.9	-31.40	-88.54	-88.54	-82.73
G41	62° 01' 54"	145° 14' 05"	1622.0	-33.03	-88.33	-88.33	-82.73
G42	62° 01' 27"	145° 14' 05"	1605.2	-33.00	-87.73	-87.73	-82.19
G43	61° 59' 34"	145° 10' 20"	1710.1	-26.97	-85.28	-85.28	-79.34

Table 4.2. (cont'd.)

Station	Latitude	Longitude	Elevation (ft.)	FAA	6 = 2.67 SBA	6 = 2.67 CBA	6 = 2.4 CBA
G44	62° 00' 56"	145° 11' 35"	1674.6	-30.46	-87.56	-87.56	-81.74
G45	62° 01' 43"	145° 11' 38"	1689.3	-30.00	-87.60	-87.60	-81.73
G46	62° 02' 26"	145° 11' 02"	1766.2	-29.25	-89.47	-89.32	-83.25
G47	62° 03' 27"	145° 11' 28"	1876.3	-26.28	-90.25	-90.25	-83.73
G48	62° 03' 47"	145° 08' 29"	2155.5	-18.48	-91.97	-91.85	-85.39
G49	62° 02' 55"	145° 09' 02"	2023.1	-22.15	-91.13	-90.98	-84.02
G50	62° 00' 34"	145° 08' 31"	1896.8	-25.12	-89.80	-89.68	-83.15
G51	61° 59' 38"	145° 05' 59"	2067.7	-19.93	-90.43	-90.19	-83.08
G52	62° 00' 23"	145° 03' 31"	2230.5	-18.14	-93.98	-93.98	-86.28
GM77, GM73							
GM 63, G53							
Upper Klawasi	62° 04' 51.96"	145° 00' 21.03"	3009.0	3.75	-98.85	-97.29	-87.09
G54	62° 03' 56"	145° 00' 25"	2663.9	- 5.18	-96.01	-96.01	-86.74
G55	62° 03' 46"	144° 57' 43"	2866.2	.42	-97.31	-97.16	-87.29
G56	62° 02' 55"	144° 59' 37"	2678.4	- 6.06	-97.38	-97.28	-88.05
G57	62° 02' 18"	145° 01' 19"	2499.2	-10.19	-95.40	-95.40	-86.78
G58	62° 00' 14"	144° 58' 10"	2548.4	-12.10	-98.99	-98.99	-90.14
GM59	62° 01' 31"	145° 06' 30"	2163.3	-17.80	-91.56	-91.56	-84.07
GM60	62° 02' 11"	145° 03' 28"	2301.1	-15.93	-94.38	-94.38	-86.44
GM61	62° 03' 17"	145° 05' 26"	2262.3	-15.54	-92.68	-92.68	-84.87
GM62	62° 04' 02"	145° 03' 32"	2453.4	-10.64	-94.29	-94.29	-85.82
GM64	62° 05' 51"	144° 58' 17"	2873.3	.70	-97.27	-97.13	-87.23
GM65	62° 06' 38"	145° 00' 42"	2667.0	- 4.43	-95.36	-95.36	-86.16
GM66	62° 10' 19"	145° 01' 20"	2546.7	- 3.43	-90.26	-90.26	-81.47
GM68	62° 06' 56"	145° 15' 13"	1757.5	-22.22	-82.14	-82.14	-76.04
GM69	62° 06' 44"	145° 23' 10"	1193.0	-38.91	-79.58	-79.47	-75.36
GM70	62° 02' 02"	145° 20' 31"	1362.6	-38.16	-84.62	-84.22	-79.56
GM71	62° 03' 58"	145° 21' 56"	1247.4	-43.18	-85.71	-85.60	-81.31
GM72	62° 05' 02"	145° 19' 35"	1561.5	-32.82	-86.06	-85.95	-80.57
G74	62° 09' 10"	145° 04' 16"	2529.3	- 2.93	-89.17	-89.03	-80.31
G75	62° 06' 11"	145° 08' 32"	2248.7	-13.52	-90.19	-90.19	-82.38
G76	62° 04' 58"	145° 09' 33"	2109.5	-20.10	-92.03	-92.03	-84.68
G78	62° 06' 22"	145° 12' 43"	1897.3	-20.80	-85.49	-85.39	-78.85
G79	62° 06' 20"	145° 18' 20"	1625.3	-25.24	-80.65	-80.65	-75.04
G80	62° 05' 06"	145° 16' 02"	1693.8	-29.86	-87.61	-87.61	-81.55
GM81	62° 06' 05"	145° 06' 43"	2403.7	- 9.27	-91.22	-91.22	-82.89

Table 4.2. (cont'd.)

Station	Latitude	Longitude	Elevation (ft.)	FAA	ρ = 2.67 SBA	ρ = 2.67 CBA	ρ = 2.4 CBA
GM82	62° 06' 40"	145° 06' 03"	2444.0	- 7.92	-91.25	-91.25	-82.78
GM83	62° 06' 25"	145° 05' 36"	2438.1	- 9.28	-92.41	-92.41	-83.96
GM84	62° 06' 31"	145° 07' 06"	2386.4	-10.24	-91.61	-91.61	-83.34
GM85	62° 07' 45"	145° 05' 32"	2444.9	- 5.02	-88.38	-88.38	-79.92
GM86	62° 03' 53"	145° 06' 53"	2275.9	-12.98	-90.58	-90.58	-82.73
GM87	62° 03' 52"	145° 07' 11"	2239.0	-14.07	-90.41	-90.41	-82.69
GA1 (≈GM27)	62° 07' 30"	145° 00' 27"	2648.3	- 3.92	-94.22	-94.22	-85.05
GA2 (≈GM66)	62° 10' 19"	145° 01' 20"	2560.4	- 2.14	-89.44	-89.44	-80.61
GA3 (≈G74)	62° 09' 10"	145° 04' 16"	2525.7	- 3.19	-89.30	-89.16	-80.46
GA4	62° 07' 13"	145° 09' 36"	2158.7	-13.10	-86.71	-86.71	-79.22
GA5 (≈GM12)	62° 06' 15"	145° 06' 37"	2393.2	-10.98	-92.58	-92.58	-84.28
GA6	62° 05' 19"	145° 02' 46"	2536.6	- 8.73	-95.22	-95.22	-86.43
GA7	62° 05' 35"	145° 08' 11"	2228.1	-14.84	-90.81	-90.81	-83.07
GA8 (≈G48)	62° 03' 48"	145° 08' 06"	2162.1	-18.17	-91.88	-91.76	-84.31
GA9	62° 04' 17"	145° 06' 45"	2243.6	-16.05	-92.55	-92.55	-84.77
GA10	62° 04' 44"	145° 11' 46"	1880.1	-25.75	-89.85	-89.75	-83.27
GA11 (≈G80)	62° 05' 06"	145° 16' 02"	1693.8	-29.76	-87.51	-87.51	-81.65
GA12 (≈G78)	62° 06' 20"	145° 12' 32"	1893.3	-21.76	-86.31	-86.21	-79.69
GA13 (≈G57)	62° 02' 18"	145° 01' 19"	2494.6	-10.07	-95.12	-95.12	-86.51
GA14	62° 01' 28"	145° 06' 11"	2132.0	-21.04	-93.73	-93.73	-86.31
GA15	62° 02' 47"	145° 06' 38"	2192.6	-18.15	-92.91	-92.85	-85.30
GA16 (≈G45)	62° 01' 43"	145° 11' 38"	1692.4	-30.74	-88.44	-88.44	-82.56
GA17 (≈G34)	61° 59' 26"	145° 16' 23"	1426.5	-32.01	-80.64	-80.40	-75.50
GA18 (≈G35)	62° 01' 16"	145° 16' 09"	1536.7	-30.14	-82.54	-82.54	-77.20
GA19	62° 02' 05"	145° 14' 20"	1653.7	-30.63	-87.01	-87.01	-81.30
GA20	62° 02' 31"	145° 13' 34"	1675.5	-32.19	-89.32	-89.32	-83.51
GA21	62° 01' 54"	145° 17' 47"	1515.0	-31.98	-83.63	-83.63	-78.35
GA22 (≈GM71)	62° 03' 55"	145° 21' 55"	1259.2	-42.28	-85.21	-85.10	-80.77
GA23 (BM D 27)	62° 04' 29"	145° 18' 38"	1580.1	-32.41	-86.28	-86.18	-80.74
GA24 FAA	62° 09' 32"	145° 27' 23"	1572.3	-18.06	-71.66	-71.66	-66.24
GA25	62° 07' 56"	145° 24' 43"	1208.9	-31.52	-72.74	-72.61	-68.45
GA26	62° 07' 57"	145° 20' 19"	1523.8	-24.50	-76.46	-76.46	-71.20
GA27	62° 07' 11"	145° 23' 01"	1230.8	-35.92	-77.89	-77.78	-73.54
GA28	62° 05' 14"	145° 22' 35"	1313.7	-40.23	-85.02	-84.91	-80.39
S94	61° 57' 08"	145° 18' 23"	1032.0	-38.98	-74.16	-74.16	-70.53

Table 4.2. (cont'd.)

Station	Latitude	Longitude	Elevation (ft.)	FAA	6 = 2.67 SBA	6 = 2.67 CBA	6 = 2.4 CBA
N90	62° 09' 35"	145° 27' 37"	1568.6	-17.71	-71.19	-71.19	-65.78
U60	62° 08' 21"	145° 28' 41"	1551.2	-21.12	-74.01	-74.01	-68.66
Z26	62° 07' 17"	145° 28' 42"	1528.0	-25.55	-77.65	-77.65	-72.38
Tazlina	62° 04' 49.20"	145° 25' 50.65"	1419.7	-37.32	-85.73	-84.86	-80.05
Q94	61° 58' 23"	145° 19' 05"	1032.1	-41.92	-77.11	-77.11	-73.50
M60	61° 58' 56"	145° 19' 41"	1039.	-42.95	-78.38	-78.38	-74.80
L60	61° 59' 52"	145° 20' 11"	1137.0	-41.57	-80.34	-80.34	-76.42
S26	62° 00' 40"	145° 20' 35"	1207.2	-40.11	-81.27	-81.05	-76.91
Glena	62° 06' 29"	145° 28' 32"	1512.0	-29.24	-80.79	-80.79	-75.57

CHAPTER 5

A Self-Potential Survey in the Eastern Copper River Basin, Alaska

by

Eugene M. Wescott and Gary Bender

Introduction

The self-potential, or spontaneous potential method of geophysical prospecting involves measuring the electrical potential (voltage difference) at points on the ground with respect to a reference point. To minimize spurious electrochemical voltages between the contacting electrodes and the ground, non-polarizing electrodes must be used. These consist of a metal and one of its soluble salts in a concentrated solution such that metal atoms may move reversibly into solution from, or plate onto, the metal electrode in response to an electric field. A copper electrode in a saturated copper sulfate solution contained in a porous cup is the most common electrode. A very high input impedance voltmeter is used to measure the voltage between electrode pairs.

The preferred measurement technique is to use a fixed electrode as a reference point, and a long wire to a second electrode which is moved to stations in a grid in the area to be surveyed. If a large area is to be surveyed, or the terrain or vegetation make the use of a long wire impractical, a pair of electrodes with a shorter separation may be leap-frogged around the area to measure the gradient. By summing the gradient a potential map or profile can be produced.

Self-potential anomalies may be the result of several natural and man-made processes. Conductive deposits of pyrite, pyrhotite, other sulfide minerals, magnetite, covelite and graphite are known to generate self-potential anomalies which are almost always negative in polarity over the top of the body. The conducting body is theorized to serve as a path

for electrons from the reducing environment below the water table to the oxidizing zone above. These anomalies are usually confined to a few hundred meters in width and about 100 mV (millivolts) in amplitude. Buried well pipes and pipelines also produce self-potential anomalies by pipe corrosion.

Self-potential anomalies that appear to be related to geothermal activity have been reported from a considerable number of geothermal areas (Corwin and Hoover, 1979). Anomalies range from 50 to 2000 mV in amplitude over distances of 100 m-10 km. Their wave forms and polarities vary widely. Steep gradients are often observed over the trace of faults which are thought to act as conduits for thermal fluids.

The flow of water through permeable rocks produces charge separation, and a significant self-potential phenomenon called the electrokinetic effect. There is considerable evidence supporting an electrokinetic origin for large anomalies over hot zones. Zablocki (1976) reported on the results of self-potential field tests in Kilauea, Hawaii, and concluded that they were the single most useful geophysical method for identifying and delineating thermal anomalies. He found positive potential differences as high as 1600 mV across distances of a kilometer or less over known fumarolic areas and recent eruptive fissures.

Morrison et al. (1978) found that the voltage - pressure relationship in the electrokinetic effect decreases with increasing salinity and increases with temperature. For a saline solution similar to the brine at the important geothermal field at Cerro Prieto, Mexico, a pressure difference of 100 atmospheres at 24°C across reservoir core samples would generate a maximum potential of 40 mV with the lower pressure side positive with respect to the high pressure side. As temperature

increased, the potential increased to an expected 200 mV at 300°C.

Temperature differences also produce self potential anomalies through thermoelectric coupling (Morrison et al., 1978). A typical coupling coefficient for sandstones is 0.060 mV/°C with the hot side positive with respect to the cold side. For a typical Cerro Prieto core and brine and a 300°C temperature difference, 18 mV would be produced by the temperature effect alone.

Potential differences can also be produced by differences in ionic concentrations in the formation fluids amounting to about 25 mV per power of 10 concentration difference (Sill, personal communication, 1982). This can be significant if there are major lateral changes in the ground water.

The Klawasi Mud Volcano Group Self-Potential Surveys

Because of limited field time the self-potential surveys were limited to the area of the Klawasi group of mud volcanoes. A long N-S seismic line located 1.75 miles west of upper Klawasi mud volcano was chosen as the major profile to be made in a search for long period anomalies. Subsidiary profiles were run from the N-S line to upper Klawasi and Shrub mud volcanoes and toward areas of previously determined helium anomalies. A separate profile over lower Klawasi was not connected to the rest of the survey due to time limitations.

Because of the large area involved and the dense vegetation, we chose to use the leap-frog method of surveying, with 100 m spacing. For almost all of the surveys we set out a 500 ft reference electrode pair which was monitored for telluric current activity. The crew making the SP survey was informed by radio when the telluric currents were quiet enough for a satisfactory reading. Voltages were measured with a Data Precision digital voltmeter of 10 megohm input impedance and a sensitivity of 10

microvolts. Copper sulfate electrodes were used and selected in pairs to have a residual potential difference of less than 1 mV when immersed in a common copper sulfate solution. Electrodes were implanted in moist soil by digging a hole through the ubiquitous vegetation mat.

Figure 5-1 and Plate 3 show the map view of the SP survey lines and potential values (in mV). As we had no SP data to compare our readings with in the area, the baseline value is arbitrary. The N-S profile was extended to the north, and the zero line A-A' was chosen near the average values there.

Profile A-A', 16.8 km long, is shown in Figure 5-2. It shows a maximum-to-minimum difference of 180 mV over 6 km. There are several shorter period dipolar anomalies of around 50 mV. The steepest gradients are located near 2-3 km S and 0-2.8 km N of the base, which may indicate the location of fault zones.

Figure 5-3 shows the self-potential profile B-B' from line A-A' east to the summit of Shrub mud volcano. Morrel Hill is the name we gave informally to a hill 2.83 km north of the base composed of Quaternary morraine deposits. The dipolar 50 mV anomaly from the top of this hill to 0.6 km east may be significant in terms of a fault zone. However, it may also be a terrain effect as the profile line went rather steeply down the hill and across a stream valley. From there eastward the potential increases gradually to a maximum at 2.1 km east. Shrub mud volcano itself may represent a small positive anomaly.

Self potential profile C-C', Figure 5-4 runs westward from the base along an E-W seismic line until the line became a swamp. At 1.7 km W the profile runs SSW towards helium anomaly #3. In general the trend is

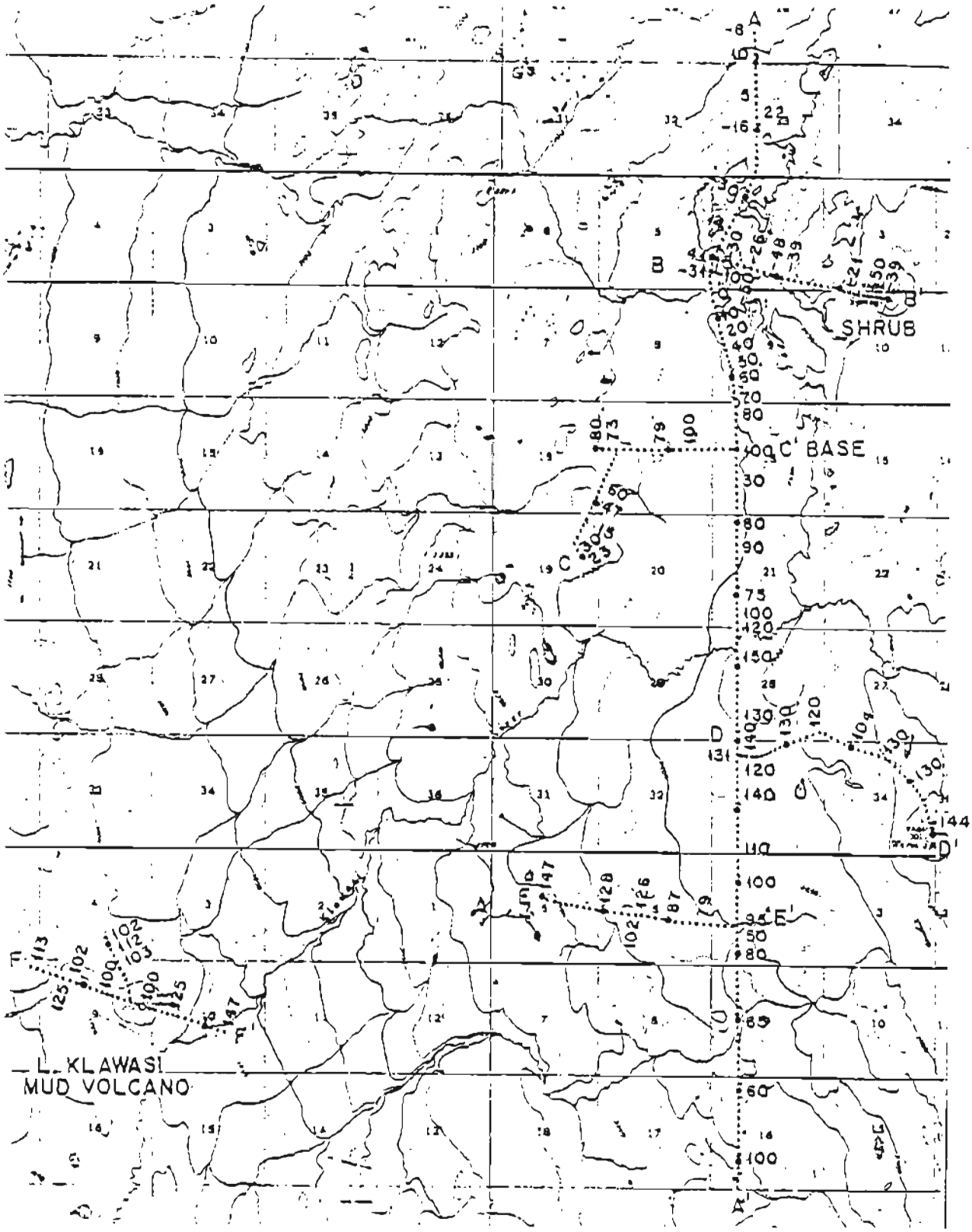

Figure 5-1. Map of self-potential profiles. Typical potentials in mV. Dots are nominally 100 m apart, larger dots 1 km apart; the baseline is arbitrary.

Figure 5-2. North-south self-potential profile A-A'. The major trend is dipolar, as would be produced by a fault crossing near 1.0 km north.

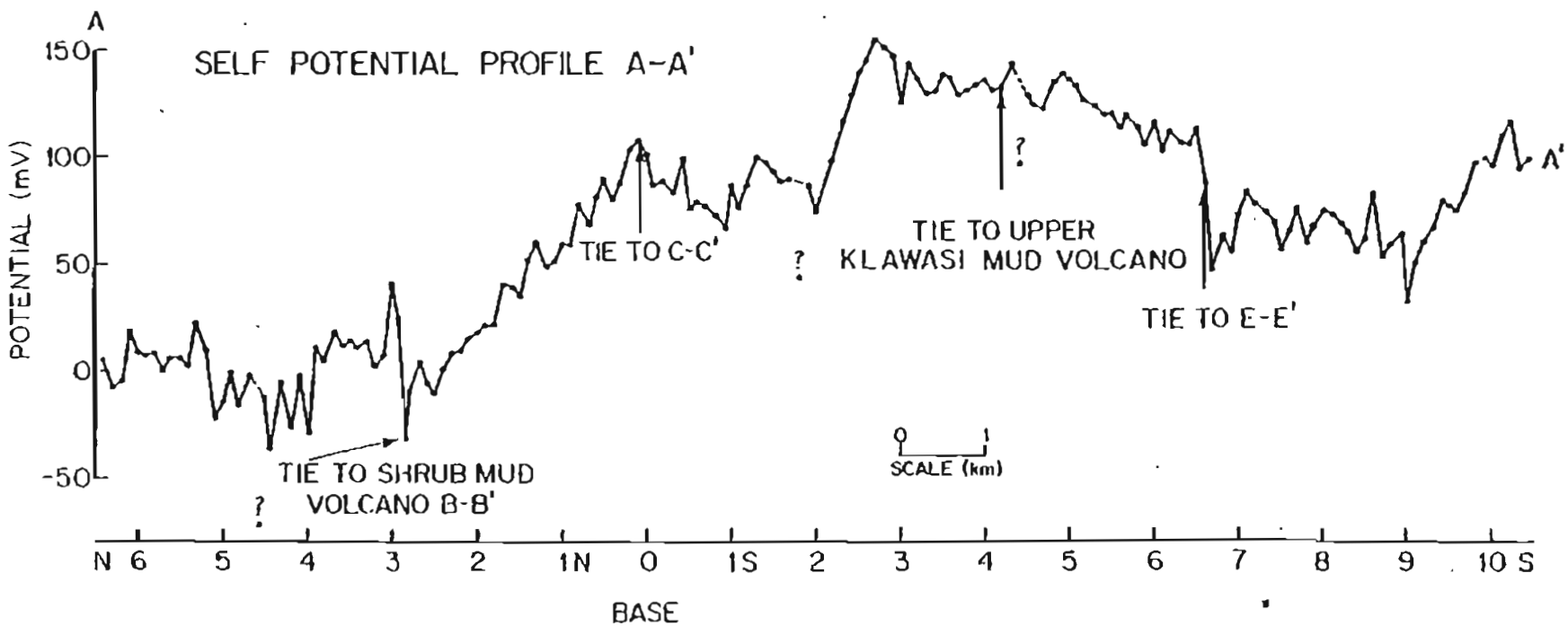

Figure 5-3. West-east self-potential profile B-B' from line A-A' to the top of Shrub mud volcano.

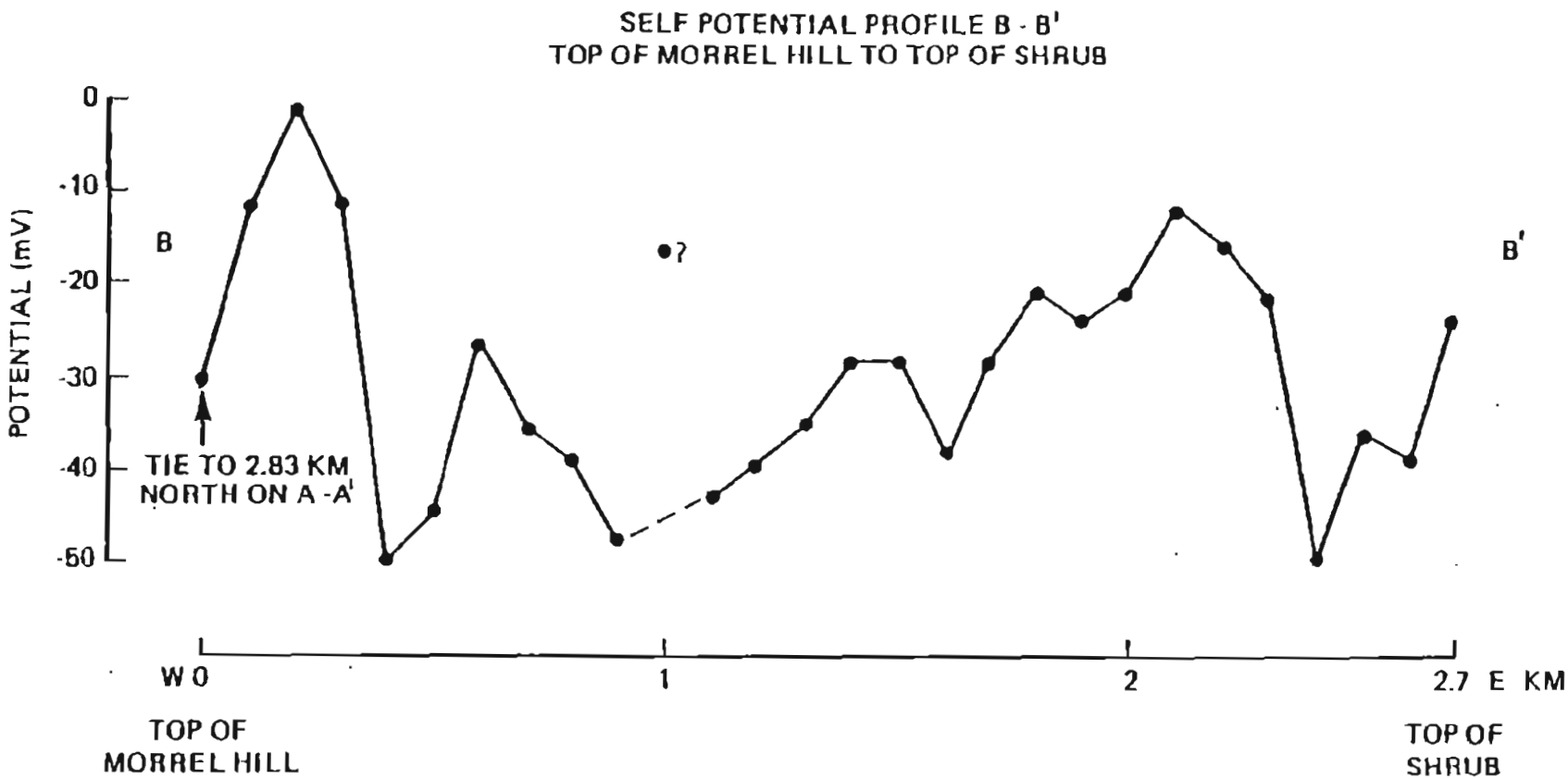

Figure 5-4. Self-potential profile C-C' from line A-A' west and SSW towards helium anomaly #3. Potential decreases towards helium anomaly area.

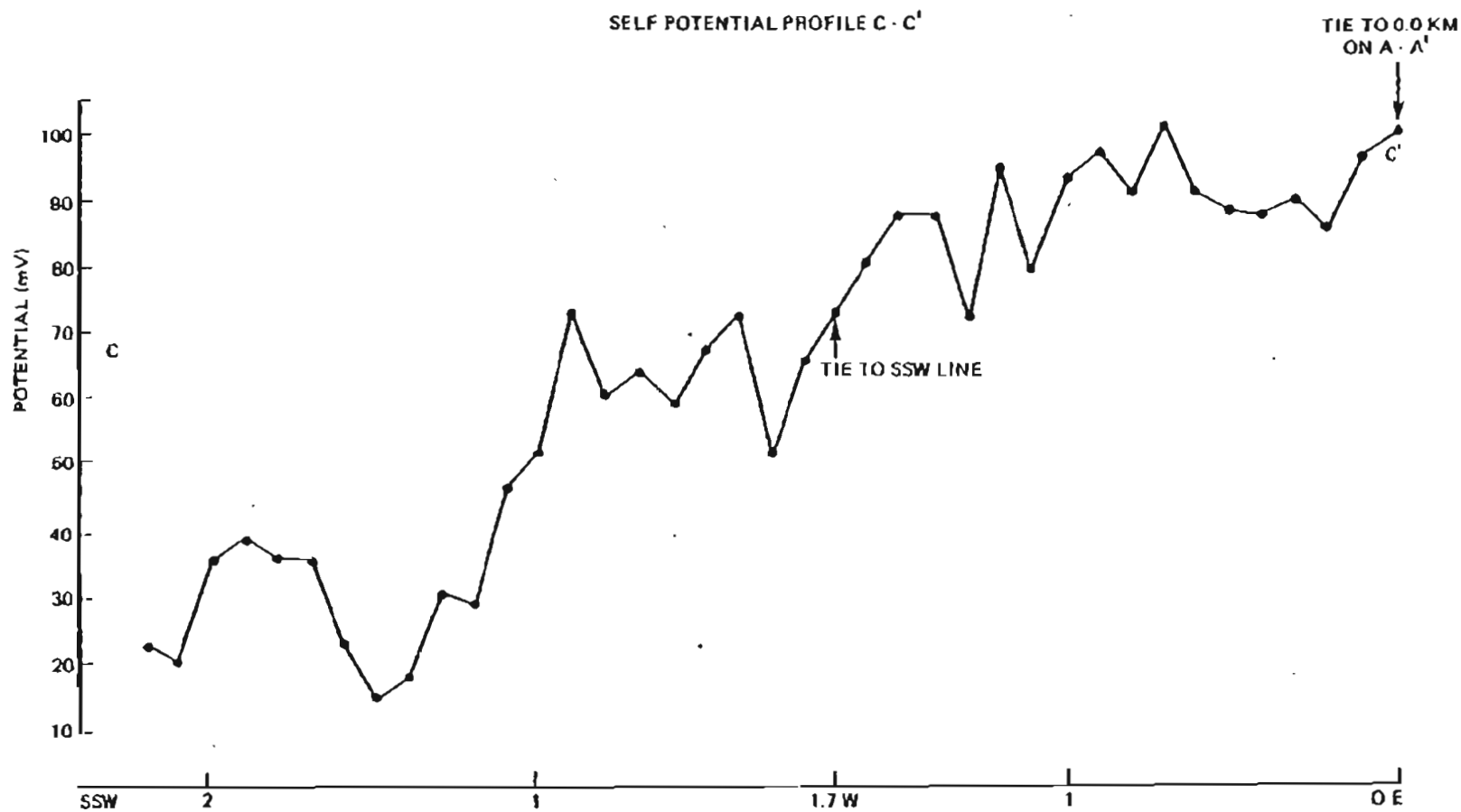

negative away from the base, reaching a 90 mV minimum at 1.4 km on the SSW line with respect to the base. As our survey approached the area of helium anomaly #3, further progress was impeded by flooding of creeks in the area. There is a possibly significant dipole-like anomaly of 35 mV with a wavelength of about 1 km near 1.65 km SSW. It suggests a fault serving as a conduit for hot water.

Profile D-D', Figure 5-5 starts at 4.2 km south of the base point and runs 3.8 km eastward to the top of upper Klawasi mud volcano. From the base line the profile trends gradually to a minimum at 2.2 km from the top of the mud volcano. There is a steep gradient from 2.2 km to 1.5 km. Upper Klawasi mud volcano itself does not seem to be a significant SP anomaly, the profile being essentially flat for 1.5 km away from the top. The potential at the top is close to the maximum positive potential on line A-A'.

Profile E-E', Figure 5-6, is one of the more important lines which were run. It runs west from 6.6 km S on line A-A' toward the general area of helium anomaly #5. There is some short period noise on the longer period trends. From line A-A' the trend is constant for 1.1 km where a positive gradient begins. A maximum of 147 mV was reached at 2.8 km from A-A', close to the maximum value on line A-A' near 3 km south of the base. The positive gradient to +147 mV near the north edge of an area with a helium anomaly and a + 2.7 mgal gravity anomaly is considered significant as discussed in the gravity and summary chapters.

Profile F-F' was run across lower Klawasi mud volcano to see if there was a significant SP anomaly from the active flow of mud and gas to the surface. As seen in Figure 5-7 the profile from the summit down to the base of the mud slope at the edge of the vegetation at 1.1 km west is

Figure 5-5. Self-potential profile D-D' from line A-A' to top of Upper Klawasi mud volcano. Note that the mud volcano does not sem to be a significant S-P anomaly.

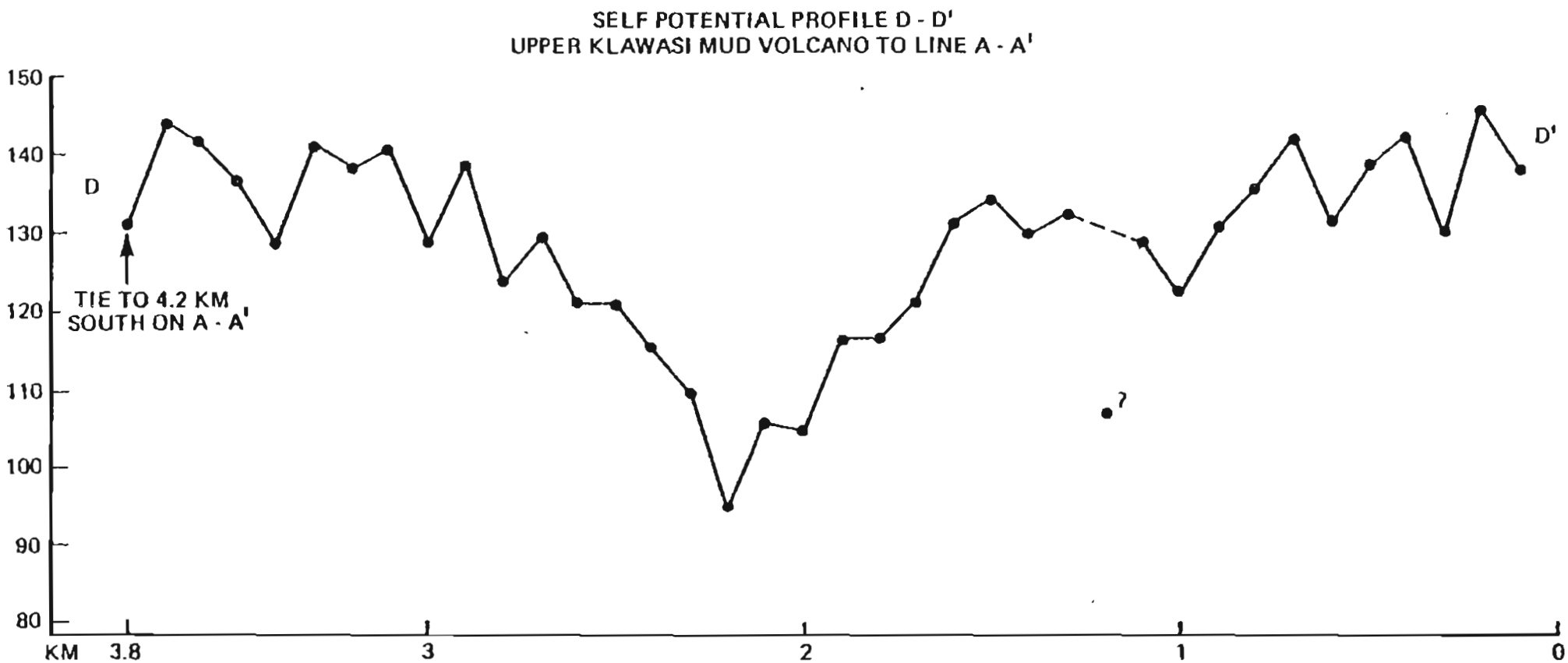

Figure 5-6. Self-potential profile E-E' west from line A-A' towards positive gravity-helium anomaly #5. The potential increases towards the anomaly area.

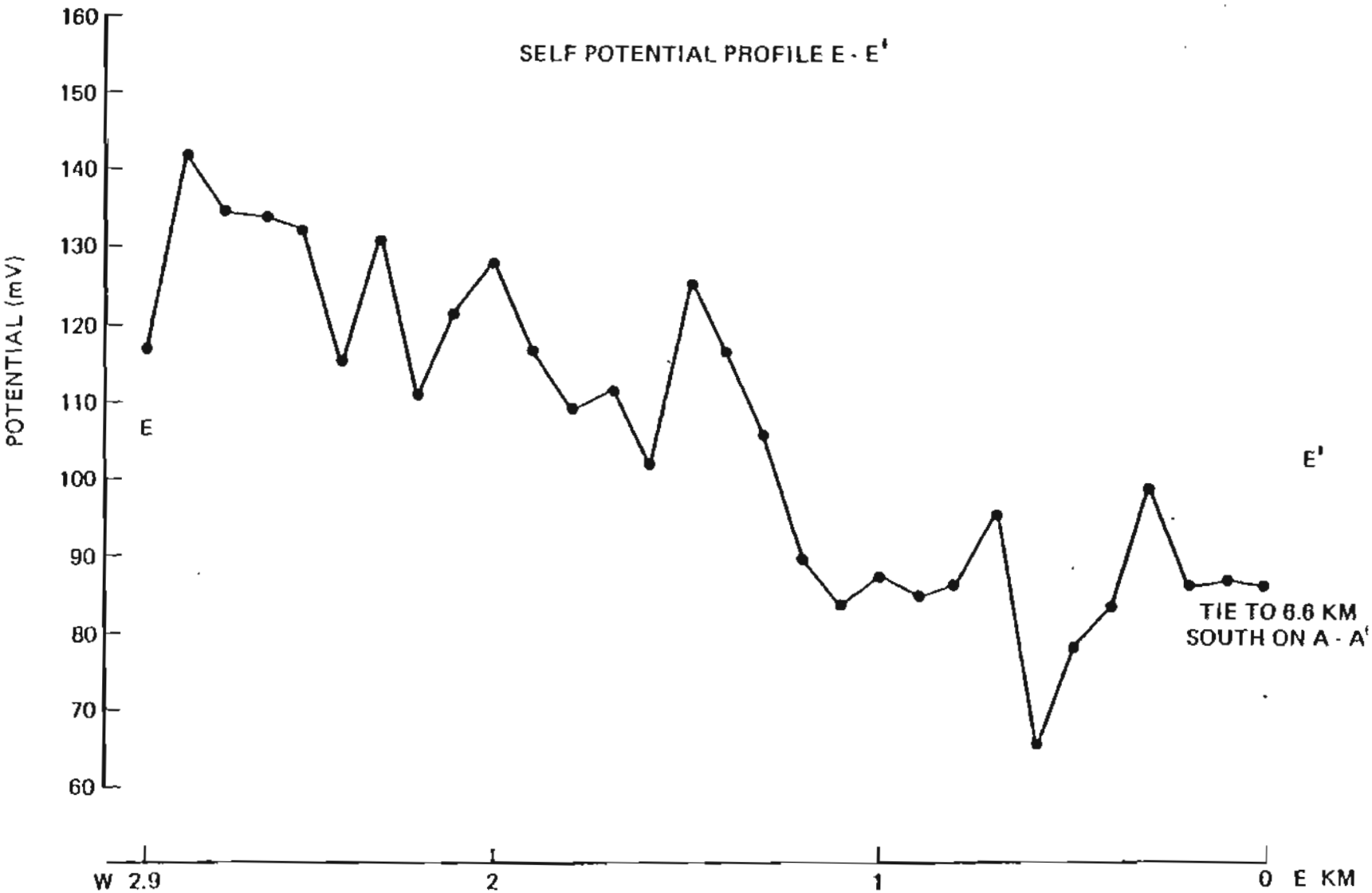

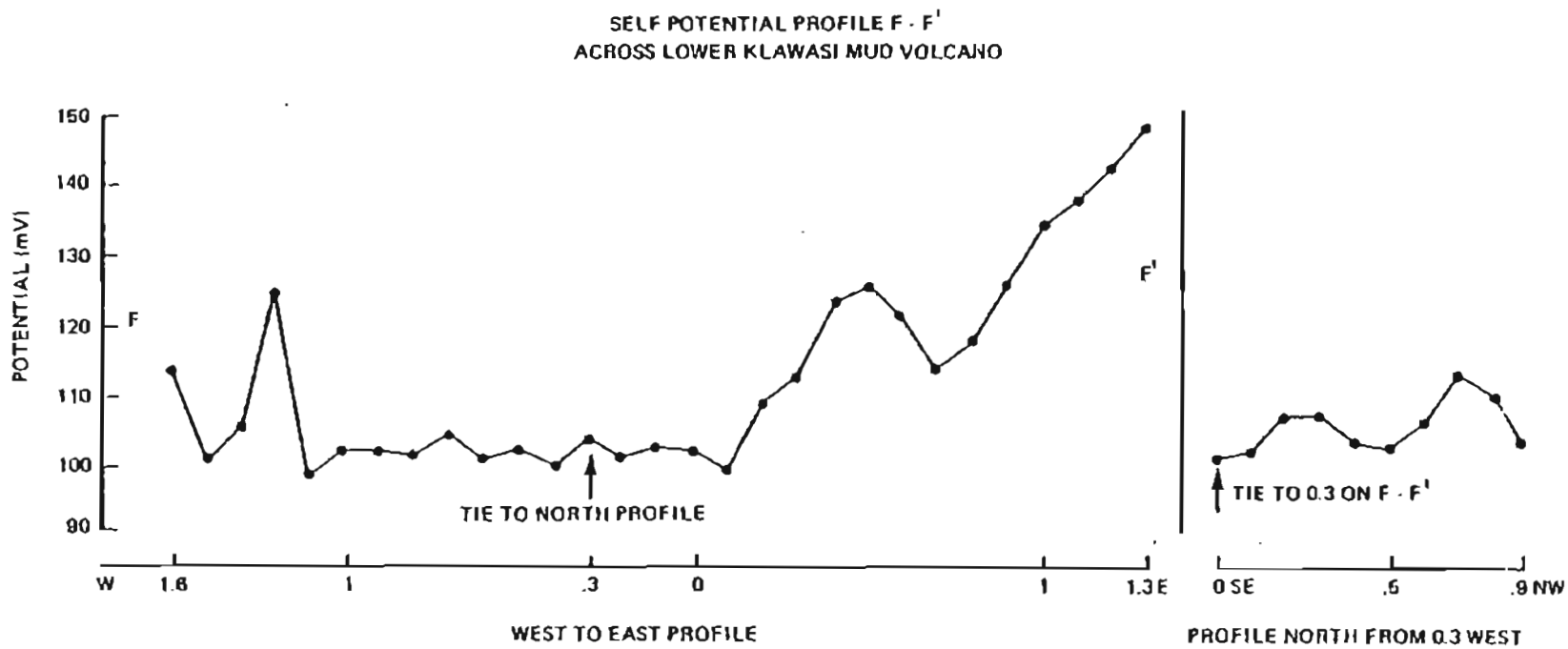

Figure 5-7. Self-potential profile F-F' across Lower Klawasi mud volcano. The flat area from the top west is the area of devegitated recent mud flow. The potential gradient is steeply positive towards the east.

very flat. At the contact between the mud flow and the taiga vegetation there is a 25 mV anomaly and an apparent positive trend to the west. To the east of the summit the trend is generally positive with respect to the arbitrary summit baseline. At 1.3 km east the potential difference is 47 mV. Unfortunately the line could not be extended to tie in with line E-E' due to the end of the field season. We note, however, that the potential was increasing toward helium anomaly #5. A short line northwest from 0.3 km west of the summit is also shown in Figure 5-7. Again on the mud flow the SP is almost constant. This may be a result of the high conductivity of the mud, as the spring water is quite saline.

Discussion of Self-Potential Surveys

It is unlikely that the self-potential anomalies found in our exploration are due to oxidation of sulfide bodies. From the topography and stream patterns, we would expect the subsurface ground water flow to be generally from east to west, producing a regional east-west potential gradient. Groundwater migration is therefore unlikely to produce the long period 180 mV anomaly observed on the 17 km line A-A'.

Figure 5-8 shows an interesting comparison of self potential profile A-A' plotted to the same scale and superposed on a profile across the economically important Cerro Prieto geothermal field in Baja California, Mexico (after Corwin and Hoover, 1979). Note the similarity in amplitude, wavelength, profile shape, and gradient. By this comparison we are not implying that our results prove a geothermal area equivalent to Cerro Prieto exists under the area of the mud volcanoes. However, since the area is located on the flank of a major volcanic region, our results are consistent with the existence of a significant geothermal resource at depth. The SP lines were not extensive enough nor were they sufficiently

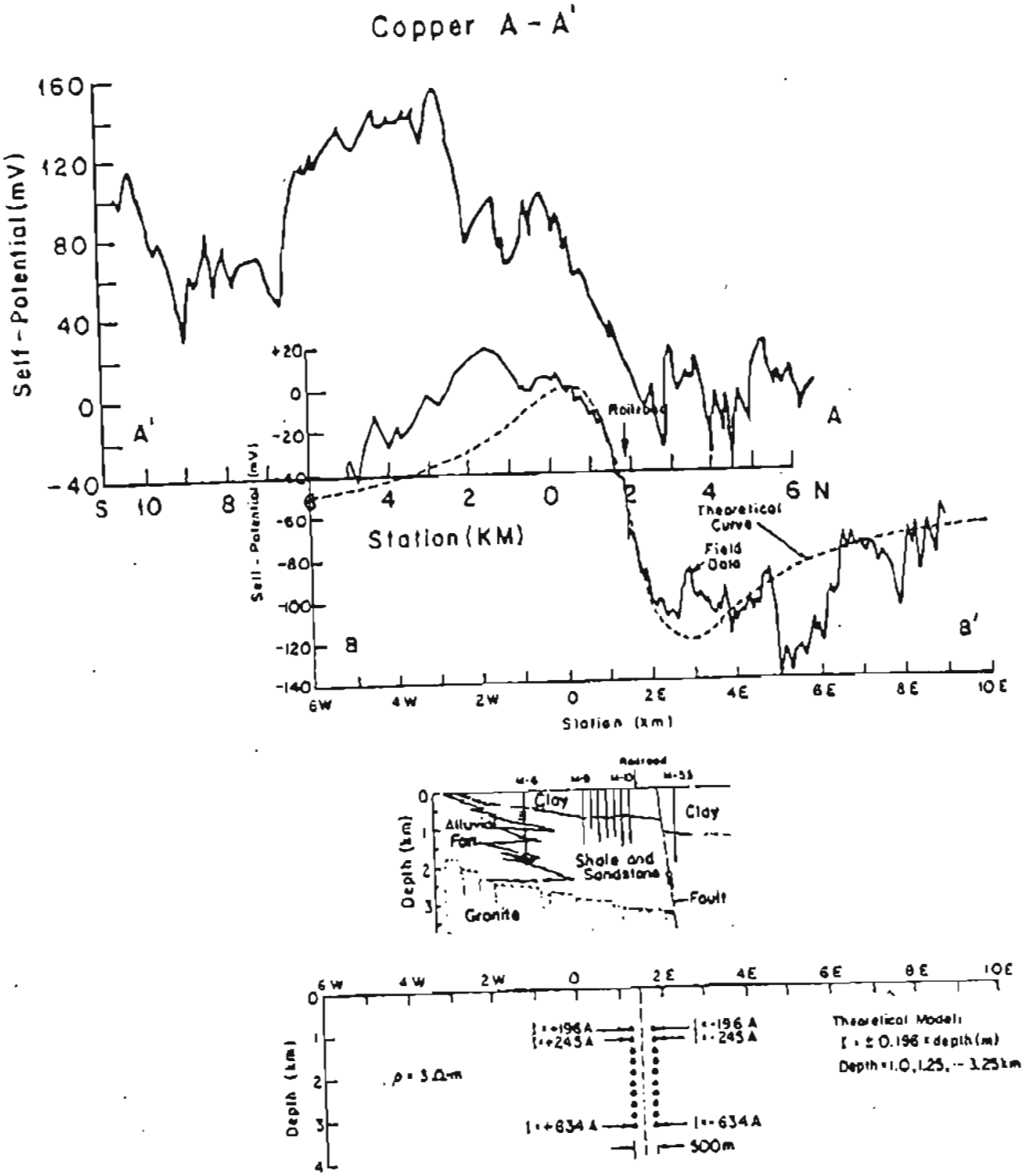

Figure 5-8. Comparison of S-P profile A-A' with an S-P profile across the Cerro Prieto geothermal field plotted to same scale. Top: profile, Copper Basin A-A'. Second from top: Cerro Prieto, observed data solid lines and dipole fault model dashed. Third from top: geological cross section of Cerro Prieto. Bottom: electrical model for line B-B', Cerre Prieto. Cerro Prieto data from Corwin and Hoover (1979).

intertied to allow contouring of the data. However, from what can be seen the data are consistent with a northeast-trending dipolar pattern, with a positive area southeast of a line joining lower Klawasi and Shrub, and negative on the northwest side of the line. This same NE trend is apparent in the gravity and magnetic data.

References

Corwin, R. F. and D. B. Hoover, 1979. The self-potential method in geothermal exploration, Geophysics, 44(2): 226-245.

Morrison, H. F., R. F. Corwin, G. de Moully and D. Durand, 1978. Semi-annual technical progress report, contract 14-08-0001-16546, Univ. of California, Berkeley.

Zabloski, C. J., 1976. Mapping thermal anomalies on an active volcano by the self-potential method, Kilauea, Hawaii: Proc. 2nd. U.N. Symposium on the Development and Use of Geothermal Resources, San Francisco, CA, U.S. Govt. Printing Office, Washington, D.C., v. 2, p. 1299-1309.

CHAPTER 6

Aeromagnetic Surveys of Part of the Eastern Copper River Basin

by

Eugene M. Wescott

Introduction

As part of the program to evaluate the geothermal potential of the Copper River Basin, the Alaska Division of Geological and Geophysical Surveys commissioned an aeromagnetic survey of parts of the Gulkana A-2 and A-3 quadrangles. ERTEC Airborne Systems, Inc. flew the survey and produced a total field, 1:63360 scale contour map, reproduced here as Plate 4. The flight lines were flown at a nominal 500 ft elevation above the terrain. The total field data were processed by subtracting the theoretical total field (the 1975 International Geomagnetic Reference Field) and then adding a constant 55,000 gammas. Flight paths were 1/2 mile apart in the north-south direction, with east-west tie lines every three miles. The data were computer contoured at 10 gamma intervals. In contrast, the previous aeromagnetic data covering part of the area was flown at a constant altitude of 4000 ft (Andreasen et al., 1958).

To augment the aeromagnetic data our gravity survey crew took total field magnetometer readings on the ground at many of the stations, and a ground magnetic profile was run across lower Klawasi mud volcano.

Discussion of Magnetic Results:

Andreason et al., (1964), in their interpretation of the 1958 aeromagnetic map, observed a well defined semicircular pattern at the eastern edge of the map apparently centered on Mt. Drum. This feature resembles a pattern of lava flows coming off of Mt. Drum, and Andreasen et al., (1964) postulated that explanation. They suggested the depth to

the lava flow unit as about 500 ft at the western edge, a few miles west of the Copper River.

Contrary to this interpretation, the Amoco Ahtna A-1 well is located within the fan-like pattern, but there is no evidence in the log of a volcanic flow unit. This does not rule out the lava flow explanation because the fan would be composed of many individual flows which would not necessarily form a continuous layer, especially near the outer margin.

In the area of our detailed surveys the trend of the Andreasen et al. (1958) map is east-west while the trend of the 1982 map (Plate 4) is generally north-south. We note that the earlier aeromagnetic survey was flown at a much higher altitude, which would eliminate smaller near-surface features and emphasize broader or deeper features. The 1982 survey at 500 ft altitude above terrain was much more sensitive to smaller, near-surface features.

Plate 4 includes the area of Mt. Drum, with its conspicuous, large amplitude dipolar anomalies. Moving westward from Mt. Drum there is about a 4-mile-wide N-S-trending zone of relatively smooth contours. Upper Klawasi mud volcano is near the middle of this zone, and Shrub is at the western edge. There is a prominent magnetic high ridge at the western edge which runs SSW from Shrub. West of this ridge the map appears very noisy with many short wavelength positive and negative anomalies of about 100 gammas amplitude. We made a semi-quantitative estimate of the average anomaly wavelength west and east of the ridge, and found they were similar: 1.20 ± 0.45 and 1.12 ± 0.28 miles respectively. The amplitude is less east of the ridge, and there are fewer anomalies.

We also measured the statistical anomaly half width, which is useful to estimate the maximum depth to the body causing the anomaly. The

average half width, $X_{1/2}$ was the same east and west of the ridge: 0.25 ± 0.10 miles. Standard half width depth rules are: sphere, $z = 2X_{1/2}$; vertical cylinder, $z = 1.3X_{1/2}$; edge of a narrow dike, $z = X_{1/2}$; and a horizontal cylinder, $z = 2X_{1/2}$. Thus we conclude that the maximum depth to the noisy appearing anomalies is between 820 and 1640 ft below the surface, but they may be at shallower depths or on the surface.

On Plate 4, there is a magnetic high of peak value 200 gammas, covering an area of about 4 square miles north and west of Shrub mud volcano. We note a close correlation of this feature with a glacial morraine mapped by Nichols and Yehle, 1969. This morraine deposit probably contains gravel and boulders of high magnetic susceptibility, perhaps derived from glaciers heading at Mt. Drum. We speculate that in other areas of the map similar morraines may be buried under lake sediments and cause the noisy aeromagnetic pattern seen in Plate 4.

At the northwest corner of Plate 4 there is a broad magnetic high of about 400 gammas above average. This corresponds to the area of the gravity high shown on Plates 2 and 3. Since the basement greenstone has a high magnetic susceptibility (Table 4-1, chapter 4), we believe these data indicate a topographic basement high.

We ran a ground magnetometer traverse across lower Klawasi mud volcano, along self-potential survey line C-C; Plate 3, from point C to the summit. Other spot readings were taken at gravity stations east of the summit. These data show a symmetrical negative anomaly of 180 gammas centered on the summit mud crater. No modelling was attempted of the gravity and magnetic anomaly here, but it seems clear that they are due to a cylinder of low density-low magnetic susceptibility mud pushed up from depth.

In Chapter 4 we noted that the positive gravity high coincident

with helium anomaly #5 appeared to also correspond with a magnetic low. The actual magnetic anomaly is better described as a narrow pinching of a magnetic ridge with magnetic lows on either side. If we make the assumption that the ridge is a smooth continuous feature which a separate, lower susceptibility body has perturbed, we can calculate the negative contours of the anomaly due to that second body. We ran a computer program to see if the proposed intrusive gravity body A, shown in Figure 4-2, Chapter 4, could produce the magnetic anomaly if it had low magnetic susceptibility. The result was conclusive - it could not. The speculated magnetic anomaly is much sharper than the broad anomaly that model A would produce. The conclusion is that the cause of the necking of the ridge is much closer to the surface than the modelled intrusive body.

Geothermal water is capable of causing magnetic minerals to be altered to non-magnetic alteration products. It is possible that this process is the cause of the magnetic pattern over the gravity anomaly. It is also possible that unrelated variations in a morraine deposit could be the source of this magnetic anomaly.

CHAPTER 7

Summary and Recommendations

by

Eugene M. Wescott and Donald Turner

The two groups of mud volcanoes, Tolsona and Klawasi do not themselves seem to be direct indications of geothermal energy resources. We have concluded that the major methane ~~with~~ significant helium content of the gas emanating from the Tolsona group can be explained by a source in the overpressured zone with a methane and hydrocarbon show found in the Moose Creek #1 well. There is no need to invoke a geothermal heat source to drive them.

The Klawasi group of mud volcanoes have a different gas composition - primarily CO_2 with a minor helium content. Motyka (personal communication) suggests that the CO_2 gas may be the result of high temperature decomposition of calcium carbonate in the sedimentary section. Motyka also reports that the geothermometers on the Klawasi group are inconclusive; some can be interpreted as suggesting a cold water source, but others indicate a source of greater than 150°C.

The wildcat well closest to the Klawasi group - AMOCO Ahtna A-1, is about 13 miles to the northwest. It did show an overpressured zone at a depth of 2,300 ft. with some natural gas. The temperature of the water coming from these mud volcanoes (about 20°C) could be explained by the normal temperature gradient to this zone, as the springs are located topographically higher than AMOCO Ahtna A-1. The CO_2 gas might also result from acid - carbonate cement reactions in the underlying sedimentary section.

Lower Klawasi is the only mud volcano showing a significant geophysical signature. It has a negative gravity anomaly and a negative magnetic anomaly. As the mud has a very low magnetic susceptibility and a low density,

these two geophysical observations are consistent with a mud diapir. Significantly it has no helium anomaly, so it is likely that there is no need for a geothermal driving force. Similarly, Shrub and Upper Klawasi are not significant helium anomalies, nor do they have geophysical signatures.

The helium survey revealed the existence of three major areas of interest. Plate 1 shows them as shaded areas 1, 3 and 5. There are other scattered helium anomalies which may or may not be significant - further sampling would be needed to determine that.

Helium anomaly area #1 is a linear zone near the junction of the Tazlina River and the Copper River. It is primarily on the west side of the Copper River, but may extend across the Copper River. From the linear configuration it is likely due to a fault acting as a conduit for helium. We believe there is a significant likelihood that hot water rising along a fault zone may have produced the anomalous helium flux. Our largest helium concentration was found at sample site CP-15G in this anomaly (Table 2-1). Because it was discovered in the data analysis after our field season, no detailed geophysical measurements were carried out in the area. If further geophysics, i.e. self-potential profiling and gravity measurements, were confined to the west side of the Copper River no helicopter time would be necessary. One of our recommendations is that geophysics and some further helium sampling be carried out in this area.

Helium anomalies 3 and 5 were explored with gravity and aeromagnetic surveys and self-potential profiles also came close to them. Figure 7-1 shows superposed helium samples, the gravity residual anomaly contours (shaded patterns), and the aeromagnetic 100 gamma contours. The gravity trough joining Lower Klawasi and Shrub is the unshaded area. Helium anomaly area 3 coincides very well with a negative offshoot area from this trough. Self-

Figure 7-1. Composite map of gravity and aeromagnetic contours and helium soil and soil gas localities. Gravity contours in 1 mgal intervals are shaded patterns. Aeromagnetic contour intervals 100 gammas. Open circles are background helium values, solid dots are anomalous He values greater than 5.4 ppm.

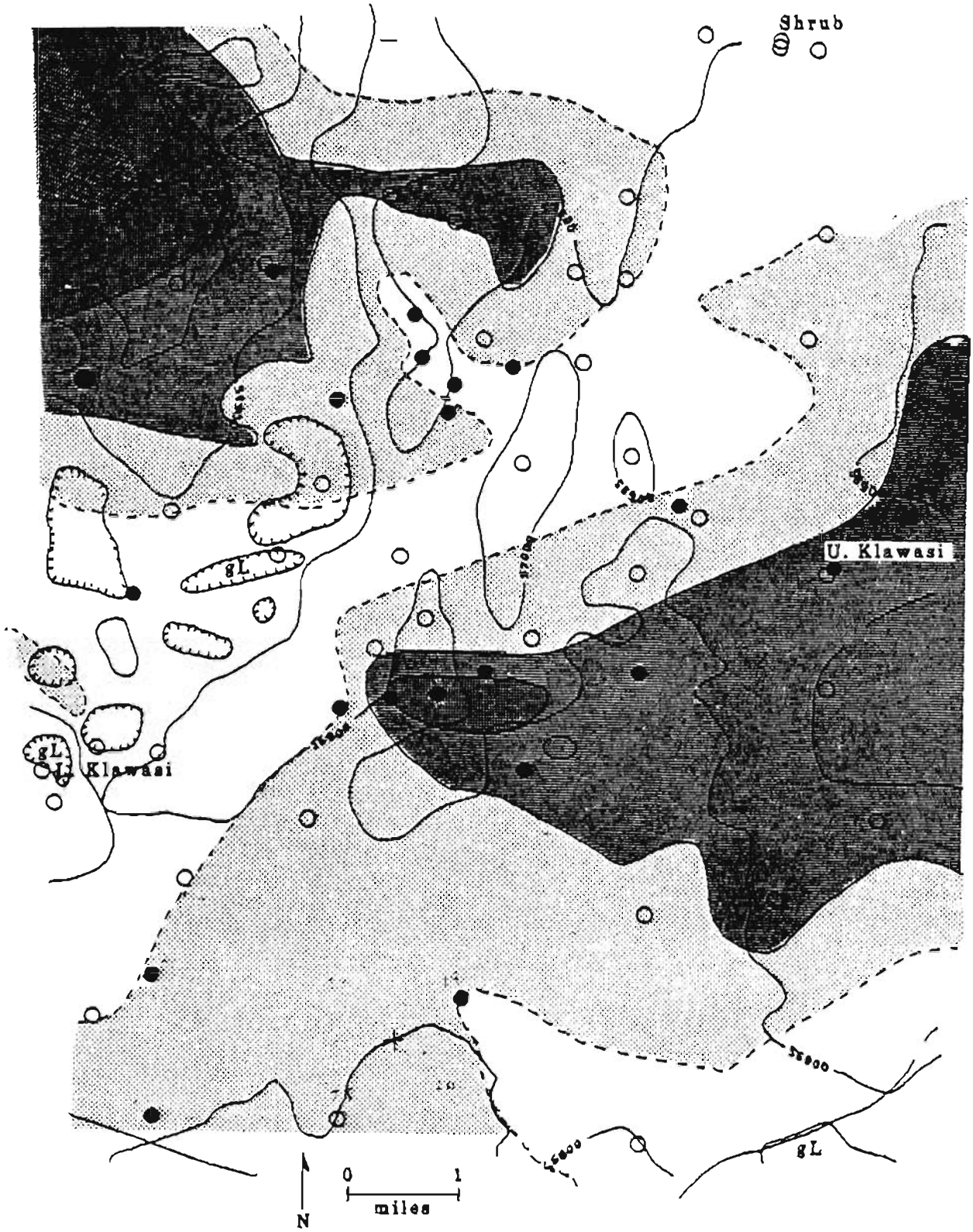

potential profile C-C' which approached this area showed a significant negative gradient. The aeromagnetic contours also suggest a negative anomaly. The negative magnetic anomaly may be due to hot water oxidizing the magnetic minerals in the rocks beneath this area. The gravity low is suggestive of a mud diapir, but other explanations are also possible. We recommend the completion of the self-potential survey in detail over this area.

Helium anomaly area 5 is the most likely geothermal prospect. Taken by themselves the four types of anomalies in this area can have several interpretations, but taken together they comprise strong evidence for a geothermal source. The helium anomaly corresponds very well with a gravity high and a magnetic low. There is a significant positive self-potential gradient along the northern edge of the anomaly. We highly recommend the completion of self-potential surveys over this area. It is a prime drilling target.

The general self-potential anomaly pattern shown is not sufficiently defined to draw firm conclusions. The map pattern, Plate 3, and profile A-A' in particular suggest that there is a large-scale dipolar pattern with a northeast trending axis, perhaps aligned with the gravity trough. We recommend that the self-potential survey be extended to complete this picture.

ACKNOWLEDGEMENTS

Financial support for this project was provided by a contract from the Alaska Division of Geological and Geophysical Surveys. Roman Motyka and John Decker of DGGS provided liason and planning for the aeromagnetic survey. Motyka also supervised helicopter logistics and interfacing of ongoing DGGS geochemical studies with our work. Clay Nicholls of DGGS visited the field site and made many helpful suggestions, as well as assisting with logistics problems.

We thank William Sill of the University of Utah Research Institute for his helpful comments on our self-potential survey and David Barnes and William Isherwood of the USGS for sharing their unpublished data and useful comments on our gravity survey. Juergen Kienle made many helpful suggestions regarding interpretation of the gravity and aeromagnetic data.

William Witte, Gary Bender and Becky Petzinger assisted with data analysis. Field assistance was ably provided by Gary Bender, Becky Petzinger, Robin Cottrell, Gabrielle de la Roche and Mary Moorman. We thank Bob Hites of Soloy Helicopter Operations for his consistently excellent flying.

Additional field support for follow-on helium soil gas surveying was provided by Ahtna Regional Corporation, arranged by Tom Craig and Clyde Stoltzfus of the Copper River Native Association.

We also thank Mrs. Katherine Ashley and her staff at the Copper River Lodge for their hospitality during our field work.